

**VOLCANIC FACIES ARCHITECTURE OF THE  
CHILCOTIN GROUP BASALTS  
AT CHASM PROVINCIAL PARK, BRITISH COLUMBIA**

by

Rebecca-Ellen Farrell

B.A., Smith College, 2004

A THESIS SUBMITTED IN PARTIAL FULFILLMENT OF THE REQUIREMENTS  
FOR THE DEGREE OF

MASTER OF SCIENCE

in

The Faculty of Graduate Studies

(Geological Sciences)

THE UNIVERSITY OF BRITISH COLUMBIA  
(Vancouver)

August 2010

© Rebecca-Ellen Farrell, 2010

## ABSTRACT

The Chilcotin Group basalt (CGB) of south-central British Columbia, Canada defines a medium-sized igneous province (*ca.* 17, 000 km<sup>2</sup>), characterized by basaltic lavas, volcanoclastic deposits, and paleosols with minor ash deposits. The CGB has previously been mapped only at reconnaissance scale (1:250 000), and most studies concentrated on geochemical and petrological studies; no stratigraphic relationships or volcanological models were attempted. Chasm canyon exposes one of the thickest successions of the CGB. Here, I explicate the volcanic facies architecture at Chasm to reconstruct the emplacement history and volcanism in the Neogene using geological mapping, cross-sections, and graphic logs. Specifically, seven discrete facies are recognized. The coherent facies are: i) vesicular/amygdaloidal pahoehoe lobes; ii) columnar-jointed, sheet-like lava; and iii) intact basaltic pillow lava. The clastic facies are: iv) paleosols; v) pillow-fragment breccia; vi) hyaloclastite; and vii) lacustrine sandstone. Facies are grouped into broad facies associations including the subaerial facies and interstratified subaqueous and subaerial facies. The subaqueous facies are a minor component in the canyon stratigraphy.

The geometry of the lavas is indicative of the eruptive style of volcanism at Chasm, which defines the volcanic facies architecture. Four architectural elements have been observed: i) tabular-classic (TC), which represents a steady continuous supply of subaerial effusive basaltic lavas; ii) compound-braided (CB), which is typical of a shield volcano where anastomosing, branching flow fields result; iii) transitional-mixed, a combination of TC- and CB-type suggestive of bimodal emplacement, perhaps sourced from coalesced shield volcanoes and flank fissures; and iv) foreset-bedded indicative of subaqueous lavas. The exposed rocks record the evolution of CGB volcanism through ten distinct eruptive episodes and intermittent lakes, with periods of quiescence characterized by the paleosol development. Whole-rock Ar-Ar dates were obtained; the duration of volcanism is calculated as  $1.28 \pm 0.61$  m.y. Emplacement is suggestive of shield volcanoes and small fissure eruptions with a northerly flow direction.

Laterally extensive paleosols, classified as Brunisolic soils, were examined closely and display a range of morphological features suggestive of the paleo-environment. Lateral variability amongst paleosols have been mapped over a distance of more than 8 km, including a subaqueous to subaerial transition.

# TABLE OF CONTENTS

<b>ABSTRACT.....</b>	<b>ii</b>
<b>TABLE OF CONTENTS.....</b>	<b>iv</b>
<b>LIST OF TABLES.....</b>	<b>vi</b>
<b>LIST OF FIGURES .....</b>	<b>vii</b>
<b>ACKNOWLEDGEMENTS .....</b>	<b>x</b>
<b>DEDICATION.....</b>	<b>xii</b>
<b>CO-AUTHORSHIP STATEMENT .....</b>	<b>xiii</b>
<b>1 OVERVIEW .....</b>	<b>1</b>
<b>1.1 – Statement of the Problem.....</b>	<b>1</b>
<b>1.2 – Organization of the Thesis .....</b>	<b>2</b>
<b>2 REGIONAL GEOLOGY .....</b>	<b>3</b>
<b>2.1 – Previous Work.....</b>	<b>3</b>
2.1.1 Nomenclature of rock types in the CGB .....	3
2.1.2 Thickness and styles of volcanism in the CGB .....	4
2.1.3 Aerial extent of the CGB .....	4
2.1.4 Regional mapping .....	6
2.1.5 Landslides.....	8
<b>2.2 – Detailed Geology at Chasm Provincial Park .....</b>	<b>10</b>
2.2.1 Cache Creek Group .....	12
2.2.2 Kamloops Group .....	12
2.2.3 Deadman River Formation .....	13
2.2.4 Chilcotin Group basalt .....	14
<b>3 CHILCOTIN VOLCANIC STRATIGRAPHY.....</b>	<b>15</b>
<b>3.1 – Facies Analysis.....</b>	<b>16</b>
3.1.1 Introduction .....	16
3.1.2 Methodology .....	17
<b>3.2 – Facies Descriptions.....</b>	<b>23</b>
3.2.1 Coherent facies.....	23
3.2.2 Clastic facies .....	25
3.2.3 Mineralogy .....	27
<b>3.3 – Facies Associations &amp; Interpretations.....</b>	<b>34</b>
3.3.1 Facies associations .....	34
3.3.2 Discussion.....	40
3.3.3 Geochronology .....	40

<b>4</b>	<b>PALEOSOL CLASSIFICATION .....</b>	<b>51</b>
4.1	<b>– Introduction.....</b>	<b>51</b>
4.1.1	Paleosol overview .....	52
4.2	<b>– Paleosol Profiles at Chasm .....</b>	<b>53</b>
4.2.1	Field methods .....	54
4.2.2	Horizon definition .....	68
4.2.3	Colour and thickness of horizons .....	68
4.2.4	Horizon boundaries .....	69
4.2.5	Results .....	76
4.3	<b>– Discussion.....</b>	<b>79</b>
4.3.1	Duration of hiatuses between lava flow flows.....	79
4.3.2	Soil maturity.....	82
4.3.3	Paleoclimate .....	83
4.3.4	Comparative studies .....	83
4.3.5	Soil geochemistry.....	85
4.4	<b>– Future Work .....</b>	<b>88</b>
<b>5</b>	<b>VOLCANIC FACIES ARCHITECTURE .....</b>	<b>90</b>
5.1	<b>– Introduction.....</b>	<b>90</b>
5.1.1	Methodology .....	91
5.1.2	Volcanic facies architecture.....	101
5.1.3	Stratigraphic analysis of Chasm lavas.....	104
5.2	<b>– Volcanic Interpretation.....</b>	<b>111</b>
5.2.1	Subaqueous to subaerial succession.....	111
5.2.2	Lateral mapping of the paleosols .....	113
5.2.3	Locating eruptive centre(s).....	116
5.2.4	Emplacement model at Chasm canyon .....	118
5.3	<b>– Implications for Regional Chilcotin Group .....</b>	<b>123</b>
	<b>REFERENCES.....</b>	<b>125</b>
	<b>APPENDICES .....</b>	<b>135</b>
	<b>APPENDIX A- Field Methodology.....</b>	<b>135</b>
	<b>APPENDIX B- Ar/Ar Sample Preparation.....</b>	<b>138</b>
	<b>APPENDIX C- Regional Geochronological Data (See Included CD).....</b>	<b>140</b>
	<b>APPENDIX D- Structure Data.....</b>	<b>142</b>
	<b>APPENDIX E- XRD Results.....</b>	<b>144</b>

## LIST OF TABLES

<i>Table 3.1: Volcanic and sedimentary facies of the Chilcotin Group in the Chasm study area.....</i>	<i>24</i>
<i>Table 3.2: Facies associations within the Chilcotin Group in the Chasm study area.....</i>	<i>33</i>
<i>Table 3.3: Chasm magnetic susceptibility data.....</i>	<i>39</i>
<i>Table 3.4: Chasm geochronology.....</i>	<i>48</i>
<i>Table 4.1: Paleosol samples from Station 069.....</i>	<i>61</i>
<i>Table 4.2: Paleosol samples from Station 070.....</i>	<i>62</i>
<i>Table 4.3: Paleosol samples from Station 071.....</i>	<i>63</i>
<i>Table 4.4: Micromorphological data.....</i>	<i>67</i>
<i>Table 4.5: Paleosol chemistry.....</i>	<i>86</i>
<i>Table 5.1: Architectural-type comparison to relevant volcanic provinces.....</i>	<i>119</i>
<i>Table C1: Regional geochronology.....</i>	<i>141</i>
<i>Table D1: Chasm structure measurements for map.....</i>	<i>143</i>
<i>Table E1: Results of qualitative analysis.....</i>	<i>146</i>

## LIST OF FIGURES

<i>Figure 2.1:</i> Simplified geological map of the southern Interior Plateau region.....	5
<i>Figure 2.2:</i> Chasm Provincial Park & vicinity geological map (1:20 000).....	7
<i>Figure 2.3:</i> Photo plate of basement rocks at Chasm Provincial Park.....	9
<i>Figure 2.4:</i> Photograph of 3 of the 4 rock formations in the canyon and a schematic vertical section summarizing the stratigraphy.....	11
<i>Figure 3.1:</i> Composite graphic log for eastern wall of the Chasm canyon.....	19
<i>Figure 3.2:</i> Composite graphic log for the western wall of the Chasm canyon.....	20
<i>Figure 3.3:</i> Photo plate of the lacustrine sandstone facies (lsS).....	28
<i>Figure 3.4:</i> Overview of petrographic observations at Chasm highlighting the younger lavas.....	29
<i>Figure 3.5:</i> Petrographic stratigraphic log for eastern main section.....	30
<i>Figure 3.6:</i> Magnetic susceptibility plots.....	37
<i>Figure 3.7:</i> Histogram of the magnetic susceptibility values for Chasm.....	38
<i>Figure 3.8:</i> Representative geochronology plots for Chasm (Plate 1).....	42
<i>Figure 3.9:</i> Representative geochronology plots for Chasm (Plate 2).....	43
<i>Figure 3.10:</i> Representative geochronology plots for Chasm (Plate 3).....	44
<i>Figure 3.11:</i> Representative geochronology plots for Chasm (Plate 4).....	45
<i>Figure 3.12:</i> Representative geochronology plots for Chasm (Plate 5).....	46
<i>Figure 3.13:</i> Representative geochronology plots for Chasm (Plate 6).....	47
<i>Figure 3.14:</i> Plot of the $^{40}\text{Ar}/^{39}\text{Ar}$ ages for Chasm and related CGB outcrops.....	50
<i>Figure 4.1:</i> Field photographs of paleosols exposed at Station 068.....	55
<i>Figure 4.2:</i> Field photographs of paleosols exposed at Station 069.....	56
<i>Figure 4.3:</i> Field photographs of paleosols exposed at Station 070.....	57

<b>Figure 4.4: Field photographs of paleosols exposed at Station 071.....</b>	<b>58</b>
<b>Figure 4.5: Paleosol profile for Station 069.....</b>	<b>59</b>
<b>Figure 4.6: Paleosol profile for Station 071.....</b>	<b>60</b>
<b>Figure 4.7: Summarizing the key soil micromorphology .....</b>	<b>71</b>
<b>Figure 4.8: Clay coating with fine laminations microphotograph.....</b>	<b>72</b>
<b>Figure 4.9: Station 069 micromorphology thin section plate.....</b>	<b>73</b>
<b>Figure 4.10: Station 070 micromorphology thin section plate.....</b>	<b>74</b>
<b>Figure 4.11: Station 071 micromorphology thin section plate.....</b>	<b>75</b>
<b>Figure 4.12: Duration of hiatuses between lava flows.....</b>	<b>80</b>
<b>Figure 5.1: Inset map showing lateral extents of the 3 cross section.....</b>	<b>92</b>
<b>Figure 5.2: Lookout photomosaic.....</b>	<b>93</b>
<b>Figure 5.3: Liden photomosaic.....</b>	<b>94</b>
<b>Figure 5.4: Eastern photomosaic.....</b>	<b>95</b>
<b>Figure 5.5: Generalized composite Chasm canyon stratigraphic log.....</b>	<b>97</b>
<b>Figure 5.6: Field photographs illustrating volcanic facies architecture.....</b>	<b>98</b>
<b>Figure 5.7: Photomosaic of a section of the western wall of Chasm canyon illustrating the irregular, non-linear geometry of the canyon wall.....</b>	<b>99</b>
<b>Figure 5.8: Detailed view of interpreted line-diagram of a section of the eastern wall illustrating the stratigraphic complexity of the paleosols.....</b>	<b>102</b>
<b>Figure 5.9: Paleosol truncates against a local paleo-topographic high formed by pre-existing lobe of lava.....</b>	<b>103</b>
<b>Figure 5.10: Schematic diagram illustrating the transition from the intact pillow basalt (ipB) and pillow-fragment breccia (pfB) facies transitioning into the paleosol (P) facies.....</b>	<b>108</b>



<b><i>Figure 5.11: Schematic representation of stratigraphic relationships in a portion of the western canyon wall.....</i></b>	<b><i>109</i></b>
<b><i>Figure 5.12: Field photograph and interpreted line-diagram showing the relationship between paleosol thickness and lava architecture.....</i></b>	<b><i>114</i></b>
<b><i>Figure 5.13: Emplacement model for Chasm canyon.....</i></b>	<b><i>117</i></b>
<b><i>Figure E1: X-ray diffractogram of sample 08REF030A02.....</i></b>	<b><i>147</i></b>
<b><i>Figure E2: X-ray diffractogram of sample 08REF034A01.....</i></b>	<b><i>148</i></b>
<b><i>Figure E3: X-ray diffractogram of sample 08REF030A01.....</i></b>	<b><i>149</i></b>
<b><i>Figure E4: X-ray diffractogram of sample RE-CH07-53.....</i></b>	<b><i>150</i></b>
<b><i>Figure E5: X-ray diffractogram of sample RE-CH07-58.....</i></b>	<b><i>151</i></b>

## ACKNOWLEDGEMENTS

This M.Sc. research was funded by the Targeted Geoscience Initiative- III Project (TGI-03), through the Geological Survey of Canada. Field costs were covered by Kelly Russell and the Geological Survey of Canada, courtesy of Bob Anderson. Geoscience BC contributed funding to the regional Chilcotin Project.

Firstly, thanks to my supervisor, Kelly, you were available and eager to discuss science nearly twenty-four hours of the day, I appreciated your knowledge, support and feedback while writing this thesis. I would like to thank my committee members, Bob Anderson, Kirstie Simpson and Jim Mortensen, for their time during many informative research discussions. I am grateful for their assistance and geological mentorship in the field, lab, and involvement in the Chasm map. I want to extend a special thanks to Paul Sanborn, for providing his time and soil science guidance for this thesis. I learned a great deal through the Chasm soil fieldwork, the Nazko trip, and your mentorship for my micromorphological study at UNBC. In addition, I want to thank the researchers, who were part of the regional Chilcotin project, Graham Andrews, Jackie Dohaney and Sarah Gordee for their collaboration. I want to thank Lucy Porritt for research discussions and her review of earlier drafts of the thesis. I want to thank Stephen Moss for this feedback on two of the chapters. Thank you Carol Wagner, Stephen Williams, Scott Smith, Brett Gilley, Arne Toma for technical and field support. Thank you Jenny Lai for the XRD work. Thank you to my field assistants: Nina Schwartzman, Ryan Emperingham, Agatha Soful, Emiliano Sepulveda, Mandy Tang and Nimmi Dhada. I want to thank the residents of Clinton, Chasm, Dog Creek and Canoe Creek, especially the Hancock family, John Grawhler, Gerhard and Florence Singer, Casa Blanca at 59 Mile, and Skookum Horse.

Thank you to the members of the VPL, past and present- Stephen, Nils, Jenny, Genevieve, Curtis, Jackie, Krista, Betsy, Shelley, and Chanone. So many off-the-cuff research discussions, daily encouragement, and friendship, I thank each of you!

Thank you to my family for their constant love and encouragement during my time in Vancouver- Dad, Anne, Hayley, Thomas, Melissa, Gigi and Pop-Pops. I will love each of you for the next 220 million years! I am utterly blessed.

And thank you to my friends for all of your support: Sandra, Channele, Julie, Emily, Silke, Jenny, Brian, Elspeth, Ines, Bram, Heather, Rosie, Lucy H., Lucy P., Emiliano, Julia, Sasha, Sarah, Erica, Jennifer Telford, Bin Lim, Heli McPhie, Laura Louie, Carolyne Abrams, Lindsay Stewart, Ailsa Le May, Keven Fitzpatrick, Brandon McNamee, Elsbeth Ruder, Emily Ferry, Steph Loetze, Emma Anderson, Ray Daniels, Ari, and the members of the VSSC.

## DEDICATION

*“If your Nerve, deny you-  
Go above your Nerve-”*

*Emily Dickinson  
(P292)*

## CO-AUTHORSHIP STATEMENT

This thesis comprises a published geological map, cross-sections, and portions of two Current Research publications make up parts of Chapters 2 and Chapter 3.

Figure 2.2 is the published geological map (January, 2010), titled 'Chasm Provincial Park & Vicinity' (scale 1:20 000). It holds a joint citation of 1) Geological Survey of Canada: Open File 6230, 2) Geoscience BC, Map 2009-16-1. I am the first author, and Dr. R.G. Anderson, Dr. K.A. Simpson, Dr. G.D.M. Andrews, and Dr. J.K. Russell are my co-authors. J. Mortensen reviewed the geochronological calculations. Field assistance (geological mapping, graphic logging, and cross-sections) has been provided by Dr. K.A. Simpson, Dr. G.D.M. Andrews and Dr. J.K. Russell.

Figures 5.2, 5.3, and 5.4 cross-sections are *in review* for publication with the Geological Survey of Canada, as an Open File and Geoscience BC map. The title is 'Bedrock cross-sections for Chasm Provincial Park.' I am the first author, and Dr. J.K. Russell and Dr. K.A. Simpson are my co-authors. All authors assisted in the field. I mapped the cross sections, and constructed the final digitized panoramas and interpreted line-diagrams. Dr. J.K. Russell was involved in the final review of the stratigraphic analysis of the Chasm lavas, and assisted in discussing the descriptive model used for the lateral mapping of the paleosols.

Portions of Chapter 2 and Chapter 3 have been published in a Geological Survey of Canada Current Research Paper 2008-13. I am first author, and Dr. K.A. Simpson, Dr. G.D.M. Andrews, Dr. J.K. Russell, and Dr. R.G. Anderson are my co-authors. All authors contributed edits during the review process to text and figures.

A portion of Chapter 3 has been published in a Geological Survey of Canada Current Research Paper 2007-A5. I am first author, and Dr. G.D.M. Andrews, Dr. J.K. Russell, and Dr. R.G. Anderson are co-authors. All authors contributed edits during the review process to text and figures.

## **CHAPTER 1      OVERVIEW**

---

### **1.1      STATEMENT OF THE PROBLEM**

The Chilcotin Group basalt (CGB) covers approximately 17, 000km<sup>2</sup> of the Intermontane Belt (Dohaney 2009) of British Columbia, Canada, and extends from Kamloops to Prince George. Previous work comprises reconnaissance and regional scale mapping and geochemistry (Tipper 1971; Bevier 1981). To date, there has been no descriptive physical volcanology of the CGB. The primary goal of this study is to provide descriptive or interpretive data on the physical volcanology studies of the CGB. Specifically, this study will examine the emplacement events in Chasm canyon, which exposes one of the thickest successions of the CGB.

The Chasm canyon is a late-glacial erosional feature exposing a 100 m thickness of the CGB including a series of sub-horizontal to gently dipping basalt lavas. Distinctive red, orange, or buff paleosols are commonly interstratified with the basalt lavas and are interpreted to represent periods of quiescence between volcanic episodes.

This study provides map, stratigraphic and facies details of the basaltic lavas and the paleosols at a variety of scales with the intent of reconstructing the volcanic events responsible for creating the basalt rocks in Chasm Canyon. Stratigraphic logging and analysis of field data helped to identify discrete lithological units, and divided them into separate volcanic facies i.e., units that share characteristic properties of mappable units (e.g., textures, geometry, lithology etc.). Mapping of the canyon walls helped discriminate between lavas, and correlate them from one wall of the canyon to another, thereby providing a spatial and temporal context for the stratigraphy. These data lead to an emplacement model for Chasm Canyon of the CGB consisting of a description and explanation of the facies architecture, and interpretations of the sub-aqueous to emergent succession eruption duration and style, and paleo-landscape in the canyon.

## **1.2 ORGANIZATION OF THESIS**

In addition to this introductory chapter, four additional chapters provide the following descriptions, data and interpretation.

Chapter 2 provides a systematic description of rock units in Chasm Canyon, expanding on summaries in a Geological Survey of Canada Current Research paper (Farrell et al. 2007). Data collection in the field and subsequent interpretations of the basement rocks at Chasm are compared to the geological descriptions from previous workers.

Chapter 3 describes the volcanic stratigraphy of the canyon, comprising coherent and clastic rocks that are divisible into separate facies. The Chilcotin Group basalt is characterized using mineralogy, magnetic susceptibility, and geochronology. This data is then correlated to the volcanic facies based on the descriptive physical volcanology of the units. The descriptions and spatial and temporal relationships of these facies allow interpretation of subaerial and subaqueous lava emplacement. Further associations are made based on geometry, morphology and textures of the lavas.

Chapter 4 is a field and laboratory study of the paleosols interstratified with the lavas within the canyon walls. Chasm paleosols are described in detail and separated into different horizons using soil profile logs. Thin section soil micromorphology is used to further characterize the soil.

In Chapters 5, a conceptual model for the emplacement of the basalt exposed in the Chasm Canyon is presented, using lateral mapping of the cliff exposures (Architectural Element Analysis). Architectural-type comparisons are compared to similarly-sized igneous provinces. The graphic logs (Chapters 2, 3) provide tests of the model and incorporate interpretations of the various textures of the lavas.

## **CHAPTER 2      REGIONAL GEOLOGY**

---

### **2.1      PREVIOUS WORK**

The Chilcotin Group basalt (CGB) constitute a volcanic field situated in the Intermontane Belt of south-central British Columbia. The CGB is expressed physiographically as a series of aerially extensive plateaus (e.g., Cariboo, Chilcotin, and Fraser) (Mathews 1991) that are incised by large rivers, and surrounded by higher topography underlain by basement rocks. Chasm canyon is situated on the southern margin of the Fraser Plateau, approximately 20 km north of the town of Clinton and 7 km east of Highway 97. Previous studies of the CGB involved mainly regional-scale mapping or geochemistry studies (e.g., Mathews 1963; Tipper 1978; Bevier 1983; Rouse and Mathews 1986; Matthews 1988; Read 1989; Dostal et al. 1996; Anderson et al. 2001). The CGB are transitional basalts (Bevier 1982; Dohaney 2009), which imply olivine-normative basalts with either hypersthene or nepheline-normative.

#### **2.1.1 Nomenclature of rock types in the CGB**

The earliest description of the CGB lavas noted them as ‘flat-lying basalt lavas’ (Dawson 1879; 1895). The ‘Chilcotin Basalts’ were named by Tipper (1978) and included the basaltic lavas and the underlying sedimentary units in terms of color, rock type, general mineralogy and common structures such as columnar joints. The ‘Chilcotin Basalts’ were then formally defined as a mappable rock unit by Matthews (1988). The extent is specified as ranging from the Okanagan Highlands to the Nechako Plateau, but does not include the Anahim belt (Bevier, 1979) ‘valley basalts’ (Matthews, 1964). Matthews (1964) described the basalts as ‘plateau basalt,’ (Farquharson and Stipp, 1969), although previously the name ‘plateau lavas’ had been used (Rice, 1947). In the Chasm study area, Read (1989b) used the term ‘Chasm Formation,’ to describe the CGB basalts in the canyon.



### **2.1.2 Thickness and styles of volcanism in the CGB**

Recent work has indicated that the thickness of the CGB (Andrews and Russell 2007, 2008; Mihalynuk 2007) and the styles of volcanism (Gordee et al. 2007; Farrell et al. 2007; Farrell et al. 2008) vary significantly. The CGB is spatially and temporally complex, rather than being a relatively homogeneous sheet, yielding locally unique exposures. Bevier (1982) interpreted that the CGB and the Columbia River Flood Basalts (CRFB) are different volcanic fields and furthermore describes the CGB as 'basaltic plains volcanism' (Greeley 1977), where there are numerous overlapping shield volcanoes that result in a lava plateau. Matthews (1988) described the CGB as significantly smaller in scale than the CRFB, and can be characterized by a single lava in some exposures (i.e., many small scale outcrops), or a stacked succession of lavas, typically less than 100 meters thick. Bevier (1982, 1983) and Matthews (1988) used K-Ar (whole rock) geochronology to identify distinctive eruptive pulses of volcanism. The nature of the bedrock, underlying the CGB is unknown except where exposed in small basement windows. The CGB is typically overlain by thick (>15 m) Pleistocene glacial deposits that are best exposed along valleys and canyons walls such as found at Chasm canyon.

### **2.1.3 Aerial extent of the CGB**

CGB had been considered to have an aerial distribution of ~ 25,000 km<sup>2</sup> (Mathews 1988). Previous work indicated the aerial extent of the CGB map region to be ~55,000 km<sup>2</sup> (Bevier 1981). The aerial extent has recently been recalculated using new compilations (NTS- map sheets: 92O and 92P) and GIS modeling to indicate a significantly decreased area of ~17,000 km<sup>2</sup> (Dohaney 2009). Variations in the estimated areal extent of the CGB may be explained by several factors. First, variations in the aerial extent and volume are primarily due to the scale of mapping of the CGB (reconnaissance-scale vs. detailed scale). Second, the interpretations of different mappers in identifying the geologic boundaries of the CGB may lead to significant variations in the mapped areal extent (pers.

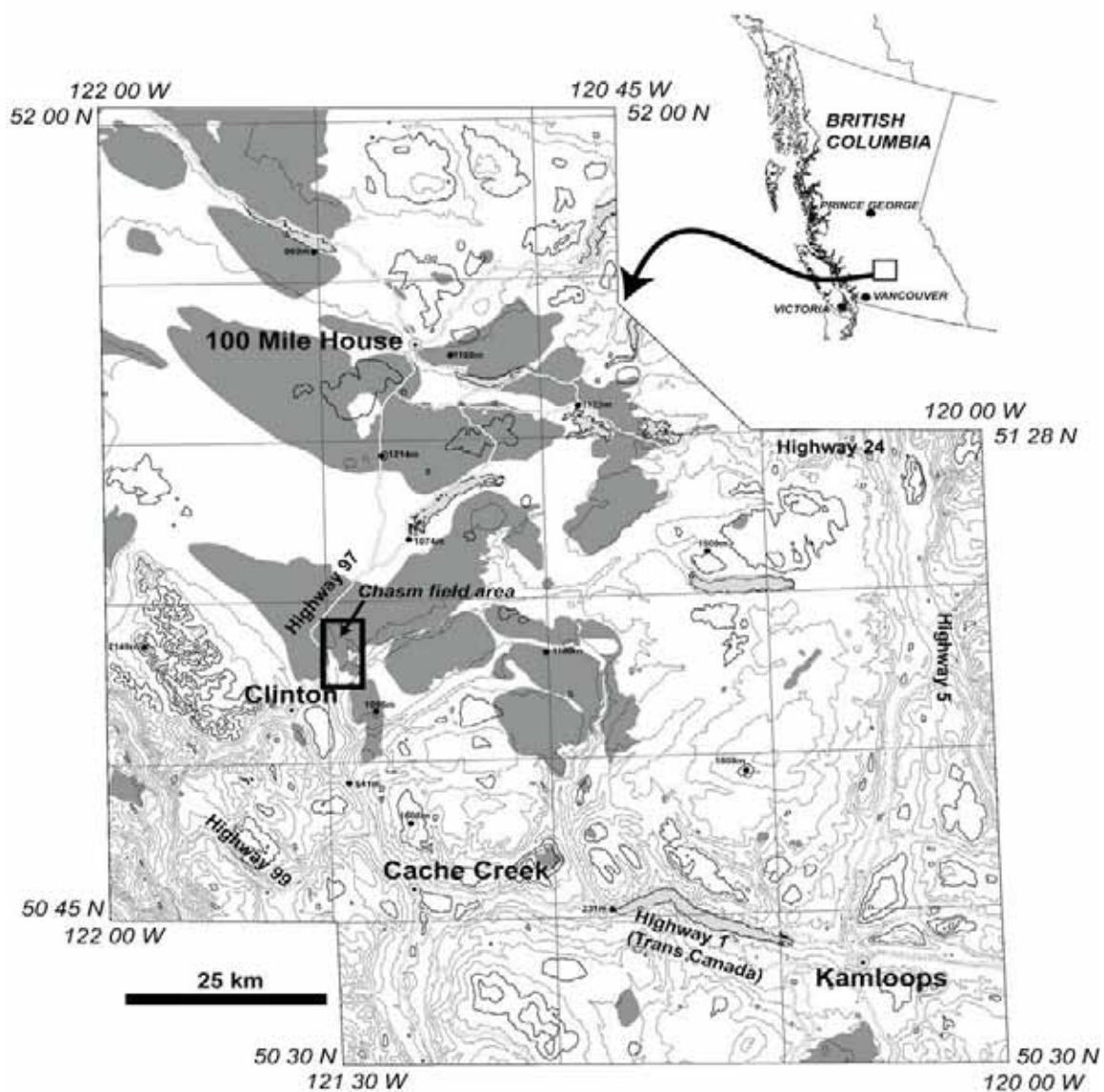


**Figure 2.1:** Simplified geological map of the southern Interior Plateau region, including the Chasm study area (outlined). The distribution of the Chilcotin Group basalt is represented in dark grey, and delineates an areal extent of 17, 000 km<sup>2</sup> (Dohaney, 2009).

comm. Dohaney 2009). Moreover, the discrepancies between what defines the CGB (e.g. basalts or basalts and underlying sediments etc), and the varying ages of the basalts has created confusion among researchers mapping the CGB lavas. Previously, the total volume of the CGB was reported to be  $\sim 3,500 \text{ km}^3$  (Bevier 1983; Matthews 1988), however the most recent volume estimate is  $6,000 \text{ km}^3$  (Dohaney 2009). To date, the vents or volcanic source points of the CGB are unknown. However plutonic plugs (e.g., Mount Begbie; gabbroic plug closest to study area) are interpreted to be the remnants of the source for at least some of the CGB volcanism (Farquaharson and Stipp 1969; Bevier 1982; Matthews 1988). Complex volcanism is inferred to exist (Matthews, 1988) because of, a) regional evidence of multiple flow directions of the lava recorded in the foreset-bedded breccias, indicative of smaller-scale flows instead of one large outpour (i.e., flood volcanism), and b) the age span of Chilcotin Group basalts is wide-ranging (38.3-1 Ma; Dohaney 2009), which may suggest multiple eruptive centres or long-lived volcanism emanating from one source point.

The study site is located within Chasm Provincial Park (NTS 092P/03; Bonaparte Lake). It is situated on the Interior Plateau, approximately twenty kilometers north of the town of Clinton and seven kilometers east of Highway 97 (Fig. 2.1). The Chasm Provincial Park contains an approximately 8 km long canyon; the canyon is approximately 300 m deep and ranges in width from 500-3000 m (Fig. 2.2). The walls of Chasm canyon expose lavas. The extreme southern end of the canyon exposes the Miocene Deadman Formation underlying the CGB. The Chasm canyon is a notch-like valley, and the shape of the canyon is due to a glacial to post-glacial outburst flooding event (Read 1991; Plouffe 2001). The incision of the canyon occurred with the retreat of the glacier during the Fraser glaciation (Fulton 1969, 1975; Plouffe 2001).

**Figure 2.2:** Chasm Provincial Park and vicinity geological map (scale: 1:20 000) (Farrell et al. 2010). The map provides the distribution of geological units, location of graphic logs, georeferenced magnetic susceptibility data, geochronology sample locations, and location of mineral deposits. Actual figure available at the UBC Library or online at The Geological Survey of Canada ([http://geopub.nrcan.gc.ca/index\\_e.php](http://geopub.nrcan.gc.ca/index_e.php))

#### **2.1.4 Regional mapping**

The most recent geological map covering the Chasm area is the 1: 250, 000 Bonaparte map sheet (NTS map 092P) of Campbell and Tipper (1965). Bedrock exposure is poor but includes rocks ranging in age from late Precambrian to Neogene.

The first general regional stratigraphy, petrological descriptions and K-Ar ages for the CGB derives from Bevier (1982). Bevier's type-localities for the CGB included Bull Canyon, Dog Creek, Cardiff Mountain and Deadman River. Typical stratigraphic sections of the CGB comprised basaltic lava, pillow lavas, and tephra. Although the lavas could not be traced laterally, correlations between areas were undertaken using similar chemical compositions, magnetic susceptibility, and physical attributes of the lavas. Bevier also included the Chasm Canyon in her studies, although it was not one of her type sections.

At Chasm canyon, Bevier (1982) defined the minimum thickness of the lavas to be 69.1 meters, consisting of at least 11 separate lava units characterized by horizontal vesicle sheets, vertical vesicle chimneys and the presence of zeolites were noted in the amygdalites (Bevier 1982; Read 1989). No subaqueous facies were recognized. There have been no isotope age dates available for the Chasm area; however, north of the Provincial Park, at Fifty-Seven Mile, on the east side of the Highway 97. There is one K-Ar age of  $9.02 \pm 0.4$  Ma (Matthews 1988; Fig. 2.2, Table 2).

#### **2.1.5 Landslides**

Evans (1983) described three landslide complexes in Chasm canyon (Chasm West Landslide complex, Chasm East Landslide complex, and the North Landslide complex). The North landslide complex is the most recent slope failure and is located near the nick point/apex of the canyon. The East and West complexes are located where the valley widens (Fig. 2.2). Each landslide deposit consists of an upper resistant cap of rock and softer underlying units, constituting a 'block-type' landslide (Evans 1983). The underlying softer units for the West Landslide complex were not described, but are inferred to be



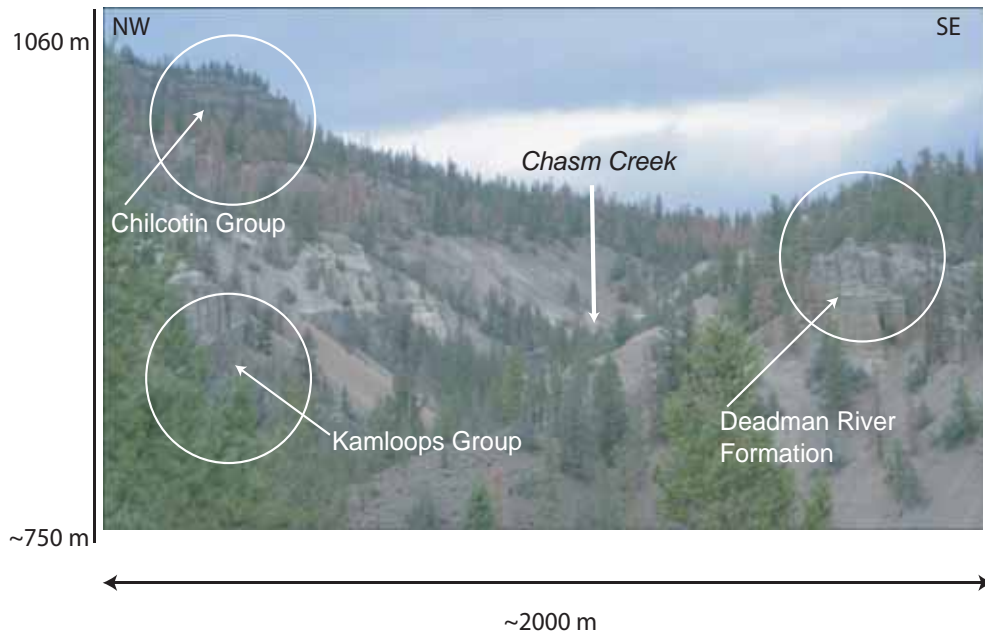


**Figure 2.3:** a) Small-scale folds in the Cache Creek Group phyllite. b) Kamloops Group, part of the Skull Hill formation. c) Bedded volcaniclastic sandstone and breccia, which are a part of the Deadman River formation. d) Angular to subangular clasts belonging to the Skull Hill formation (andesite?) in a breccia bed within the Deadman River formation. e) Imbricated angular clasts in a breccia layer within the Deadman River formation indicating a northwesterly transport direction. View is to the southeast. Pen for scale is 9 cm.

clastic units derived from a pillow fragment breccia succession. The Deadman River Formation sedimentary rocks are inferred to be the 'softer units' in the East Landslide Complex. Evans (1983) interpreted that the erosional processes of Chasm creek are not substantitive enough to produce large slope failures. Instead, Evans (1983) interpreted the landslides are a result of multiple failure events and is on-going to the present-day. The slumped basalt blocks mapped on Fig. 2.2 are rotated blocks associated with these landslide processes. The landslide complexes have not been dated, however field evidence suggests they occurred post-glacially (Evans 1983). Evans (1983) speculated that the first landslides in the canyon occurred approximately 8,200 years ago and began near the completion of the 'stress-relief phase', meaning after the canyon had been incised and erosional processes had begun to take affect. Slope failure is an ongoing process in the Chasm canyon, and contributes to the overall weathering and erosional processes taking place in the canyon. The evolution of the canyon landscape, including the landslide events, is important to understand as it provides the context for mapping the rock units. The exposures as a result of the current canyon landscape allow for detailed description and interpretation of the CGB lavas and the interpretation of the paleo-landscape conditions at the time of emplacement of the lavas.

## **2.2 DETAILED GEOLOGY AT CHASM PROVINCIAL PARK**

Detailed field studies in 2006 -2008 focused on CGB rocks that overlie a varied basement sequence of Cache Creek Formation, Kamloops Group and Deadman River Formation rocks (Fig. 2.3). The stratigraphic section, and in particular the CGB units, are exposed in the walls of Chasm Canyon (Fig. 2.4). Four stratigraphic units, the Chilcotin Group, Deadman River Formation, Kamloops Group, and Cache Creek Group, were mapped within the Chasm study area. There are no exposed contacts between the CGB and the underlying basement rocks.



## Generalized Vertical Section

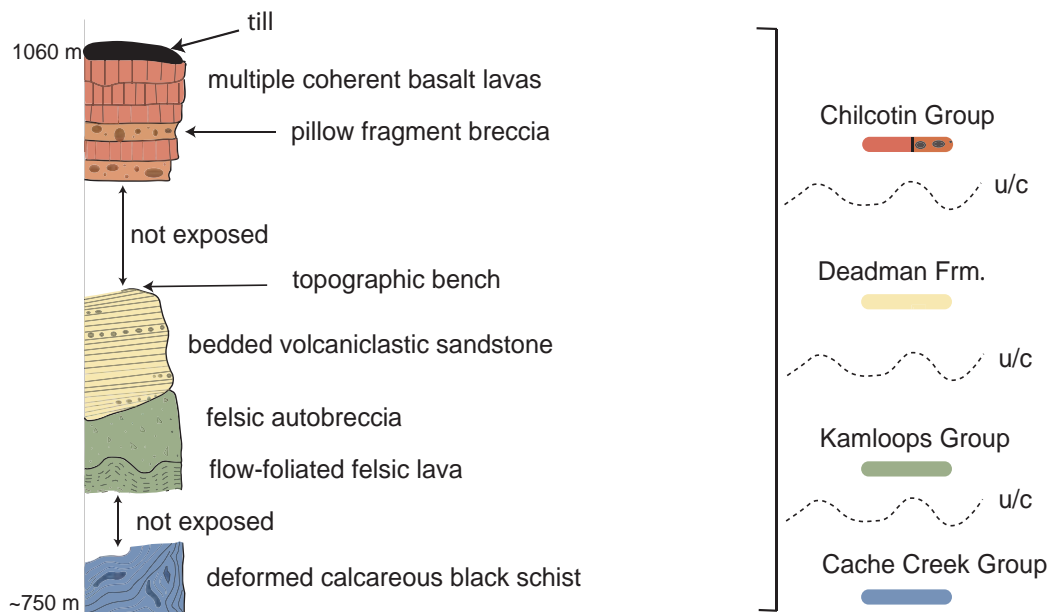


**Figure 2.4:** a) View looking north along Chasm Creek to three of the four rock formations present in the canyon. b) Schematic generalized vertical section summarizing the stratigraphy present in the Chasm study area. Unconformities are labeled u/c. Elevations represent the y-axes.



### **2.2.1 Cache Creek Group**

Campbell and Tipper (1965) described the Cache Creek Group in the Chasm as a collection of greenstones, argillites, cherts and limestones. Near the study area, the rocks are typically deformed and sheared. Brachiopods and fusulinids were used to infer a Permian age for the rocks.

Three outcrops of the Permian Cache Creek Group are located along Fifty-Seven Mile Creek (Figs. 3, 4), consisting of strongly folded calcareous phyllites (Fig. 3). These rocks are locally unconformably overlain by rocks assigned to the Deadman River Formation. The Chasm Canyon area is considered to be the western extent of the Cache Creek Group (Campbell and Tipper 1965).

### **2.2.2 Kamloops Group**

The Eocene Kamloops Group is subdivided into two formations, the Chu Chua Formation and the Skull Hill Formation (Uglow 1922; Cockfield 1948; Mathews and Rouse 1961, 1963). The Chu Chua Formation is a sedimentary succession consisting of conglomerates, arkoses and shales with coal seams. The Skull Hill Formation consists of coarse, unsorted volcanic breccias, and dacite, trachyte, basalt, andesite, and rhyolite lavas and associated flow breccias (Campbell and Tipper 1965). Loon Lake, is the type locality for the Skull Hill Formation. Lavas range in colour, and are typically vesicular. The thickness of the lavas can be up to 14 meters, however generally the outcrops are isolated remnants and the geometry of the lavas cannot be determined. The Kamloops Group is undated in the study area.

Rocks tentatively assigned to the Skull Hill Formation of the Eocene Kamloops Group are exposed discontinuously along 3 km of Sixty-One Mile Creek and Chasm Creek (Fig. 2.2). The exposed thickness of the Skull Hill Formation in this area ranges from 3-60 m. At the junction of Chasm Creek and the Bonaparte River, the Kamloops Group is unconformably overlain by the Deadman River Formation (Fig. 2.4). Two associated rock

units were observed (Fig. 2.3b); the first unit is a red-brown, plagioclase-phyric, coherent andesite with trachytic texture (Fig. 2.3). Flattened vesicles are aligned parallel to the small (>1 mm) plagioclase phenocrysts. The second unit is a monomict volcanic breccia that conformably overlies unit 1 and consists of clasts of trachyte. Collectively the two units are interpreted as the coherent and autobrecciated components of a single lava.

### **2.2.3 Deadman River Formation**

The Deadman River Formation as defined by Campbell and Tipper (1965) and Read (1989) consists of cream-colored to brown tuffs, breccias, diatomites, siltstones, arenites and conglomerates and are interpreted to have been deposited in a fluvio-lacustrine environment. The type locality is on the eastern shore of Skookum Lake in the Deadman River Valley. Within Chasm Provincial Park, Campbell and Tipper (1965) identified three ‘possible’ exposures of Deadman River Formation, with the best outcrop located at the junction of Chasm Creek and the Bonaparte River although it is dissimilar to rocks in the type-section (Campbell and Tipper 1965). Sandstones and breccias were mapped by Campbell and Tipper (1965), and interpreted to have been deposited as flat-lying units. The present bedding dips are attributed to post-depositional slumping, compaction from the overlying CGB basalts, or draping of paleotopography. The thickness of the Deadman River Formation varies considerably from centimeters to a maximum thickness of ~150 meters. The Deadman River Formation (DRF) is undated, however the formation is inferred to be late Miocene based on regional correlations (Matthews and Rouse 1986).

The main exposures of the Deadman River Formation occur along Chasm Creek, at the junction of Chasm Creek with the Bonaparte River and north of Rickett’s Ranch (Figs. 2.2 and 2.3). Thin (<5 m thick) limited exposures are structurally above the Cache Creek Group in Fifty-Seven Mile Creek. The cliff forming exposure (Fig. 2.3c) is underlain by cream-colored sandstones and bedded volcanic breccias. Breccia clasts, in a sand-sized matrix, are dominantly angular to subangular and imbricated (Figs. 2.3d and 2.3e). Three

distinct clast size populations are present (mean sizes = 39.1 cm, 8.6 cm, and 1.1 cm; Fig 2.3). Clast imbrication indicates a northwesterly transport direction (Fig. 2.3e), and the angularity of the clasts suggests minimal transport from their source.

#### **2.2.4 Chilcotin Group basalt**

The Chasm area is host to one of the best-known and thickest exposures of the CGB and for this reason was selected for the current detailed study. Cliff-forming exposures occur continuously for 8 km along Chasm Creek, but away from the canyon walls exposures are limited (Fig. 2.2). The width of the canyon varies between 500 m and 3000 m. The canyon is approximately 300 m in depth. The Chasm lavas are considered a stacked succession of basalt (Mathews 1988), of variable thickness, however, the total succession is typically less than 100 m, indicative of a relatively minor succession. The CGB lavas dominate the landscape and bedrock geology in the canyon.

In the study area, the CGB is estimated to be approximately 140 m thick. The CGB is divided into seven distinctive volcanic facies, (described in Chapter 3) and include:

1) basaltic pahoehoe lava comprising vesicular/amygdaloidal pahoehoe lobes (vlB), 2) aphyric, columnar-jointed and sheet-like basalt lava (acB), 3) dominantly intact basaltic pillow lava (ipB), 4) fine-grained paleosols (P), 5) pillow-fragment breccia (pfB), 6) rare hyaloclastite (hB) and 7) lacustrine sandstone (lsS) (Figs. 3.1 and 3.2).

## **CHAPTER 3      CHILCOTIN VOLCANIC STRATIGRAPHY**

---

In this chapter, the key physical volcanological characteristics of the CGB at Chasm are introduced, including: i) a general field description; ii) facies analysis; and iii) delineation of seven discrete facies. Recent research on the CGB has resulted in a significant database of information such as magnetic susceptibility, porosity, density, and conductivity (Dohaney 2009; Andrews 2008; Farrell et al. 2008; Farrell et al. 2007).

Facies analysis is an effective method in understanding volcanic stratigraphy (McPhie and Allen 1992; Jerram 2002), and has been used in this research to complement the existing CGB database in order to understand the volcanism in the Chasm canyon. Historically, facies analysis is used in sedimentary basin analysis where the assigned facies are directly linked to a depositional environment. This is the routinely used method in sequence stratigraphy (Walker 1984; Miall 2000). There are key differences to the analysis for volcanic stratigraphy, such as a de-emphasis of the depositional setting, and a greater attention to emplacement processes (McPhie 1992, 1993; McPhie 1993). Facies and facies associations are used for understanding the style of eruptive, transport, and emplacement processes and proximity to source which collectively make up the volcanic facies architecture of a given area.

The defined facies include: 1) basaltic pahoehoe lava comprising vesicular/amgdaloidal pahoehoe lobes (vLB); 2) aphyric columnar-jointed and sheet-like basalt lava (acB); 3) fine-grained red coloured paleosols (P); 4) intact pillow lava (ipB); 5) pillow-fragment breccia (pfB); 6) hyaloclastite (hB); and 7) lacustrine sandstone facies (lsS). Within the established facies framework, next the magnetic susceptibility, chemistry and geochronology of the basalt facies are reported and interpreted. The volcanic facies architecture and evolution of the stratigraphy at Chasm is presented in Chapter 5.

### **3.1 FACIES ANALYSIS**

In this section, facies analysis methods as described by Cas and Wright (1995) are applied to Chasm sections. The principal goal of facies analysis is to understand the emplacement events at Chasm canyon, and provide evidence for the location for one or multiple eruptive centres.

#### **3.1.1 Introduction**

The principal goal of facies analysis is to identify features that allow for interpretation of eruption style, transport, and depositional processes, depositional environments, proximity to vent and timing with respect to major eruptions. The definition of facies used for this study is a grouping of rocks, which are interpreted to have formed (i.e., ‘emplaced’ etc., for volcanic rocks) under similar conditions (Miall 2000). Volcanic stratigraphy, facies analysis and architecture are used in relatively young volcanic successions such as Large Igneous Provinces (LIPS) (Mangan 1986; Self et al. 1996; Self et al. 1997; Hooper 1997; Jerram et al. 1999; Jerram 2002; Jerram and Widdowson, 2004; Bondre et al. 2004; Passey and Bell 2007; Elliot and Fleming 2008), and ancient volcanic successions (Cas et al. 1989; McPhie and Allen 1992; Paulick and McPhie 1999; Simpson and McPhie 2000; Moore et al. 2000).

To clarify, a flood basalt is a subcategory of a LIPS, which consist of thick basaltic lavas with an areal extent greater than 130,000 km<sup>2</sup> and volume greater than 80,000 km<sup>3</sup> (Tyrell, 1937; Jerram and Widdowson, 2004). For definitive purposes, LIPS can either be extrusive or intrusive, mafic to silicic in composition, and continental or oceanic (Jerram and Widdowson, 2004). Jerram (2002) emphasized the need of defining facies in order to understand flood basalt architecture. He hypothesizes whether or not a repeatable sequence can be observed in emplacement scenarios between different flood basalts. The CGB is significantly smaller in size when compared to a flood basalt province (e.g., CBG covers 17,000 km<sup>2</sup> with a volume of 6,000 km<sup>3</sup> in south-central British Columbia (Dohaney 2009)),

however the physical volcanology can be comparable in many instances. In particular, the Chasm Canyon, is approximately 8 km in length, ranging from 500 to 3000 m in width, and 300 m deep, hosting a diverse suite of facies symbolic of a range of emplacement events and processes, which will be discussed towards the end of this chapter.

### **3.1.2 Methodology**

The methodology used in this study can be broken into six stages, each of which are described below.

#### ***Stage 1: Geological Map 1: 20 000 scale***

A detailed geological map of the Chasm Canyon at a 1: 20 000 scale was prepared (Fig. 2.2; Farrell et al. 2010). Detailed field studies in 2006-2008 focused on the CGB, which overlie a varied basement sequence of Cache Creek Formation, Kamloops Group, and Deadman River Formation rocks (Fig. 2.4). The CGB are exposed in the walls of the Chasm Creek canyon.

Mapping provides the framework for the study. At this scale, the canyon was traversed on foot, mapping by hand using a printed digital base map from Terrain Resource Information Management Program (TRIM). Global Positioning System (GPS) data was received using a PDA (Personal Digital Assistant) supplied by the Geological Survey of Canada. The PDA uses the Ganfeld operating system, which digitally stores all stations, samples, field photographs, and field notes, all of which are geo-referenced simultaneously. There are no roads into Chasm Canyon; however, there are two tracks that permit access. The first access route is from the northern end of the canyon beginning at the Chasm Provincial Park Lookout site, using a track that runs parallel to the eastern canyon wall. The alternative is using a private track, owned by Mr. John Grawhler, which allows for a south-west starting point for traversing (Fig. 2.2). Stages 1 through 3 occur simultaneously.

### ***Stage 2: Structure at Chasm***

There are no observed faults in the Chasm canyon. Post-depositional slumping and landslides are observed in places along the canyon walls. They have displaced stratigraphic packages downslope, therefore the slumped blocks founded in the canyon (not on cliffs) are not in-situ (Evans 1983). The only geological instability in the canyon is due to landslides, beginning in 8,200 B.P. and there is continued slip in the present time (Evans 1983). The CGB lavas are sub-horizontal (dip  $<3^\circ$ ), and from the Chasm Lookout, the lavas dip to the NE towards the head of the canyon. Approximately, 1 km downstream from the head of the canyon, is a lava package that thickens to the NW, has a wedge-like morphology and is interpreted to be in-situ.

Structural data of the CGB also includes bedding orientations from pillow lobes, and bedding measurements in the Deadman River Formation (Fig. 2.2 and Appendix D).

### ***Stage 3: Identifying Facies***

Detailed graphic logging as outlined in McPhie et al. (1993) was undertaken along the canyon walls to produce two main composite graphic logs. The composite graphic log along the eastern wall, covers a lateral distance of approximately 950 m (Fig. 3.1) and the composite graphic log for the western wall of the canyon, covers a lateral distance of approximately 1060 m (Fig. 3.2). The extent of each of the graphic log can be seen on the map (Fig. 2.2). A combination of both symbology (McPhie et al. 1993) and line drawing was used to illustrate the textures and structure present in the cliff outcrops. The majority of the legend associated with the logs was created specifically for the features found at Chasm, aiming for accuracy and precision.

Sampling was conducted simultaneously with graphic logging as well as from additional exposures within the canyon, from outcrops along Highway 97 and from basement exposures. In the East and West composite graphic logs, all coherent lavas were sampled. Clastic rocks were sampled with discretion such as pillows, pillow rinds, the

## Chasm East Composite Log

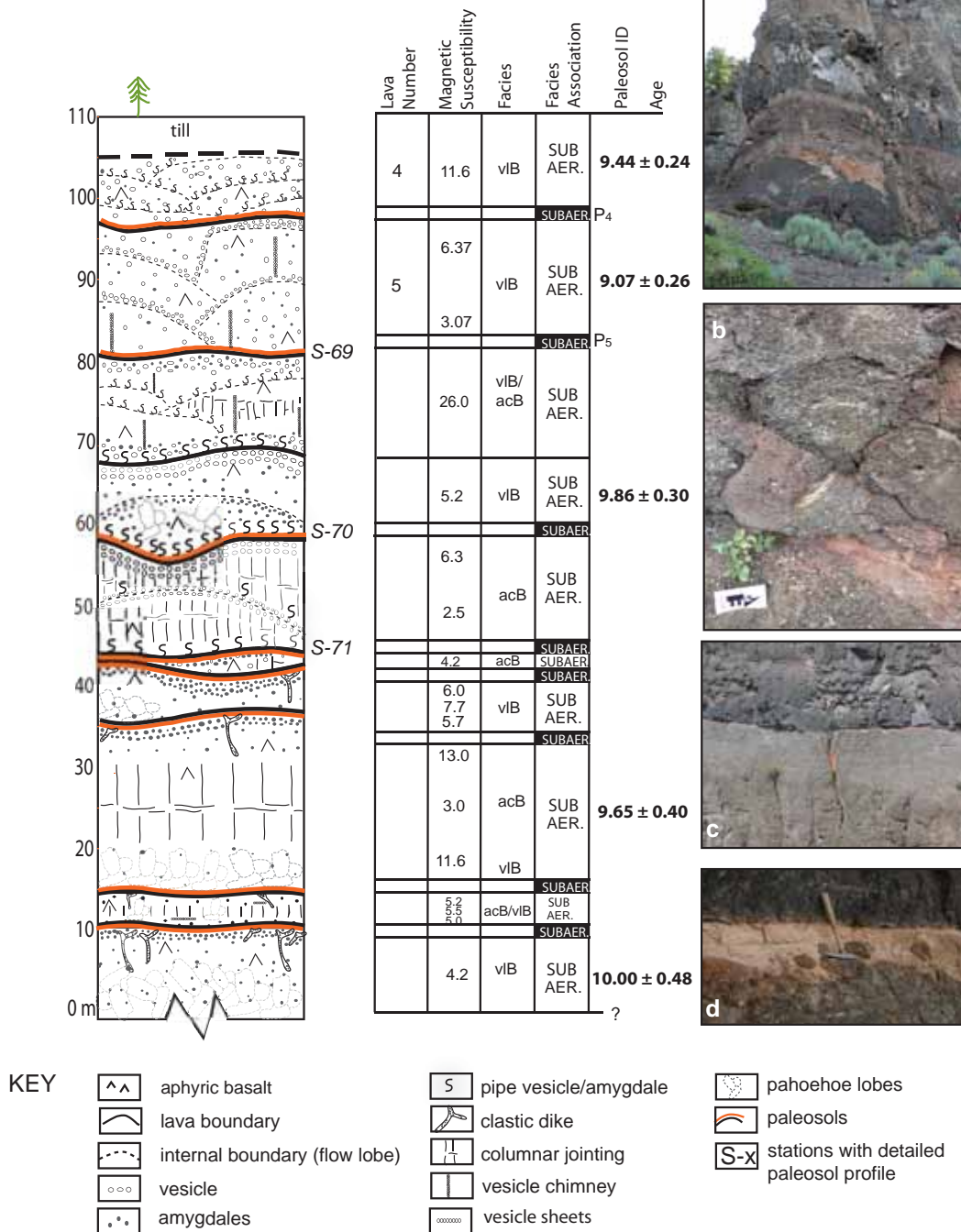


**Fig. 3.1:** Composite graphic log for eastern wall of the Chasm canyon. Lateral distance covered is approximately 950 m. Representative field photographs of major units, including: a) oblique view of representative section (~30 m in height), b) amygdaloidal pahoe-hoe lobes (vlB), c) clastic dike in top lava (acB) and below paleosol (P), d) paleosol (P) with basaltic core stones (~30 cm long rock hammer for scale). Photograph courtesy of Paul Sanborn. Magnetic susceptibility values in 10<sup>-3</sup> SI units.



**Figure 3.2:** Composite graphic log for western wall of the Chasm canyon. Lateral distance covered is approximately 1060 m. The horizontal axis on the graphic log represents the average grain size. Coherent units are illustrated by symbols only and are drawn to the maximum grain size as outlined in McPhie et al (1993). The grain size for units containing variably sized pillow-fragments in a finer-grained matrix was calculated using the average size of the smallest pillow fragments. Intact pillow lobes and larger pillow fragments (> 64 mm) are shown schematically and protrude outside the log where they are abundant within a unit.

Representative field photographs of major units: a) Typical exposure of western log section. Person for scale (~170 cm), b) Upper lava (acB) with vesicle chimneys underlain by pillow lava (ipB) with dipping pillows to the SE. Hammer for scale ~40 cm, c) Pillow lava with prismatic jointing and tiny normal joints. Hammer for scale is ~40 cm, d) Pillow fragment and associated breccia (pfB). Pencil is 14.5 cm long, e) Smaller-sized pillow fragments and breccia (pfB). Pencil is 14.5cm, f) Large pipe amygdaloides and pahoehoe ropes (vlB), g) Vesicle sheets. Hammer for scale ~40 cm. h) Large Pahoehoe rope (vlB), i) Cross-section through amygdaloidal lobes (vlB). Pencil is 14.5cm. Actual figure available at UBC Library.

interstitial material between the pillow fragments, and the matrix of the unit. Observations were made with a hand-lens, and discrete protocol (Cas et al. 2008) followed for coherent and clastic rocks. An abbreviated outline of the method is listed below:

*Coherent rocks (lavas, intrusions)*

- 1) Porphyritic or aphyric/aphanitic
- 2) If porphyritic: note a) crystals (phenocrysts or xenocrysts), b) groundmass, c) xenoliths
- 3) If aphyric/aphanitic: note a) xenoliths (cognate or exotic), b) groundmass (uniform, clastogenic, segregationary or vesicular/amygdaloidal)
- 4) For porphyritic and aphyric: determine a) textures, b) contacts, c) geometry (outcrop-scale), and d) colour

*Clastic rocks (fragmental)*

- 1) Clasts/fragments or interstitial medium
- 2) Clasts/fragments (free crystals, juvenile clasts, lithic clasts)
- 3) Interstitial medium (clastic matrix, primary cement, alteration minerals)
- 4) Geometry, shape, texture, composition

All samples are found in the regional CGB database (Dohaney 2009), along with stratigraphic reference, and any analyses undertaken on the samples (geochronology, geochemistry, or any physical property measurements. Detailed observations resulted in the identification of 7 facies (Table 3.1), which are described in section 3.2.

***Petrography***

Petrographic analysis was undertaken on eighteen coherent rock samples in the eastern composite log, and vicinity. In addition, paleosol samples, from stations 069, 070, and 071, were analysed. Paleosols are discussed in detail in Chapter 4.

#### ***Stage 4: Age relationships of the facies***

Geochronological sampling was focused on the Eastern Composite Log and highway locations north of the Chasm canyon (Table 3.4). Other areas of the canyon were also sampled (Fig. 2.2) and are stratigraphically referenced by using cross-sectional mapping, which is discussed in Chapter 5 (Figs. 5.2, 5.3, 5.4). The goal of the geochronostratigraphy is to understand the age relationships between the facies in the Eastern Composite log, and the overall age relationships in the entire canyon, which contributes to the emplacement model discussed in Chapter 5.

#### ***Stage 5: Facies Associations***

The grouping of facies together into facies associations is based on any of the following components: a) the geometry or thickness of the facies; b) lateral continuity and shape of the rock units; c) rock types; or d) sedimentary structures (McPhie 1992). For Chasm, the facies associations allow for the interpretation of the lavas, where the rock types (coherent and clastic) and the environment of final deposition as well as emplacement style are considered. The facies associations are Chilcotin Group-Subaerial (Mcb1) or Chilcotin Group-undivided sub-aqueous and subaerial (Mcb2) (Table 3.2). This distinction is emphasized by colour on the map (Fig. 2.2), where the south-west exposure of the CGB in the canyon to be Mcb2 is shown in light blue and the Mcb1 in green. Refer to Table 3.1, for the descriptive data on the individual facies.

#### ***Stage 6: Facies Architecture***

The final step in facies analysis at Chasm is determining the facies architecture, which is discussed in Chapter 5. At Chasm, mapped cross-sections of the length of the canyon walls were drafted, followed by mapping on these sections using a modified (volcanology focused) method of Architectural Element Analysis (AEA) outlined in Miall

(2000). Sequence stratigraphy was not attempted for this study due to accessibility of the vertical cliffs. The data obtained from the facies analysis yields the framework for a descriptive emplacement model, with preliminary interpretations regarding the eruptive centre(s).

### **3.2 FACIES DESCRIPTIONS**

Coherent and clastic facies were mapped at Chasm. The three coherent facies are vesicular basaltic pahoehoe lobe facies (vLB), aphyric columnar-jointed basalt facies (acB), and intact pillow lava facies (ipB). The four clastic facies are fine-grained paleosol facies (P), pillow-fragment breccia facies (pfB), hyaloclastite facies (hB) and lacustrine sandstone facies (lsS). Refer to graphic logs (Fig. 3.1 and 3.2) for photographs of facies and the facies sequence for each log. Table 3.1 summarizes the facies.

#### **3.2.1 Coherent facies**

##### ***Vesicular basaltic pahoehoe lobe facies (vLB)***

The dominant facies is 'vLB,' and consists of aphyric, vesicular (and/or amygdaloidal) pahoehoe lobe lavas (Fig. 3.2, photo i). Lavas are poorly (20-40%) vesicular. Vesicles are randomly distributed and pipe vesicles (average height of 10 cm) commonly occur at lobe contacts and help to differentiate them. Vesicles are <1 mm in size and amygdaloidal with infillings of zeolites, specifically phillipsite-K and chabazite-Ca (Appendix E). Pahoehoe ropes and wrinkled textures are common. Colours of vLB lavas range from dark grey (fresh) to maroon (weathered). Single pahoehoe lobes range from 6 cm-3 meters across and overlap one another resulting in lava units approximately 2-10 m thick. The lobe shapes vary significantly, ranging from bulbous ellipses to elongated thin flow lobes. Typically, the contacts between the vLB and other facies are concordant and sharp or irregular.

**Table 3.1:** Volcanic and Sedimentary facies of the Chilcotin Group in the Chasm study area.

Table 3.1: Volcanic and sedimentary facies of the Chilcotin Group in the Chasm study area

Facies Code	Facies	Characteristics	Thickness
<b>Coherent units</b>			
vlB	Vesicular basaltic pahoehoe lobe	dark grey to maroon, lobate structures, pipe vesicles (avg. height 10cm) are common, pahoehoe ropes and wrinkles noted <u>Vesicles/Amygdales</u> : spherical, 20%, < 1-2 mm <u>Contacts</u> : concordant, sharp or irregular	individual emplacement units 2-10m thick single pahoehoe lobes 6cm-3m
acB	Aphyric columnar-jointed basalt	dark grey, tan or maroon, commonly amygdaloidal and/or vesicular. <u>Amygdales</u> : spherical, 3-40%, < 1 mm <u>Phenocrysts</u> : olivine microphenocrysts <u>Contacts</u> : concordant and sharp	individual emplacement units 5-20m thick
ipB	Intact pillow basalt	dark grey, prismatic jointed, tiny normal joints around periphery of pillow; pillows packed together with little or no interstitial material <u>Amygdales</u> : spherical, < 15% <u>Contacts</u> : chilled fine-grained black rim (1-3cm thick)	average pillow size 70cm
<b>Clastic units</b>			
hB	Hyaloclastite	monomitic basalt breccia, weakly vesicular; jigsaw-fit texture <u>Clasts</u> : ~ 3-10mm angular to subangular fragments <u>Matrix</u> : sand-sized comprised of fine basalt fragments <u>Contacts</u> : irregular	~ 2m thick
pfB	Pillow fragment breccia	orange, massive, lensoidal, pillow fragments, intact basalt pillows <u>Clasts</u> : ~ 1-20 mm, angular to subangular, pillow fragments <u>Matrix</u> : angular, glassy basalt fragments, 1-20 mm <u>Pillows</u> : Average dimension 0.5 m, irregularly shaped, prismatic jointed with tiny normal joints around the periphery of pillow <u>Contacts</u> : irregular	~ 5-30 m for each lens
P	Fine-grained paleosol	orange/red, locally vesicular/ amygdaloidal in C and R horizons, numerous basalt cobble-sized clasts set into the orange material <u>Horizons</u> : typically 1-5 separate horizons from 1-40 cm each, generally abrupt and irregular boundaries between horizons. <u>Bedforms</u> : can be thinly laminated, however bedding is not always present <u>Contacts</u> : gradational, irregular, forming sediment infilled cracks	~ 0.5-1.5m for each paleosol
lsS	Lacustrine Sandstone	medium-grained buff coloured sandstone <u>Contacts</u> : not laterally continuous / localized outcrop	~ 15-30cm thick

### ***Aphyric columnar-jointed basalt facies (acB)***

The 'acB' facies comprises massive, sheet-like lavas, with moderate to well-developed columnar joints (Fig. 3.1; photo c). Units are aphyric with sparse olivine microphenocrysts. Vesicle chimneys (1.5 – 5 m) (Fig. 3.2; photo g) and horizontal vesicle sheets (1-3 cm width, length varies) are a key feature of 'acB.' Vesicularity ranges typically from 30% (poorly vesicular) at the base of the lava, <5% (very poorly vesicular) at the middle, and 30% at the upper portion of the lava. Colour of the acB lavas ranges from dark grey (fresh) to maroon (weathered). Individual emplacement units are ~1-10m thick. Columnar joints vary in width (from ~30-60 cm) and preserved chisel marks are rare. Spheroidal weathering locally masks the columnar jointing. The contacts are concordant and sharp for the acB facies.

### ***Intact pillow lava facies (ipB)***

Dark grey, intact pillow lavas are common at the base of the sub-aqueous sequences (Fig. 3.2; photo c). The average pillow size is 70 cm, and they have quenched black glassy rims (1-3 cm thick). Locally, pillow sag structures are observed. Prismatic jointing is common at the centre of the pillow, whereas tiny normal joints are commonly preserved adjacent to the black glassy rims. Pillows are packed together with little to no interstitial material. Intact pillows dip at about 37 degrees based on the orientation of their larger plunging 'head' and a narrower 'tail' (Jones and Nelson 1970).

## **3.2.2 Clastic facies**

### ***Fine-grained paleosol facies (P)***

This facies consists of red to buff-coloured paleosols that occur between lavas on both the eastern and western walls of the canyon (Fig. 3.1; photo d). Three paleosol sites were analysed, using soil science methodology, on the eastern canyon wall (Fig. 2.2). Four to five horizons or zones were identified at each site. Blocky soil structure is rare in the field, though additional structures can be identified in thin section. Possible sedimentary

structure such as root casts or clastic dikes, of identical composition as the paleosols commonly occur at the basal paleosol-lava contact (Fig. 3.1, photo c), and are described in Chapter 4. A generalized horizon description at one of these sites would include top to base: 1) a upper red fine-grained paleosol material (2.5 YR 6/8) with an abrupt, irregular boundary that is platy due to weathering; 2) very pale brown (10 YR 8/4) and increasingly well-lithified paleosol rock; 3) a lowermost horizon of highly amygdaloidal, weathered basalt, identical in colour (10 Yr 8/4 'very pale brown' and 10 Yr 4/1 'dark grey') to the surrounding lava in the Chasm, and defines the lower limit of the paleosol. Each horizon consists of weathered basalt fragments, which include highly amygdaloidal varieties and less common dense basalt fragments (up to 10 cm in size). Lower contacts of the paleosol are typically undulating, irregular and gradational to the next horizon. The paleosols (P facies) are further discussed and interpreted in Chapter 4.

#### ***Pillow-fragment breccia facies (pfB)***

This facies is unstratified and massive (~5-30 m thick) and includes angular to blocky pillow fragments (Fig. 3.2; photos d and e). The morphology of this facies is lensoidal in shape. This facies is monomictic, however different degrees of palagonitization of the basaltic fragments are observed, colouration ranging from dark grey fragments with a orange rim, to smaller fragments completely converted to palagonite, which are orange. The clasts range in size (from approximately 3 mm - 20 cm) and shape (sub-angular, blocky, elongate, ragged to curvi-planar) (Fig. 3.2; photo e). The margins on some of the pillow fragments are fine-grained with a black glassy rim. Secondary clay minerals commonly infill voids in the breccia.

There are two types of secondary zeolite and clay mineralization observed in this facies, one is an dull red chalcedony-like material, which is shown to be analcime (associated with zeolites), and zeolite (phillipsite-K) (Appendix E). Montmorillonite (smectite) is also present, in addition to plagioclase (albite) and quartz. The second material is chalky and white analcime (associated with zeolites) and zeolite (wairakite) (Appendix

E). Montmorillonite is also present, and calcite, clinochore, plagioclase, K-feldspar, and quartz. Therefore, the secondary mineralization of this facies is dominated by zeolites and clays. Both alteration assemblages occur within the interstitial clastic matrix between pillow fragments.

### ***Hyaloclastite facies (hB)***

The facies is rare and associated with pillow lava (Fig. 3.2; refer to 72 m stratigraphic position). Monomictic basalt breccia consisting of angular to sub-angular fragments, which range in size from ~3 mm-10 mm and are weakly vesicular. The matrix is sand-sized and consists of fine-grained basalt fragments. Locally jigsaw-fit textures are preserved indicating in-situ fragmentation and no transport. More commonly, clasts are rotated relative to one another and randomly distributed indicating transport post brecciation.

### ***Lacustrine sandstone facies (lsS)***

This facies is 15 cm thick and not laterally continuous. A lens of medium-grained buff coloured quartz sandstone, with minor feldspars and mica, is found locally at the base of a sub-aqueous sequence (facies v1B; Fig 3.2 and 3.3). The upper and lower contacts are not observed in detail, on account of inaccessibility. K. Simpson is photographed at the contact for scale (Fig. 3.3), however the cliff remained too dangerous to carefully observe the entire unit. The mapped extent of this unit is shown entirely within the photo, which may be a function of accessibility. No ripple marks or other sedimentary structures were visible. The grainsize is coarse, and the shape of the grains are subangular to subrounded.

## **3.2.3 Mineralogy**

Field observations of the CGB at Chasm range from aphyric to olivine-phyric. Coherent samples from the eastern composite log section were prepared into thin sections in addition to stations near the apex of the canyon. All thin sections have a stratigraphic context and field description to accompany the petrographic notes (Fig. 3.5). To summarize 10 thin sections were studied in detail (eastern composite log samples), olivine phenocrysts





**Figure 3.3:** Lacustrine sandstone facies (lsS)

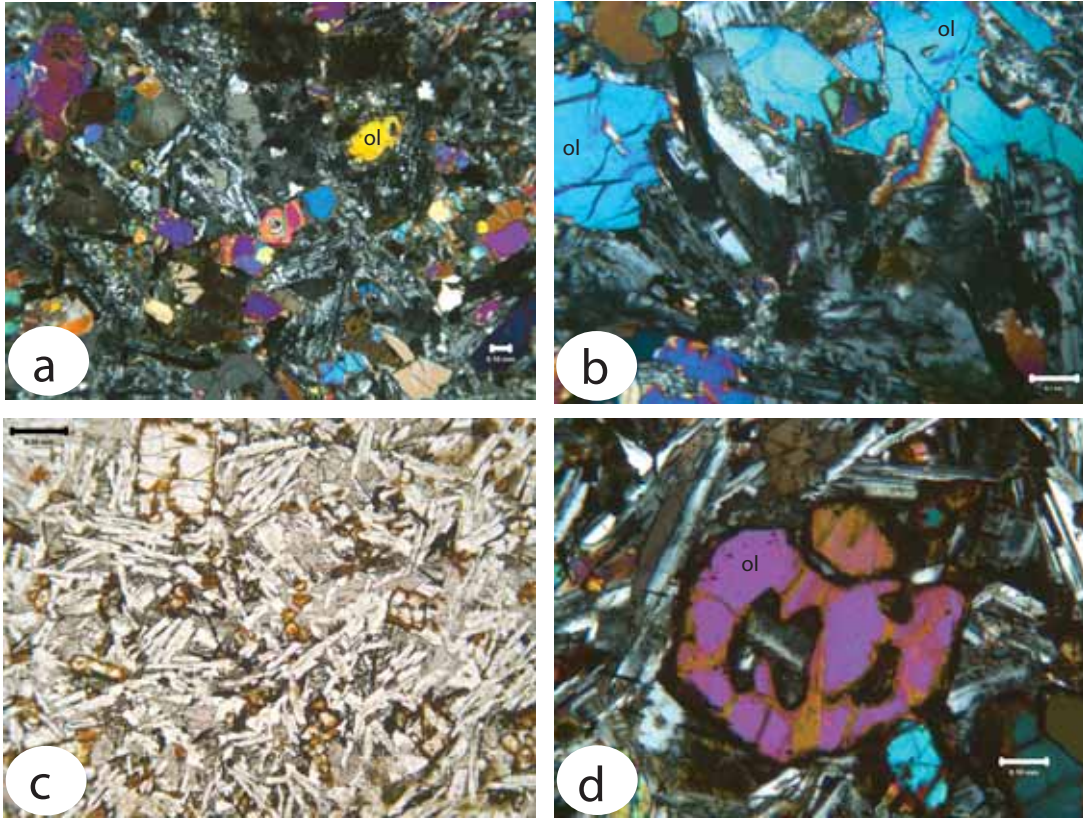
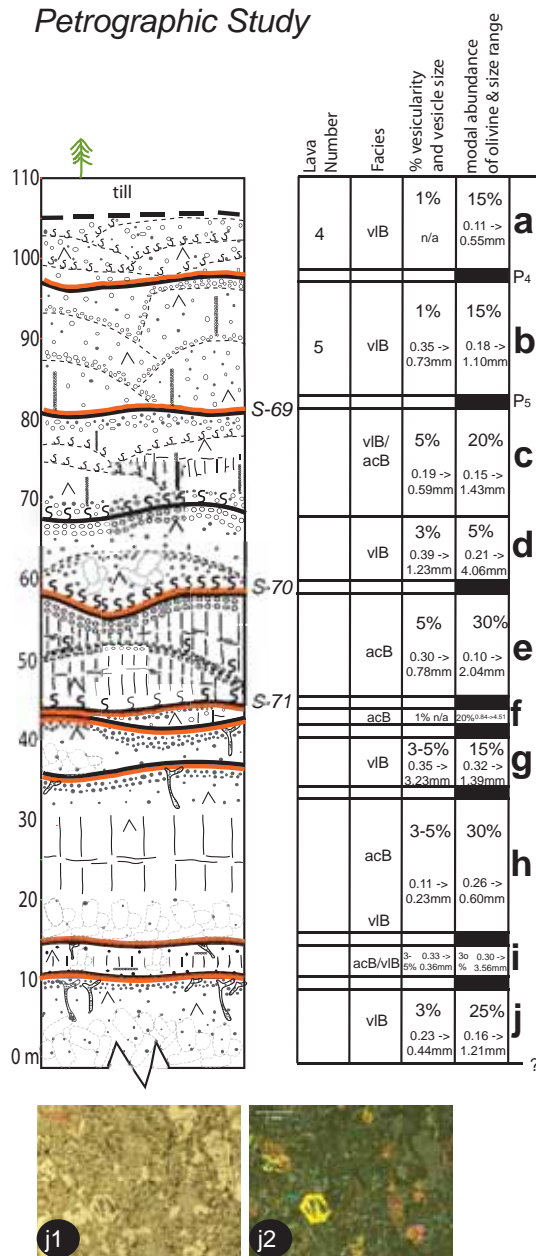


**Fig. 3.4:** Petrographic textures at Chasm highlighting the younger lavas. A) and B) are sample GA-CH06-40, from the Chasm lookout near the apex of the canyon. C) and D) are sample RE-CH08-4, which is the topmost lava in the eastern stratigraphic log. A) Typical view of olivine phenocrysts and plagioclase in the groundmass. Scale is 0.10 mm; B) Olivine and plagioclase laths. Scale is 0.1 mm; C) Brown coloration of iddingsite surrounding olivine crystals in a dominantly plagioclase groundmass with interstitial glass. Scale is 0.30 mm; D) Olivine partially chemically dissolved with iddingsite rim, surrounded by plagioclase laths. Scale is 0.10 mm.

# Chasm East Composite Log Petrographic Study



Note: Average length of plagioclase laths = 0.58mm

**Fig 3.5:** Petrographic stratigraphic log (modification of the eastern composite log). The following samples were used: a1& a2) RE-CH08-4: olivine phenocrysts and in the ground-mass; b1 & b2) RE-CH06-21; c1 & c2) RE-CH06-3; d1 & d2) RE-CH06-30: ellipsoidal amygdale; e1 & e2) RE-CH06-17; f1 & f2) RE-CH08-2; g1 and g2) RE-CH06-18: irregular and jagged amygdale and olivine phenocryst; h1 & h2) RE-CH06-16: cluster of olivine phenocrysts and bladed oxides visible; i1 & i2) RE-CH06-4; j1 & j2) RE-CH08-1: altered skeletal olivine phenocryst. The general trend of alteration shows an increase with depth. The scale on all photomicrographs is 1 mm.



are common and olivine in the groundmass, which is typical in an alkali olivine porphyritic basalt. Red-brown iddingsite is visible around and inside a portion of the olivine crystals (skeletal olivines), as an alteration product of the olivine crystal. Commonly, the olivines are zoned. Other minerals in the groundmass include plagioclase (average length of laths 0.58 mm), clinopyroxenes, augite, bladed oxides, and interstitial glass. The dominant texture is where the plagioclase laths commonly exhibit diktytaxitic texture. Other textures include ophitic and poikilitic textures. Accessory minerals are K-feldspar and nepheline in the groundmass. The modal abundance of olivine crystals varies between samples, ranging from 5 to 30%; the average modal abundance is 20.5% (Fig. 3.4). The degree of weathering varies between samples, with the freshest samples located at the stratigraphic top of the canyon. Samples range from non-vesicular, vesicular and/or amygdaloidal. The average abundance of vesicles is 3%, with the average size of the vesicles ranging from 0.28-0.95 mm. The shape of the vesicles range from ellipsoidal to irregular and jagged. All samples are similar in mineralogy but there are grain size and minor textural differences between lavas (Fig. 3.4).

### ***Petrography***

Petrographic observations demonstrated minor variability between samples, however no major distinctions are detected with the comparison of facies-type (Fig. 3.5). The basaltic subaerial facies (vLB and acB) are similar in detail, however, the vesicularity is greater in vLB facies. Mineralogy is consistent at Chasm, including the one phenocryst-type (olivine) identified in the CGB rocks. Differences in grain-size are observed in the groundmass, which are interpreted to be a result of different rates of post-emplacement cooling of the lava. Olivine phenocryst size is unchanged with stratigraphic height. Olivine in the groundmass more often retain their euhedral shape, compared with the phenocrysts, which appear to be more susceptible to weathering and alteration. The second difference is the degree of weathering in the samples, where the transformation of the olivine crystals into iddingsite is evidence for the alteration of the original basalt mineralogy. The general

trend of weathering and alteration shows an increase with depth stratigraphically. Units in the ipB, pfB, or hB facies were not analyzed petrographically.

## MAJOR FACIES ASSOCIATIONS

<i>Subaqueous facies</i>	<i>Subaerial facies</i>
<b>Intact pillow breccia (ipB)</b> <u>Interpretation:</u> This facies is found at the base of subaqueous successions, inferred that gravity moved these intact bodies downslope to the base of the temporary Chasm Lake.	<b>Vesicular basaltic pahoehoe lobe (vlB)</b> <u>Interpretation:</u> emplaced on a shallow slope, with the smallest 'toes' at the front of the flow. Anatomising across the landscape.
<b>Pillow fragment breccia (pfB)</b> <u>Interpretation:</u> The disaggregation of the pillows is interpreted to occur with movement, as the lava spalls into the temporary lake. The pillow bodies hit one other, and the impact, creates the sharp pillow fragments. Movement was limited, as the fragments are not rounded.	<b>Aphyric columnar-jointed basalt facies (acB)</b> <u>Interpretation:</u> emplaced by inflation (SWELL hypothesis; Self et al, 1998), where initially thin pahoehoe lava is then inflated with a new pulse of lava, producing a massive non-vesicular interior (cools more slowly) resulting in columnar joints.
<b>Hyaloclastite (hB)</b> <u>Interpretation:</u> Formed by quench fragmentation, a non-explosive fracturing and subsequent breakup of basalt lava.	<b>Fine-grained paleosol (P)</b> <u>Interpretation:</u> represents periods of quiescence in the emplacement of the lavas to allow for soil accumulation and development. Soil results in the weathering of the basaltic parent material and aeolian deposits.
<b>Lacustrine Sandstone (lsS)</b> <u>Interpretation:</u> sandstone grains are deposited into the temporary Chasm Lake, and accumulate at the base of the lake.	

**Table 3.2:** Facies associations within the Chilco-tin Group in the Chasm study area.

### 3.3 FACIES ASSOCIATIONS & INTERPRETATIONS

Facies associations in the CGB in the Chasm canyon include facies vlB, acB, and P, which are interpreted to have been emplaced subaerially, and facies ipB, pfB, hB, and lsS, which are interpreted to have been emplaced subaqueously (Table 3.2). The facies associations lead to division of the CGB at Chasm into two broad associations (Mcb<sup>1</sup> and Mcb<sup>2</sup>) (Fig. 2.2), wherein Mcb<sup>1</sup> comprises the subaerial facies, whereas Mcb<sup>2</sup> represents interstratified subaqueous and subaerial facies. Descriptions as well as spatial and temporal relationships of these facies support subaerial and subaqueous interpretations. The subaqueous Chasm succession was associated with a temporary lake (i.e. Chasm Lake), which is discussed further in Chapter 5. Further associations are justified based on comparing the facies geometry of the lavas, such as the sequence vlB, acB, vlB is a common occurrence at Chasm. Lastly, the petrography, magnetic susceptibility and geochronology are interpreted based on the facies and facies associations.

#### 3.3.1 Facies Associations

##### *Unit Mcb<sup>1</sup> Miocene Chilcotin basalt- sub-aerial facies association*

This association consists of sub-aerial basaltic lavas and paleosol horizons and includes: 1) basaltic pahoehoe lava comprising vesicular/amygdaloidal pahoehoe lobes (facies vlB); 2) aphyric columnar-jointed and sheet-like basalt lava (facies acB); and 3) fine-grained, red-coloured paleosols (facies P). From a distance, the sub-aerial lava appears to be thick, ‘sheet-like’ units with sparse lobate shapes and moderately developed columnar-joints (facies acB). However, in detail many of the lavas consist of small pahoehoe lobes (facies vlB).

Pahoehoe lavas (vlB facies) are interpreted to have been emplaced on a shallow slope. The smallest lobes (‘toes’) are located at the flow front, which may reflect a discontinuous, or slower emplacement with anastomosing pahoehoe lobes. The ‘acB’ facies was emplaced by inflation (SWELL hypothesis; Self et al. 1998), producing more massive,

sheet-like flows indicating a more rapid emplacement.

In Hawaii, Hon et al. (1994) observed that slopes must be no greater than 2° to form the sheet-like flows; if the slope increases than channelized flows will result. Hawaiian field data has documented inflation process, illustrating a 10-50 cm thick pahoehoe lobe can be inflated to 4 m (Hon et al. 1994). The presence of ropes imply deformation to the skin of the lava; the skin of the pahoehoe lava is flexible and when lava moves over topography disturbance in the skin results (Fink and Fletcher 1978). In modeling the emplacement of the CGB lavas into Chasm canyon, inflation processes commonly invert the surface topography, therefore the paleo-highs in the topography are subsequently termed 'inflation pits' and the paleo-lows are then 'tumuli' (Self et al. 1998). Passey and Bell (2007) state that the differences between sheet-like lavas and pahoehoe lobes (compound lavas) is related to the supply rates during emplacement. No a'a pahoehoe lava is observed at Chasm.

The presence of paleosols (P facies) suggests many hiatuses in volcanism during emplacement of the lavas in the Chasm area, and are classified and interpreted in Chapter 4. Disconformities mark all contacts between the overlying lava (typically acB) and the P facies. With the interstratified paleosols, commonly the upper contacts of the lavas are paleosol horizons, implying discrete flow fields in Chasm. This is further discussed in Chapter 4.

#### ***Unit Mcb<sup>2</sup> Miocene Chilcotin basalt- undivided sub-aqueous and sub-aerial facies association***

Within the Chasm study area, an important transition occurs between subaqueously-deposited clastic rocks and subaerially-emplaced lavas. The Mcb<sup>2</sup> facies association is best developed in the southern portion of the western canyon wall and comprises alternating sub-aqueous and sub-aerial lavas. Subaerial lavas make up 60% of the sequence. Subaerial facies of the Mcb<sup>2</sup> include subaerial lavas from the vIB and acB facies described above.



The Mcb<sup>2</sup> also includes the dominant intact pillow lava (facies ipB) and pillow-fragment breccia (facies pfB) facies and rare hyaloclastite (facies hB) and lacustrine sandstone (facies lsS) units. The subaerial flat lying lavas are correlated over 8 km, the interstratified subaqueous and subaerial sequence is a minor component in the Chasm Chasm, only exposed in the southwestern section.

The ipB facies represents subaqueous lavas flowing downslope, and accumulating into a pillow pile. The ipB facies is a dominantly 'close-packed pillow lava' (Carlisle, 1963), wherein the intact basaltic pillows are molded into each other. Corrugation, a wrinkle pattern on the outer skin of individual pillows (Yamagishi 1987), is a common surface structure. Tensional cracks are prevalent at Chasm (see West graphic log; Fig. 3.2) and form deep grooves into the pillow, and are formed due to another pulse of the molten lava from the interior of the pillow, cracking the solidified exterior crust (Yamagishi 1973, 1983), after the breakout/growth of a new pillow lobe. Pillows with pronounced tensional cracks are observed at the base, middle and top of section. Single and multiple rinds are observed in the pillows, the latter indicative of more than one surge of the molten interior of the pillow lava as this process breaks the skin of the pillow in the formation an isolated pillow (Yamagishi 1987; McPhie et al. 1993).

The pfB facies is interpreted to have formed by disaggregation of pillow lava as pillow breakouts occur from the pillow fronts to form new pillows. The transport of the pillows downslope, the mechanical impact and abrasion of one pillow upon another, and angle of depositional slope all influence the abundance of pillow fragments compared to intact pillows. Quench fragmentation also likely contributes fragments to this facies.

The hB facies is rare in the Chasm succession and is interpreted to have formed by quench fragmentation (McPhie et al. 1993). Collectively, the pillow lava, pillow-fragment breccia, and hyaloclastite facies are interpreted to have formed a lava-delta sequence as a result of subaqueous emplacement of basalt lavas (Jones and Nelson 1970). The lsS is interpreted to have been deposited into the temporary Chasm Lake, and represent the base

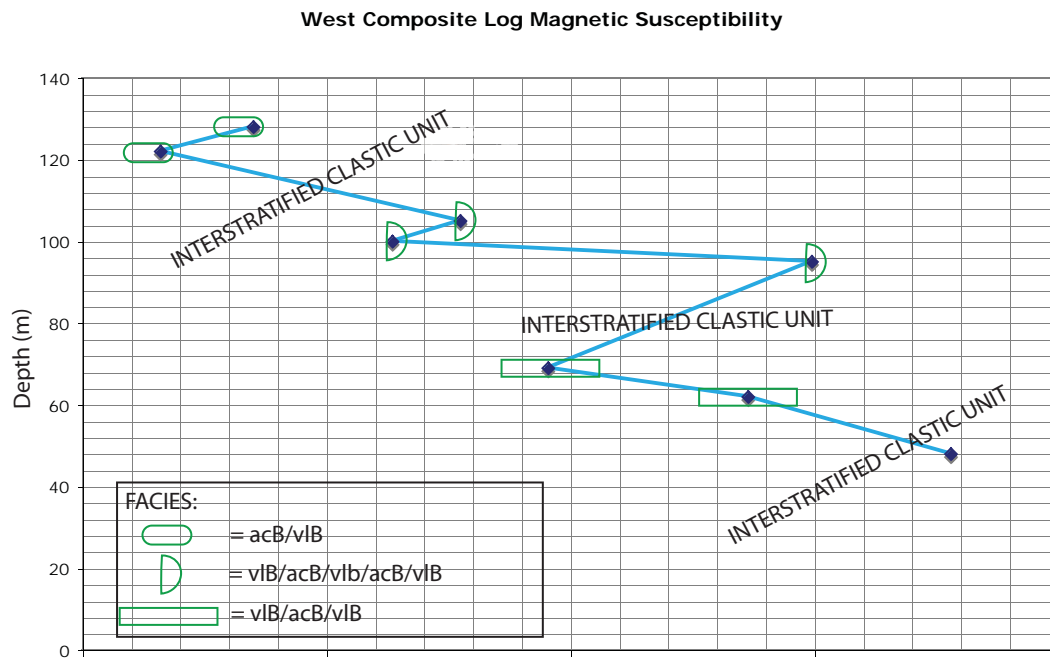
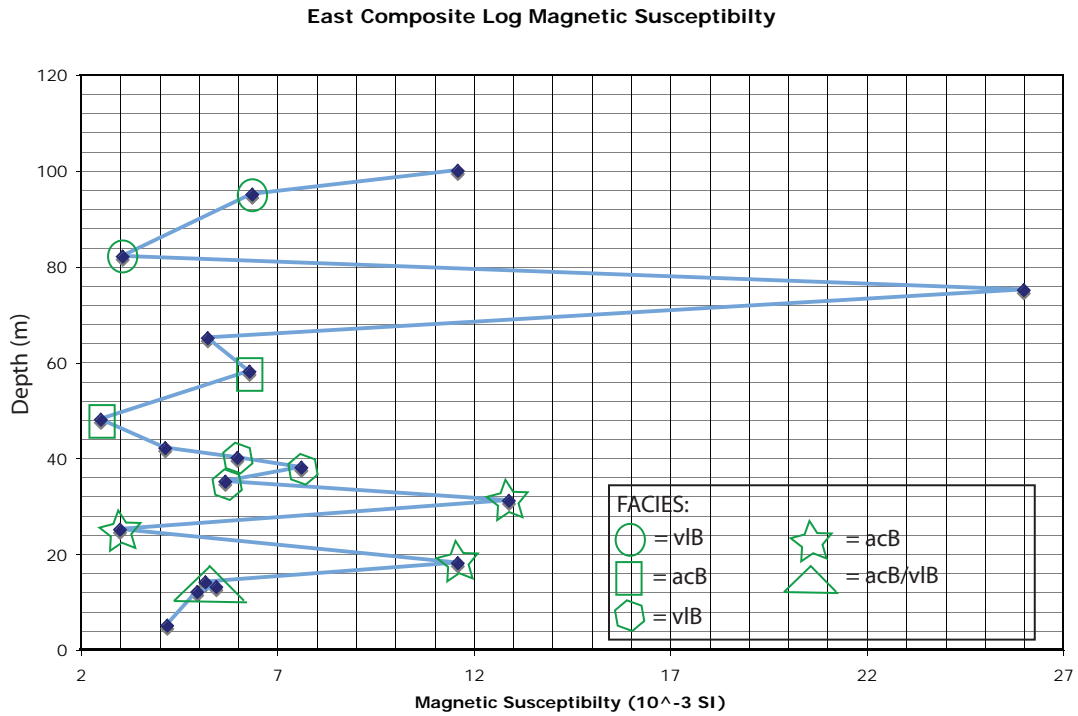


**Figure 3.6:** Magnetic susceptibility plots of eastern (upper) and western (lower) composite log sections. Identical shapes represent a single lava unit. If there is no symbol, 1 measurement was recorded for that lava unit. If there are two symbols for the same unit it implies the upper and lower facies stratigraphically. Note the scale difference between two plots. Refer to Figures 3.1 and 3.3 for corresponding graphic logs.

**Distribution of Chasm Magnetic Susceptibility**

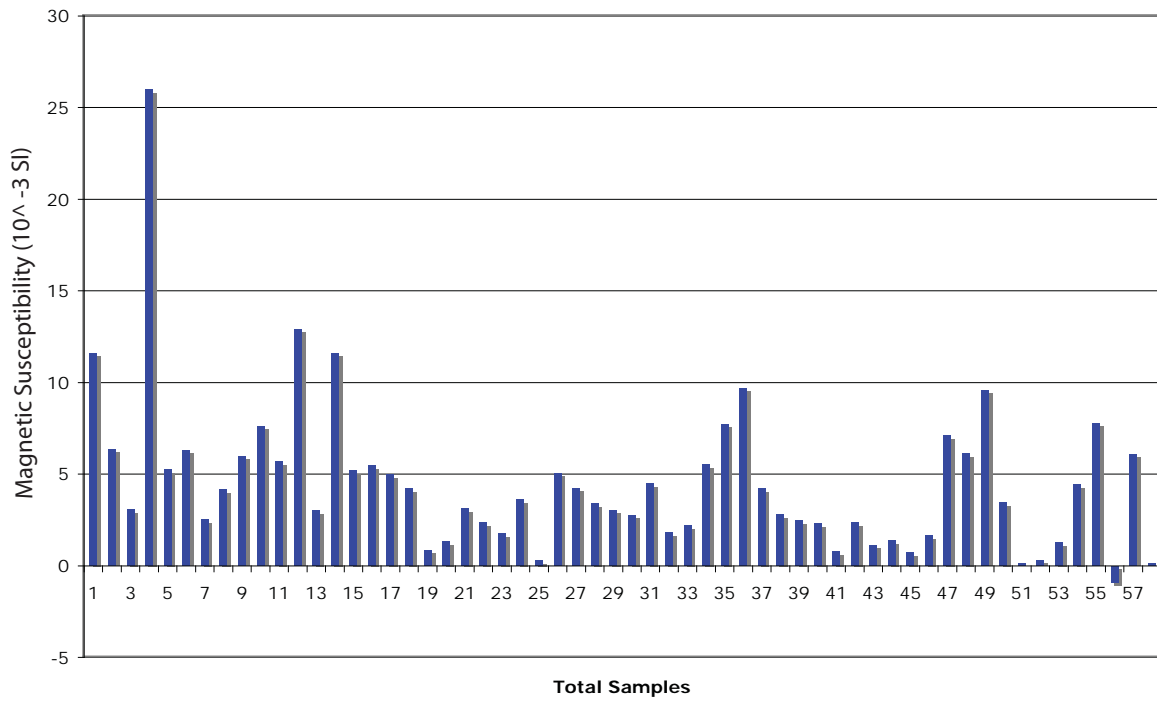


**Figure 3.7:** Histogram of the magnetic susceptibility values for Chasm. The average M.S. value at Chasm is 4.5

CHASM MAGNETIC SUSCEPTIBILITY MEASUREMENTS						
Field #	Magnetic Susceptibility <sup>1</sup>	UTM Easting (NAD83)	UTM Northing (NAD83)	Measurement Type <sup>2</sup> (n)	Unit <sup>3</sup>	Location
06REF020q	11.6	609005	5671220	Field (10)	Chilcotin Group	Eastern Log
06REF020p	6.37	609005	5671220	Field (10)	Chilcotin Group	Eastern Log
06REF020o	3.07	609005	5671220	Field (10)	Chilcotin Group	Eastern Log
06REF020n	26	609005	5671220	Field (10)	Chilcotin Group	Eastern Log
06REF020m	5.24	609006	5671220	Field (10)	Chilcotin Group	Eastern Log
06REF020l	6.3	609006	5671220	Field (10)	Chilcotin Group	Eastern Log
06REF020k	2.52	609006	5671220	Field (10)	Chilcotin Group	Eastern Log
06REF020j	4.15	609006	5671220	Field (10)	Chilcotin Group	Eastern Log
06REF020i	5.99	609006	5671220	Field (10)	Chilcotin Group	Eastern Log
06REF020h	7.62	609006	5671220	Field (10)	Chilcotin Group	Eastern Log
06REF020g	5.68	609006	5671220	Field (10)	Chilcotin Group	Eastern Log
06REF020f	12.9	609006	5671220	Field (10)	Chilcotin Group	Eastern Log
06REF020e	3	609006	5671220	Field (10)	Chilcotin Group	Eastern Log
06REF020d	11.6	609006	5671220	Field (10)	Chilcotin Group	Eastern Log
06REF020c	5.18	609006	5671220	Field (10)	Chilcotin Group	Eastern Log
06REF020b	5.45	609006	5671220	Field (10)	Chilcotin Group	Eastern Log
06REF020a	4.97	609006	5671220	Field (10)	Chilcotin Group	Eastern Log
RE-CH08-1	4.2	609093	5671017	Lab (5)	Chilcotin Group	Eastern Log
07REF143-2A	0.86	607617	5669526	Lab (3)	Chilcotin Group	Eastern Wall
07REF143-2B	1.32	607617	5669526	Lab (3)	Chilcotin Group	Eastern Wall
07REF143-1A	3.11	607617	5669526	Lab (3)	Chilcotin Group	Eastern Wall
07REF143-1B	2.33	607617	5669526	Lab (3)	Chilcotin Group	Eastern Wall
RE-CH06-04	1.75	608609	5671734	Lab (3)	Chilcotin Group	Eastern Wall
RE-CH06-12	3.61	609057	5671112	Lab (3)	Chilcotin Group	Eastern Wall
RE-CH06-16	0.289	609057	5671112	Lab (3)	Chilcotin Group	Eastern Wall
08REF037	5.06	607514	5669891	Field (10)	Chilcotin Group	Western Log
08REF034	4.23	607675	5669360	Field (10)	Chilcotin Group	Western Log
08REF033	3.41	607692	5669236	Field (10)	Chilcotin Group	Western Log
08REF011c	3.05	607682	5668454	Field (10)	Chilcotin Group	Western Log
08REF011b	2.77	607682	5668454	Field (10)	Chilcotin Group	Western Log
08REF011a	4.49	607682	5668454	Field (10)	Chilcotin Group	Western Log
08REF010b	1.82	607643	5668338	Field (10)	Chilcotin Group	Western Log
08REF010a	2.2	607643	5668338	Field (10)	Chilcotin Group	Western Log
08REF038	5.5	607347	5668138	Field (10)	Chilcotin Group	Western Wall
08REF039	7.73	607422	5668199	Field (10)	Chilcotin Group	Western Wall
08REF040	9.69	607509	5668283	Field (10)	Chilcotin Group	Western Wall
08REF077	4.21	607438	5670071	Field (10)	Chilcotin Group	Western Wall
08REF078	2.79	607431	5670121	Field (10)	Chilcotin Group	Western Wall
08REF079	2.44	607434	5670258	Field (10)	Chilcotin Group	Western Wall
06REF027	2.29	607730	5668821	Field (10)	Chilcotin Group	Western Wall
06REF027	0.78	607730	5668821	Field (10)	Chilcotin Group (pillow)	Western Wall
06REF027	2.34	607730	5668821	Field (10)	Chilcotin Group	Western Wall
06REF027	1.14	607730	5668821	Field (10)	Chilcotin Group	Western Wall
06REF027	1.38	607730	5668821	Field (10)	Chilcotin Group	Western Wall
06REF027	0.72	607730	5668821	Field (10)	Chilcotin Group (pillow)	Western Wall
07REF161	1.63	607304	5671207	Field (5)	Chilcotin Group	Western Wall
07REF162	7.11	607313	5671433	Field (5)	Chilcotin Group	Western Wall
07REF162	6.12	607313	5671433	Field (5)	Chilcotin Group	Western Wall
07REF162	9.59	607313	5671433	Field (5)	Chilcotin Group	Western Wall
07REF174	3.45	608321	5670361	Field (5)	Chilcotin Group	Western Wall
07REF-186	0.15	606782	5666970	Lab (3)	Deadman Frm	
07REF195	0.3	608019	5667749	Lab (3)	Deadman Frm	
07REF177	1.27	608447	5669850	Lab (3)	Skull Hill Frm	
07REF137-1	4.44	608262	5668917	Lab (3)	Skull Hill Frm	
07REF137-3	7.78	608262	5668917	Lab (3)	Skull Hill Frm	
07REF137-2	-0.9	608262	5668917	Lab (3)	Skull Hill Frm	
07REF176	6.1	608457	5669916	Lab (3)	Skull Hill Frm	
07REF-184	0.13	606735	5666878	Lab (3)	Cache Creek Group	
<sup>1</sup> Magnetic Suceptibility data is recorded in 10 <sup>-3</sup> SI units						
<sup>2</sup> Measurements taken with KT-9 Kappameter; Lab measurements on core						
<sup>3</sup> Chilcotin Group Basalt; Deaman Formation Volcaniclastic sandstone; Skull Hill Formation Volcanics.						

**Table 3.3:** Magnetic Susceptibility data table, specific to Chasm.

of the lake, (see Chapter 5; Fig. 3.3).

### **3.3.2 Discussion**

#### ***Magnetic Susceptibility***

The average magnetic susceptibility (MS) values for Chasm lavas is  $4.5 \cdot 10^{-3}$  SI units. MS values are plotted for the eastern and western composite log sections (Fig. 3.6), and vary between facies. In the eastern log area, the vLB facies values are often similar indicating that the overlapping pahoehoe lobes are indistinguishable based on MS. The acB facies in the East Log area, has two values plotting near 12, and one value near 3. The top and base of the lava have similar values, whereas the centre results in a dramatically lower value.

The Western Log MS plot differs from the eastern plot due to the interstratified clastic units, and because each lava measured contains 2 or more facies. Overall, there is no significant MS value variability for the entire western plot (range:  $1.5\text{--}5.5 \cdot 10^{-3}$  SI units; average value =  $3.4 \cdot 10^{-3}$  SI units) compared with the eastern plot range (range:  $2\text{--}27 \cdot 10^{-3}$  SI units; average value =  $7.3 \cdot 10^{-3}$  SI units). To summarize, the range of MS values as shown in Figure 3.7 for Chasm lavas overlap therefore the MS data are not useful for discriminating between flow fields or facies at Chasm, however there is potential for characterization of individual facies with strategic MS sampling.

### **3.3.3 Geochronology**

The  $^{40}\text{Ar}/^{39}\text{Ar}$  system was used to investigate the chrono-stratigraphy in Chasm Canyon, aiming to test correlations among lavas in a few areas of the canyon. At Chasm, extensive dating of 12 samples from the canyon was carried out, aiming to constrain the emplacement events for the basalts at Chasm and surrounding vicinity (Figs. 3.8, 3.9, 3.10, 3.11, 3.12, and 3.13). There are no ages in the literature specifically from Chasm Canyon. Matthews (1988) sampled CGB basalt from 57 Mile Creek, north of the Chasm, and

obtained a K-Ar age of  $9.2 \pm 0.4$  Ma.

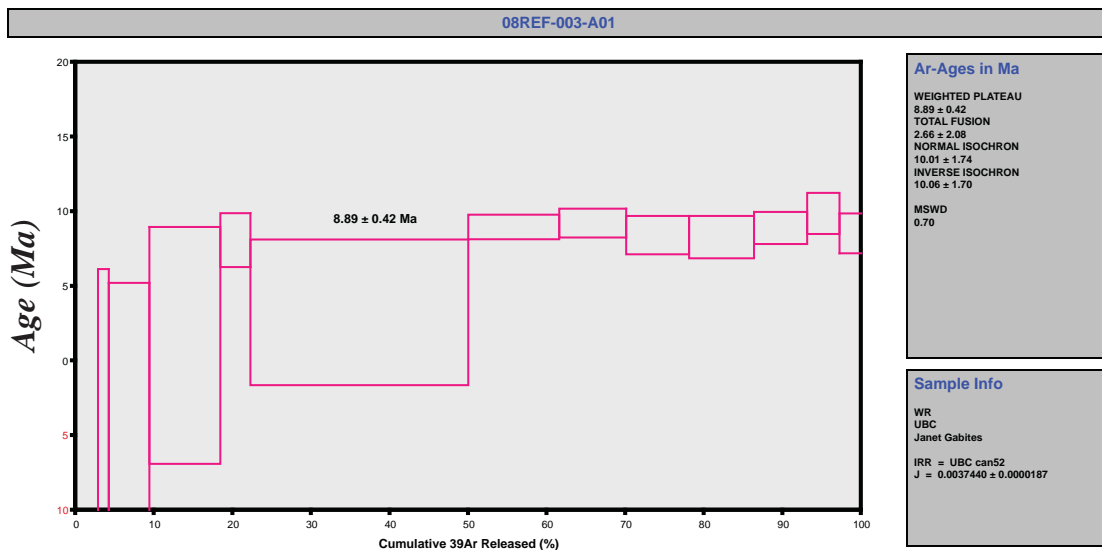
The regional CGB ages are located in Appendix C, and ages specifically from Chasm area are located in Table 3.4. Sample preparation methodology can be found in Appendix B. The ages were derived following careful analytical checks including: 1) the plateau shape; 2) observing whether all steps are within the 2 sigma error range; 3) the MSWD (mean-square weighted deviation) number should be close to 1, this provides information on the goodness of fit parameter (McDougall and Harrison 1999); and 4) if there are any additional notes from the analyst.

Geochronology samples are listed in Table 3.4, with sample number, age, geographical location in the canyon, and the corresponding lava number (see also Fig. 2.2). The 12 new Chasm whole-rock  $^{40}\text{Ar}/^{39}\text{Ar}$  ages range from  $10.00 \pm 0.48$  Ma to  $8.72 \pm 0.37$  Ma (Fig. 3.14 and Table 3.4). These samples overlap in  $2\sigma$ , but reveal a complex chronostratigraphy, discussed below.

Refer to Appendix C for CGB regional plots, and the Chasm specific plots are located in Figures 3.8 through 3.13. The errors overlap within a  $2\sigma$  error, except for one sample (RE-CH08-1<sub>b</sub>), and the entire Chasm suite and related outcrops on the Highway 97 are seen on Fig. 3.10.

All new ages are plotted on the map (Fig. 2.2), except for sample (RE-CH08-1<sub>b</sub>), which does not plot within the  $2\sigma$ -error age range. To summarize, the youngest lavas (Lava 1 etc.) are only exposed in the northern section of the canyon, whereas the older lavas are exposed at the base of the canyon due to dissection. It is not clear what caused this anomalous result ( $8.59 \pm 0.72$  Ma; plot in Appendix C), since it is a younger age compared to analysis RE-CH08-1<sub>a</sub> which yields  $10.00 \pm 0.48$  Ma; however the analytical source of the error is unclear, since both ages were conducted using two aliquots of the same sample. Stratigraphic constraints indicate  $10.00 \pm 0.48$  Ma (RE-CH08-1<sub>a</sub>) is likely to be the better age. The degree of weathering of the basalts should not create discrepancy within the geochronology.

A)



B)

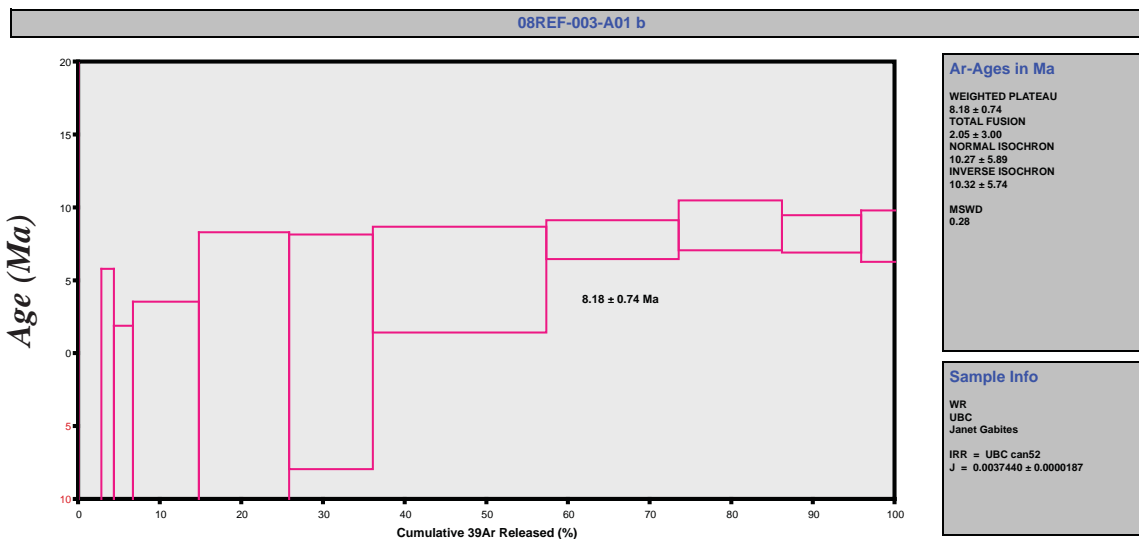
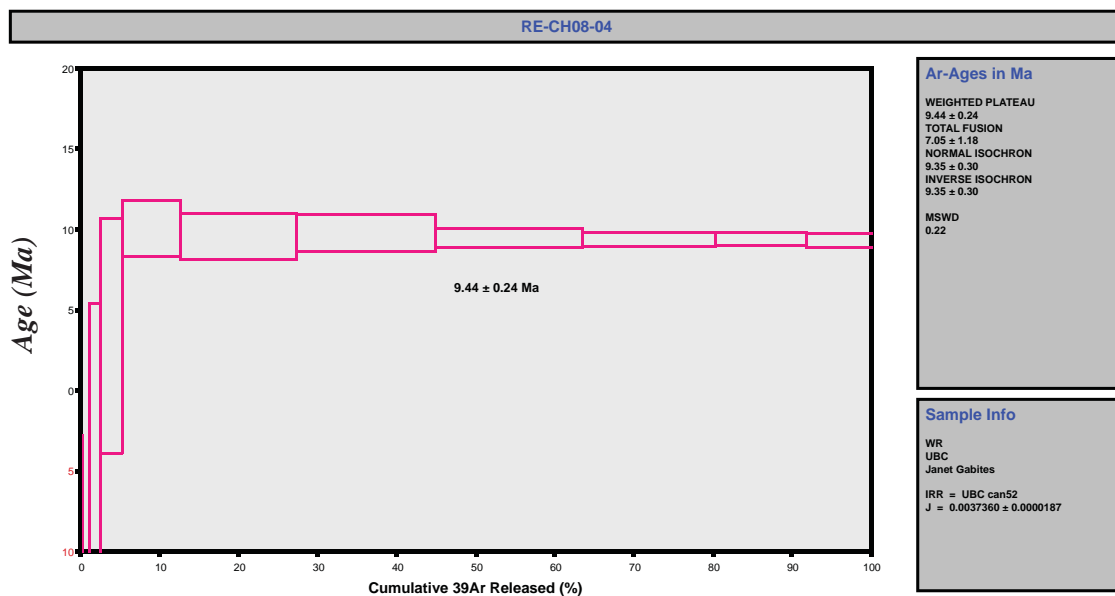
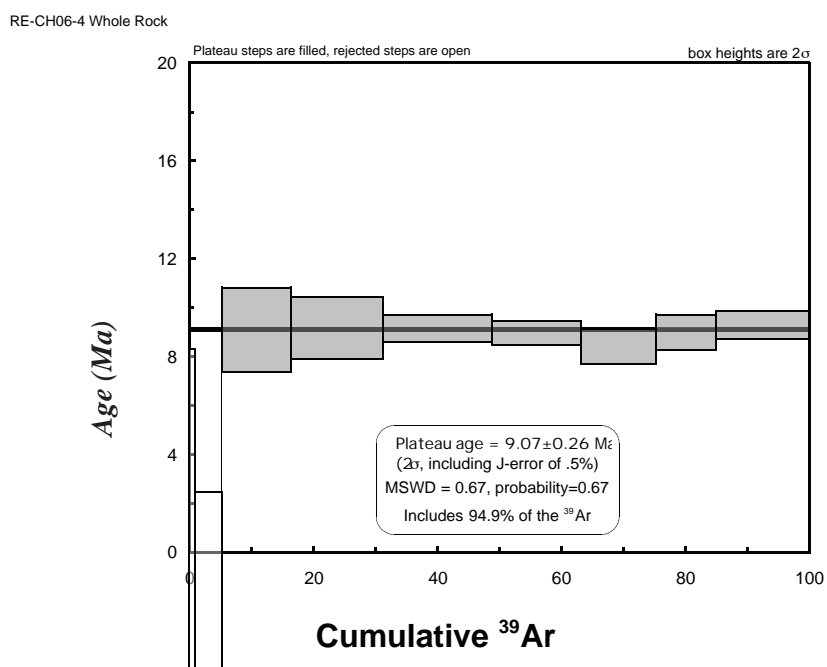


**Figure 3.8:** Representative geochronology age plots for Chasm. A) Sample (RE-CH08-91) with a plateau age =  $8.89 \pm 0.42$  Ma. B) Sample (RE-CH08-92) with a plateau age =  $8.18 \pm 0.74$  Ma.

C)



D)

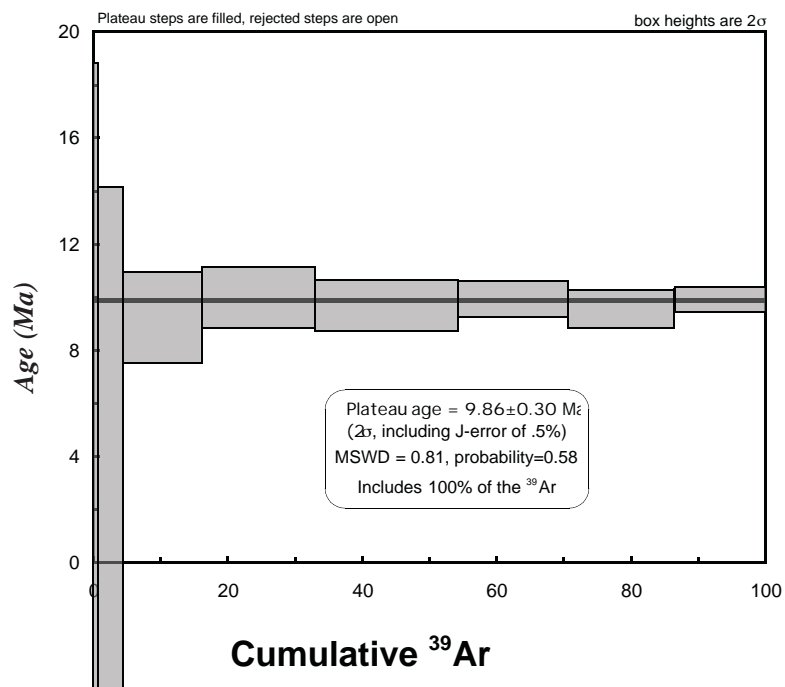


**Figure 3.9:** Representative geochronology age plots for Chasm continued. C) Sample (RE-CH08-42) with a plateau age = 9.44 ± 0.24 Ma. D) Sample (RE-CH06-4) with a plateau age = 9.07 ± 0.26 Ma.



**E)**

RE-CH06-18 Whole Rock

**F)**

RE-CH06-12 Whole Rock

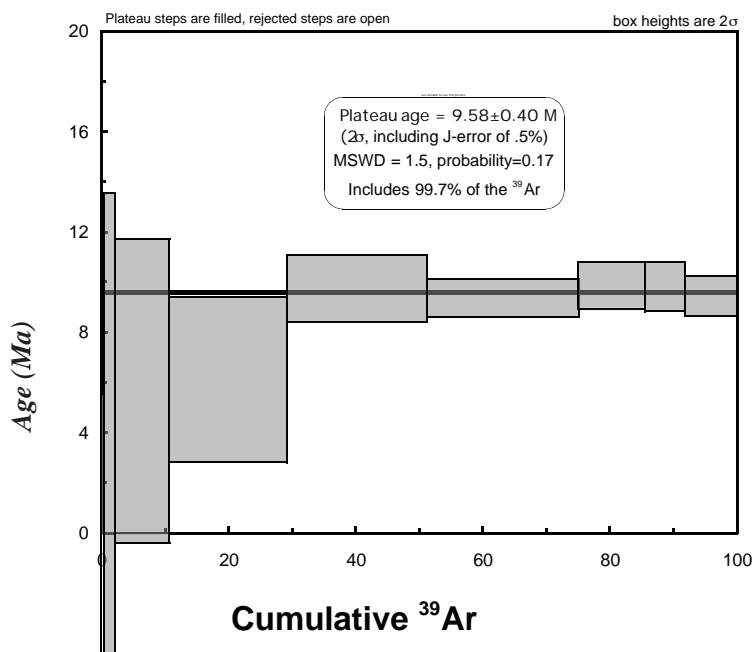
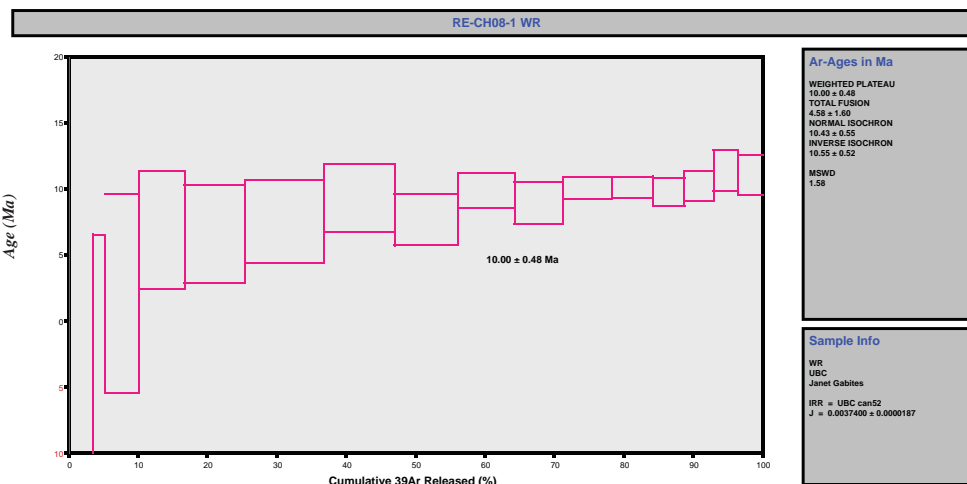


**Figure 3.10:** Representative geochronology age plots for Chasm continued. E) Sample (RE-CH06-18) with a plateau age =  $9.86 \pm 0.3$  Ma. F) Sample (RE-CH06-12) with a plateau age =  $9.65 \pm 0.4$  Ma.

G)



RE-CH06-92 Whole Rock

H)

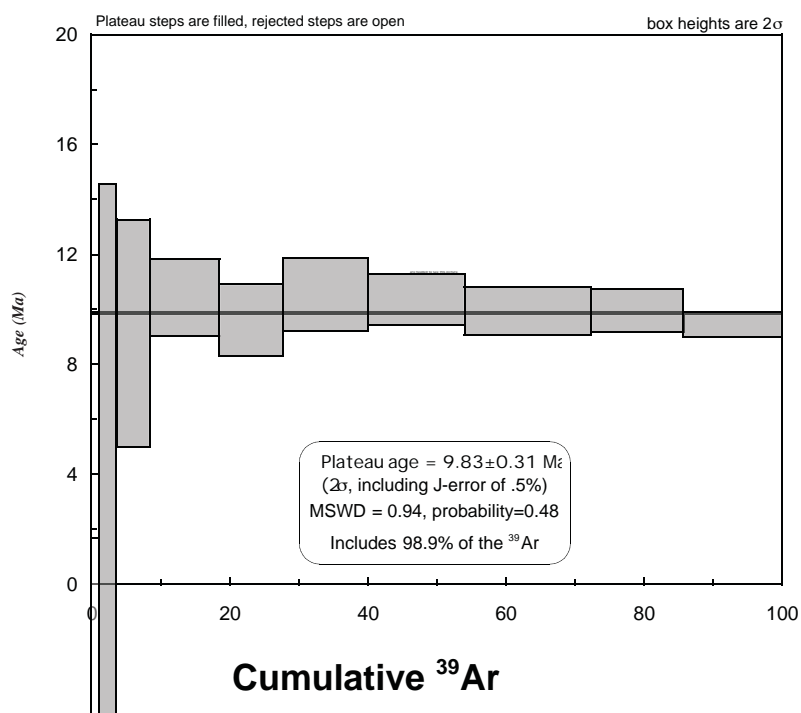


**Figure 3.11:** Representative geochronology age plots for Chasm continued. G) Sample (RE-CH08-1) with a plateau age = 10.00 ± 0.48 Ma. H) Sample (RE-CH06-92) with a plateau age = 9.83 ± 0.32 Ma.

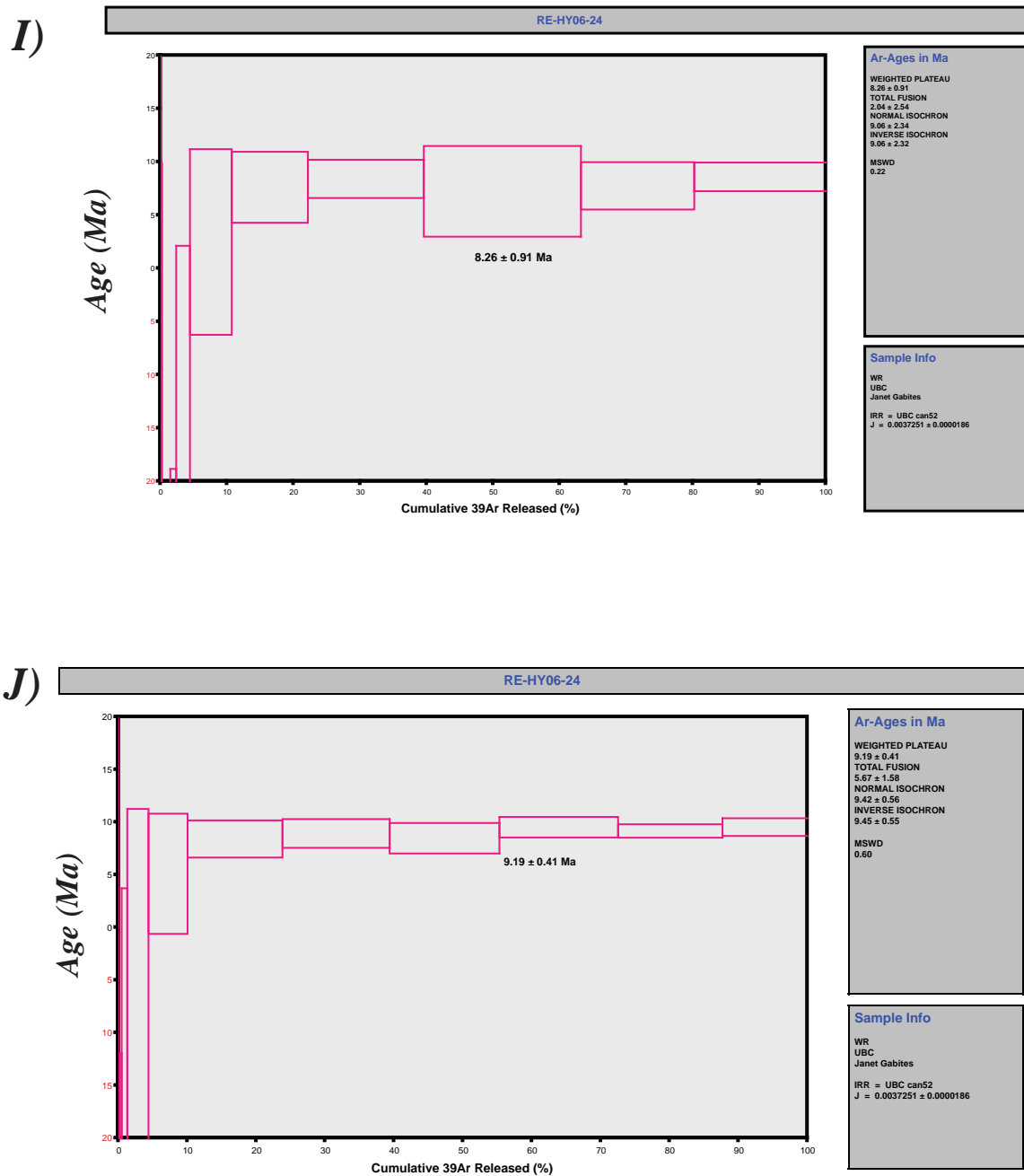
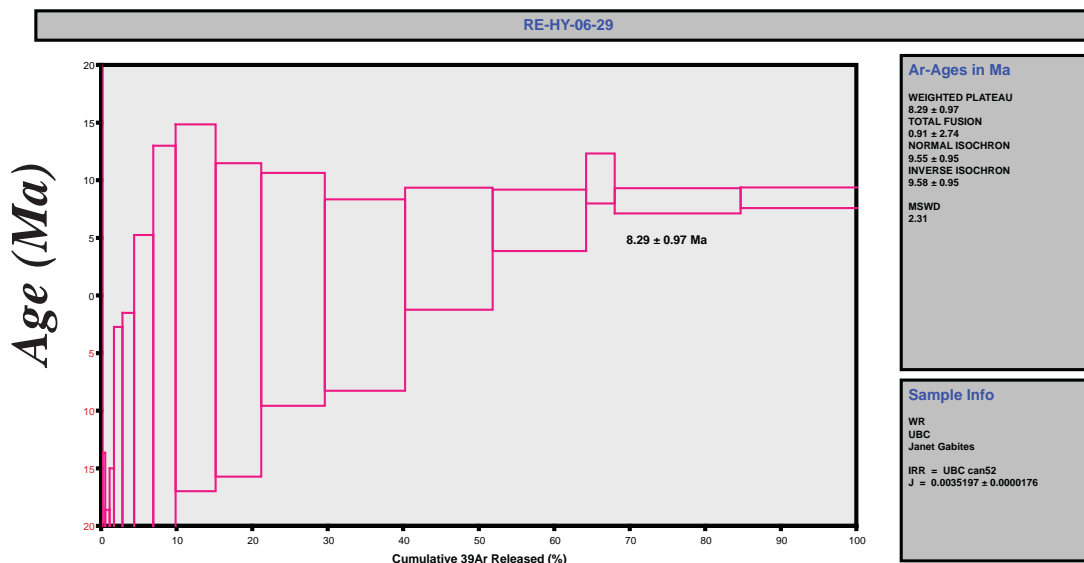


**Figure 3.12:** Representative geochronology age plots for Chasm continued. I) Sample (RE-HY06-241) with a plateau age =  $8.26 \pm 0.91$  Ma. J) Sample (RE-HY06-242) with a plateau age =  $9.19 \pm 0.41$  Ma.

K)



L)

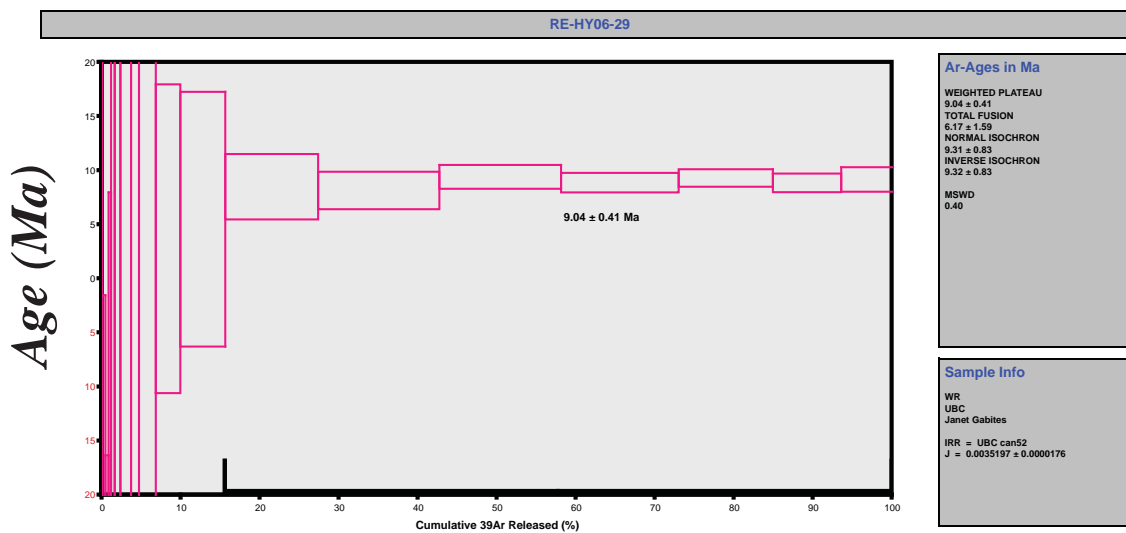


**Figure 3.13:** Representative geochronology age plots for Chasm continued. K) Sample (RE-HY06-291) with a plateau age =  $8.29 \pm 0.97$  Ma. L) Sample (RE-HY06-292) with a plateau age =  $9.04 \pm 0.41$  Ma.

GEOCHRONOLOGY OF CHILCOTIN GROUP BASALTS: CHASM CANYON AREA						
Sample Number <sup>a</sup>	AGE (Ma)	System	UTM Easting (NAD83)	UTM Northing (NAD83)	GEOGRAPHICAL LOCATION	Lava Number <sup>b</sup>
RE-CH08-9 <sup>c</sup> <sub>1</sub>	8.89 ± 0.42	Ar-Ar	606393	5675485	Eastern Chasm canyon wall	1
RE-CH08-9 <sup>c</sup> <sub>2</sub>	8.18 ± 0.74	Ar-Ar	606393	5675485	Eastern Chasm canyon wall	1
RE-CH08-4 <sup>c</sup>	9.44 ± 0.24	Ar-Ar	608769	5671521	Eastern Chasm composite log	4
RE-CH06-4 <sup>d</sup>	9.07 ± 0.26	Ar-Ar	608609	5671734	Eastern Chasm composite log	5
RE-CH06-18 <sup>d</sup>	9.86 ± 0.3	Ar-Ar	609005	5671220	Eastern Chasm composite log	Refer to Figure 3.1
RE-CH06-12 <sup>d</sup>	9.65 ± 0.4	Ar-Ar	609057	5671112	Eastern Chasm composite log	Refer to Figure 3.1
RE-CH08-1 <sup>c</sup>	10.00 ± 0.48	Ar-Ar	609093	5671017	Eastern Chasm composite log	Refer to Figure 3.1
RE-CH06-92 <sup>d</sup>	9.83 ± 0.32	Ar-Ar	607729	5668821	Western Chasm canyon wall	no stratigraphic reference
RE-HY06-24 <sup>c</sup> <sub>1</sub>	8.26 ± 0.91	Ar-Ar	603381	5671458	57 Mile, West Side of Highway 97	
RE-HY06-24 <sup>c</sup> <sub>2</sub>	9.19 ± 0.41	Ar-Ar	603381	5671458	57 Mile, West Side of Highway 97	
57 Mile Creek <sup>e</sup>	9.2 ± 0.4 <sup>D</sup>	K-Ar	604277	5670184	57 Mile, East Side of Highway 97	
RE-HY06-29 <sup>c</sup> <sub>1</sub>	8.29 ± 0.97	Ar-Ar	605595	5678011	63 Mile, West Side of Highway 97	
RE-HY06-29 <sup>c</sup> <sub>2</sub>	9.04 ± 0.41	Ar-Ar	605595	5678011	63 Mile, West Side of Highway 97	
<sup>a</sup> All samples are whole rocks.						
<sup>b</sup> Number assigned to individual lavas that can be traced laterally along the canyon, see Figures 3.1, 5.2, 5.3, and 5.4						
<sup>c</sup> UBC; J. Gabites, analyst						
<sup>d</sup> UBC; T. Ullrich, analyst						
<sup>e</sup> Matthews, 1988.						

**Table 3.4:** Geochronology of Chasm canyon.

The new whole rock ages provide the duration of volcanism at Chasm (Fig. 10; Table 3.4). The youngest lava was analyzed twice, and yielded ages  $8.89 \pm 0.42$  Ma and  $8.18 \pm 0.74$  Ma (ages overlap at a  $2\sigma$  level). The duration of volcanism calculated using the two different measured ages for the youngest lava are  $1.11 \pm 0.64$  Ma and  $1.82 \pm 0.88$  Ma. Using the weighted average for the youngest lava, the calculation yielded a duration of volcanism of  $1.28 \pm 0.61$  Ma, which is the preferred estimate for the duration of volcanism at the Chasm ( $2\sigma$  internal error, refer to summary geochronology plot in Fig. 3.10, and Table 3.4).

The addition in quadrature method was used to average the errors for the duration of volcanism calculation. This method is important for statistically calculating the correct error between two ages. This method as follows is: if 's' is the probable value for the sum (or difference) of the two measurements 'x' and 'y' and if dx and dy are the probable uncertainties in 'x' and 'y' then the most probable error in 's' ('ds') equals the square root of the sum of the squares (  $ds = \sqrt{dx^2 + dy^2}$  ).

The implication of the age results constraining the soil development for the paleosols is covered in Chapter 4 and discussion of the emplacement chrono-stratigraphy is found in Chapter 5, where the lava source direction and eruptive centre (s) are interpreted.

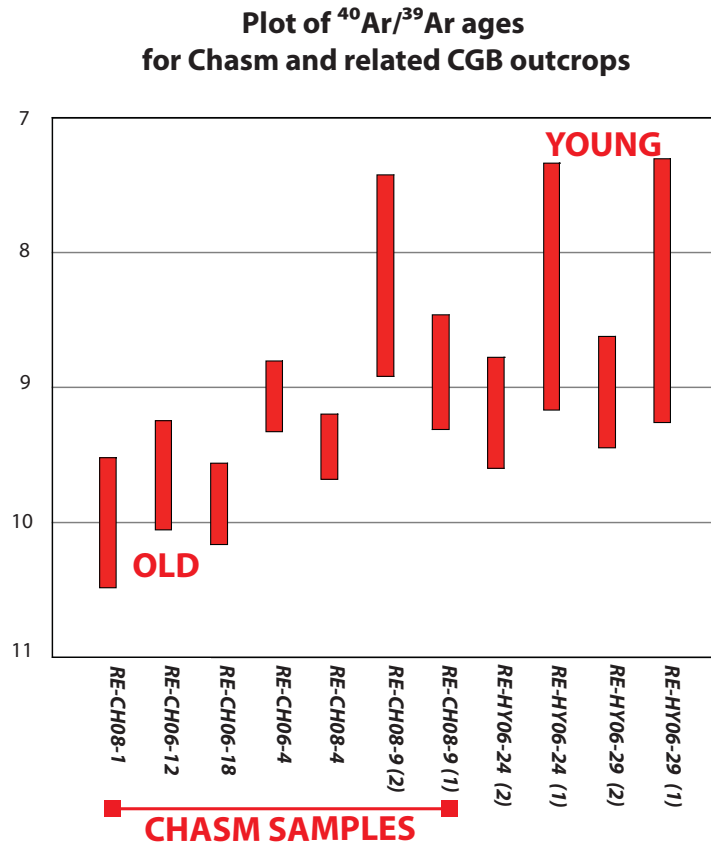


*Figure 3.14:* Plot of  $^{40}\text{Ar}/^{39}\text{Ar}$  ages for Chasm and related CGB outcrops

## **CHAPTER 4      PALEOSOL CLASSIFICATION**

---

### **4.1      INTRODUCTION**

Paleosols are ancient soils preserved in the geologic stratigraphic record. They are a common occurrence in basaltic successions and interesting to volcanologists because each sequence represents a volcanic hiatus. Paleosols are useful in volcanology where they bracket lava flows (Smith 1990), and they preserve soil-forming processes. The Chasm canyon is the only known CGB exposure to exhibit distinctive red paleosols (Farrell et al. 2007). The paleosols contain physical and chemical information useful in reconstructing paleoclimates, e.g., the type of ecological environment responsible for producing the soil, the mean annual temperature, and mean annual rainfall. However, such analysis requires multivariate datasets including that from chemical data, thin section analyses, and comparative case studies, to be able to accurately interpret attributes of the paleoclimate.

This chapter provides an overview of paleosols and the usefulness of paleosols in volcanology. Fieldwork and thin-section analyses from CGB yields a “Brunisolic soil” classification for the Chasm paleosol sample suite, a soil type, which may derive from a forest-type environment (Schaetzl and Anderson 2005). Field observations define the paleosol horizons and horizon boundaries. Laboratory study of micromorphological features illustrates the microstratigraphic relationships in the soil profiles. Combining these observations leads to a classification of the soil. Chasm paleosols differ from most Canadian soils because of the parent material. The paleosols exhibit two dominant parent materials, mafic basalt and felsic tephra. These are qualitatively described below and shown in the horizonization of the soil sites. Chasm paleosols are compared with the Miocene Porcupine basalt paleosols at the Yukon-Alaska border (Smith 1994) and the coeval Columbia River flood basalt paleosols (Sheldon 2003). Preliminary climatic interpretations such as types of vegetation, tree growth, and the soil development of the Chasm paleosols are discussed. Though preliminary climatic interpretations will be covered in this chapter, a complete paleoclimatic reconstruction is not



a part of this study.

#### **4.1.1 Paleosol overview**

Paleosols have been documented in many of the major continental flood basalt successions and igneous provinces, such as the Deccan Traps, the North Atlantic Large Igneous Province (prominent in the Faroe Islands), Karoo basin and the Columbia River Flood basalts (Smith 1990; Sheldon 2003; Sayyed and Hundekari 2006; Passey and Bell 2007; Keller et al. 2008;). For continental flood basalts, the paleosols are commonly termed “red boles”, “red beds”, “baked zones” and “red earth.” However the genetic term is paleosol and the red coloration is described by Munsell colors (Munsell 1994). Hawaii is a modern analogue for basaltic paleosols because they derive from the same parental material (Vitousek et al. 1997; Sheldon 2006). However the soil processes in Hawaii relate to its tropical and humid climates and are strongly dissimilar to the paleo-environmental conditions in interior British Columbia during Miocene time.

For the purposes of this study, soil is defined as the accumulated material on an earth surface that is altered via a combination of physical, chemical and/or biological processes (Retallack 2001). The classification of paleosols is challenging, likely due to the additional complexity of the buried soils, compared with modern fresh soils, and application of the conventional soil terminology presents a challenge in the combination of soil science and volcanology analysis required to understand the Chasm paleosols. This chapter aims to develop terminology and to classify the paleosols at Chasm.

Paleosols, literally ‘ancient soil,’ are distinguished from sediment (Retallack 2001) by evidence of roots or root casts, soil structure, and presence of soil horizons (colour variations). In contrast, a saprolite is simply a decomposing rock that progressively grades downward into coherent solid bedrock. Saprolite retains the fabric or appearance of a rock, but can be altered drastically. Regolith is a broader term, encompassing any material which ‘blankets’ the bedrock (i.e. tephra, glacial deposits, loess, organic matter, alluvium, colluvium, and soil)

(Anand and Butt 1988).

Paleosols are often subdivided into horizons; field classification of horizons is subjective as the actual horizons may be difficult to define due to compaction, weathering, and erosion. A significant amount of alteration can occur post-burial, which masks the original properties of the soil. It is simpler to recognize horizon boundaries in modern soils, where the layers have not been greatly disturbed or obliterated. The analyses of horizons in the Chasm paleosols will be described later in this chapter.

However, there are many cases in which paleosol sites will not have all three factors necessary for paleosol classification. In this case, chemical data must be obtained, and the weathering of specific elements will be useful in whether or not the material is a paleosol. In addition, study of the micromorphology of soil peds may also be used in combination with the chemistry to classify the paleosol.

Paleosols are divided into one of four classes (Schaetzl and Anderson 2005): 1) relict paleosols; 2) vetusol paleosols; 3) buried paleosols (the common type in volcanic successions); and 4) isolated paleosols. Relict paleosols are found at the modern day surface and have characteristics indicative of past environments. Vetusols can be buried or at the surface, and the climate at the time of burial is similar to the present-day climate. Isolated paleosols are a sub-category of 'buried paleosols.'

Buried paleosols occur interstratified between lavas, and are often baked by an overlying lava flow and/or tephra layer. In non-volcanological scenarios, the buried paleosols are overlain by loess, till or alluvium. The rate of burial, gradual or immediate, has direct implications for the amount of erosion.

## **4.2 PALEOSOL PROFILES AT CHASM**

In this section, I define the Master horizons at each profile site (Stn. 069, 070, 071), describe the colour and thickness of each horizon, and characterize the contacts between the horizon (i.e., horizon boundaries). The sites were chosen in the Chasm eastern composite

log section (Fig. 3.1), based on accessibility and exposure needed for detailed soil profiling. Micromorphology is a thin-section method used whereby textural and fabric analyses are carried out, and results determined, which subsequently classify the Chasm paleosols. The term 'texture' differs between the fields of soil science and volcanology. For this chapter only, the term 'texture' is specific to the soil science definition, which means proportions of different particle sizes of sand, silt and clay. The particle sizes are measured using the diameter of grain, instead of the entire grain used by geologists.

#### **4.2.1 Field methods**

Fieldwork focusing on the paleosols was carried out over two days under the guidance of soil scientists Paul Sanborn (Univ. of Northern British Columbia) and Scott Smith (Soil Classification Working Group 1998). The methods used in observation and sampling were conducted in accordance with standard soil science practices, and comprise the abbreviated following steps (the description criteria is obtained from 'Expert Committee on Soil Survey' (1983), whereas the soil horizon nomenclature is from the 'Soil Classification Working Group' (1998)):

- 1) choose profile sites
- 2) draw soil profile
- 3) define horizons
- 4) define color and thickness of each horizon with descending depth
- 5) identify and characterize the contact boundaries between horizons
- 6) record any root traces, preserved soil structures, or any other features present.

I chose stations 069 through 071 as profile sites, based on the stratigraphic context with the overlaying lava and accessibility of the paleosol. Detailed soil profiles were drawn (Figs. 4.5 and 4.6) in an approximate 2 m x 1 m format at three sites in the Chasm within the main eastern composite section (Figs. 2.2; Fig. 3.2). At each site, I used oriented and grab (unoriented) samples and samples of adjacent volcanic tephra (Tables 4.1-4.3, Figs. 4.5-

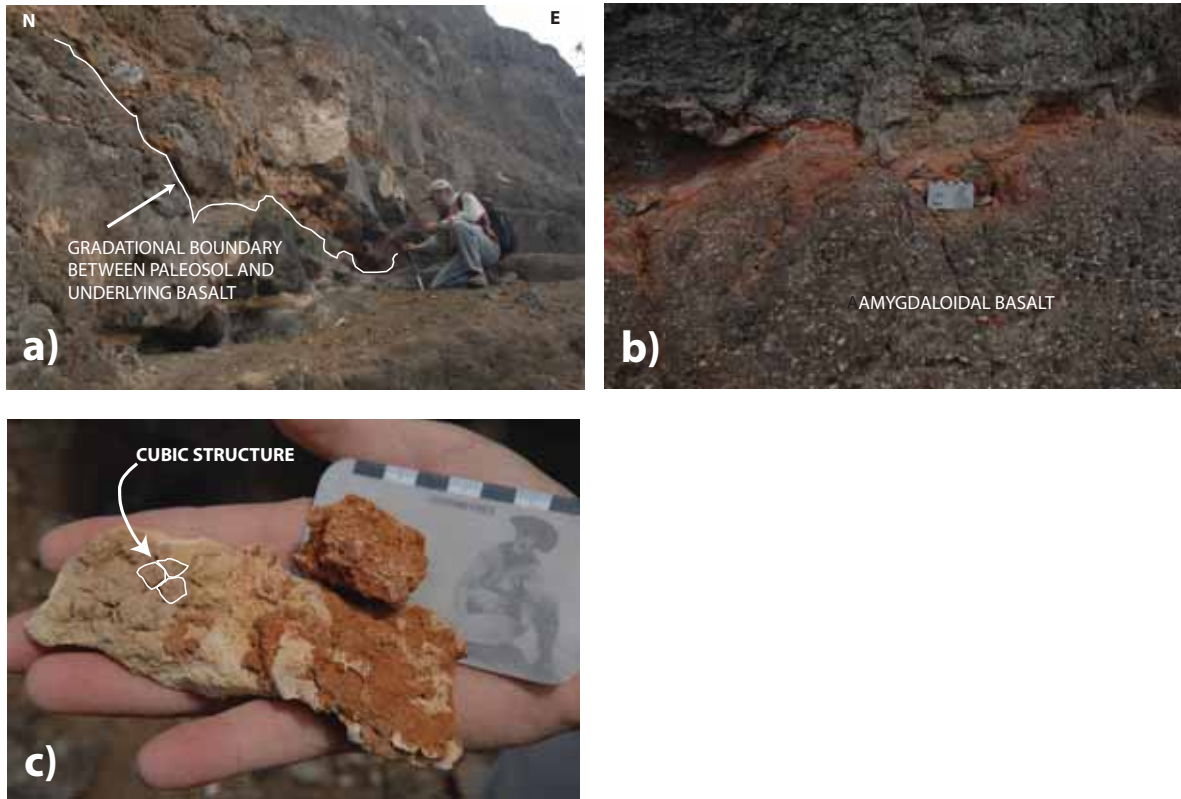


**Figure 4.1:** Field photographs of paleosols exposed at Station 68; a) Nature of contact between paleosol and the underlying basalt. Hammer for scale is 30 cm, b) Detailed view of the amygdaloidal basalt showing the diffuse boundary between the paleosol and the basalt. Scale card is 7 cm, c) Soil structures are found at Chasm. Scale card is 7 cm.

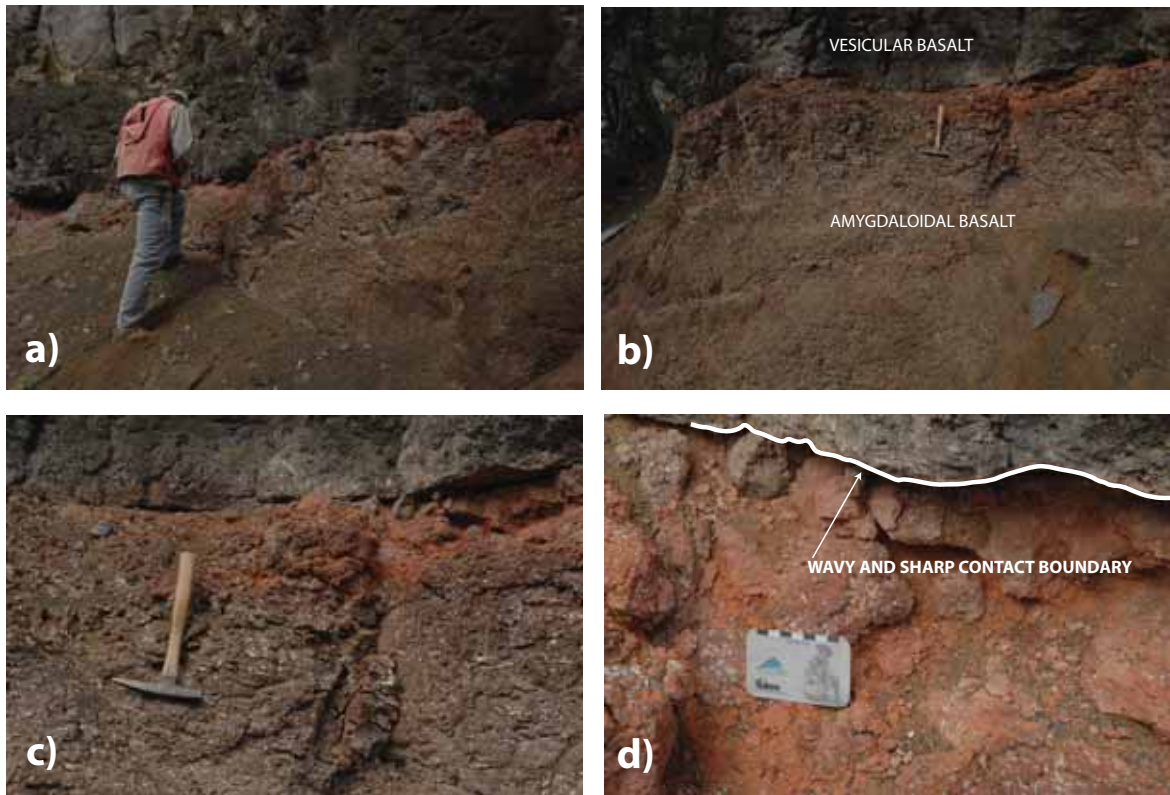


**Figure 4.2:** Field photographs of paleosol Station 69. This station is mapped in the Eastern composite log (Fig. 3.1) a) Boundary between paleosol contact and underlying basalt. Note the wavy boundary at this scale., b) Detailed view of the vesicular basalt, undulating paleosol and underlying amygdaloidal basalt emphasizing the wavy paleosol boundary, c) Detailed view of underlying amygdaloidal basalt, which is overlain by the wavy and sharp paleosol boundary, d) View of wavy and sharp contact boundary between overlying basalt and paleosol.

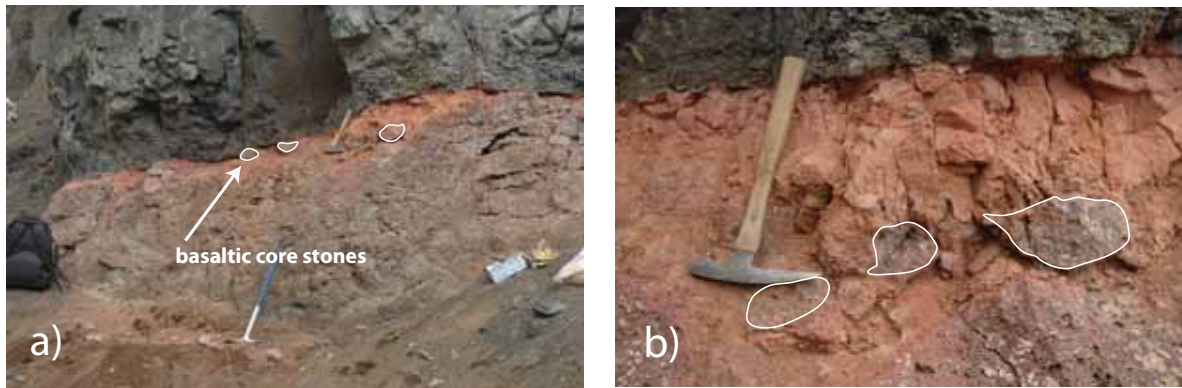


**Figure 4.3:** Field photographs at Station 70. a) Basaltic core stones are common, in the Chasm paleosols, and set into the uppermost paleosol horizon (Bmb), b) Detailed view of core stones. Hammer for scale is 30 cm. The core stones are weathered, rounded to sub-rounded, vesicular basalt.



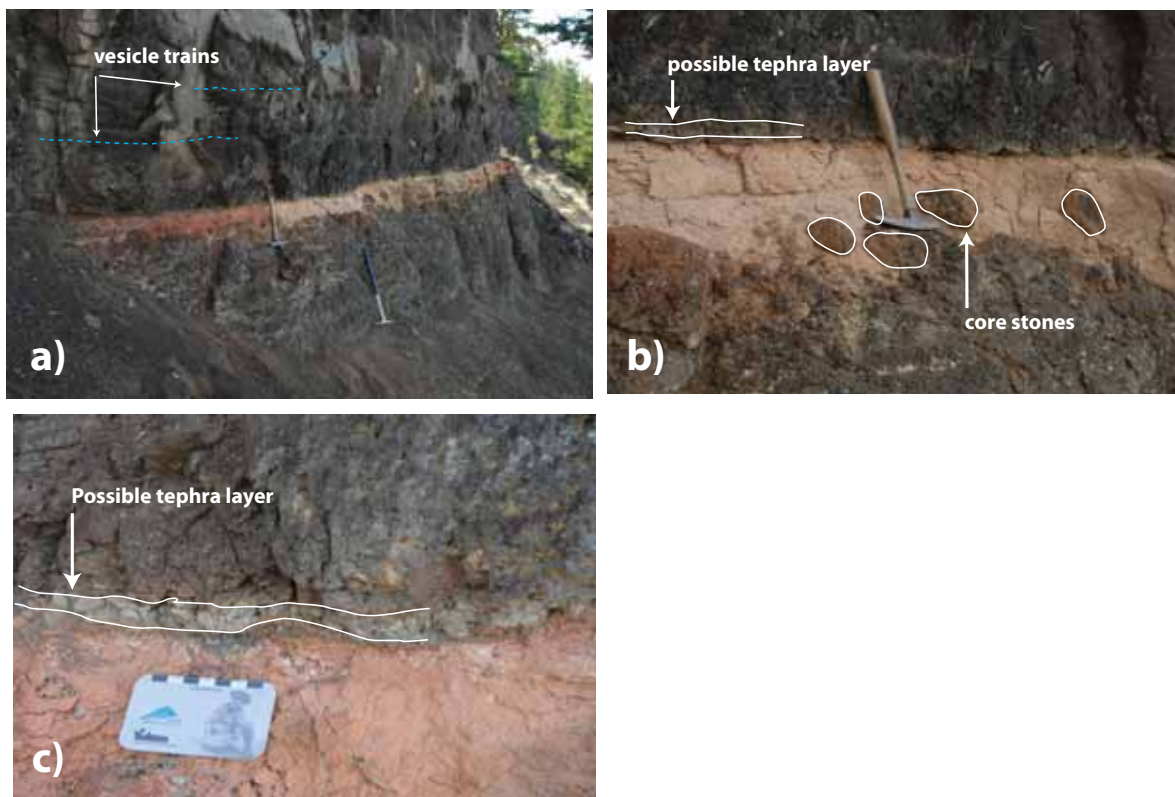


**Figure 4.4:** Field photographs of paleosol at Station 71. a) View of the abrupt, smooth boundary of the paleosol. In addition, horizontal vesicle trains are observed in the overlying basalt. b) Note the core stones in horizon, IIBmb1, and overlying tephra layer, horizon Bmb. c) Detailed view of tephra layer.

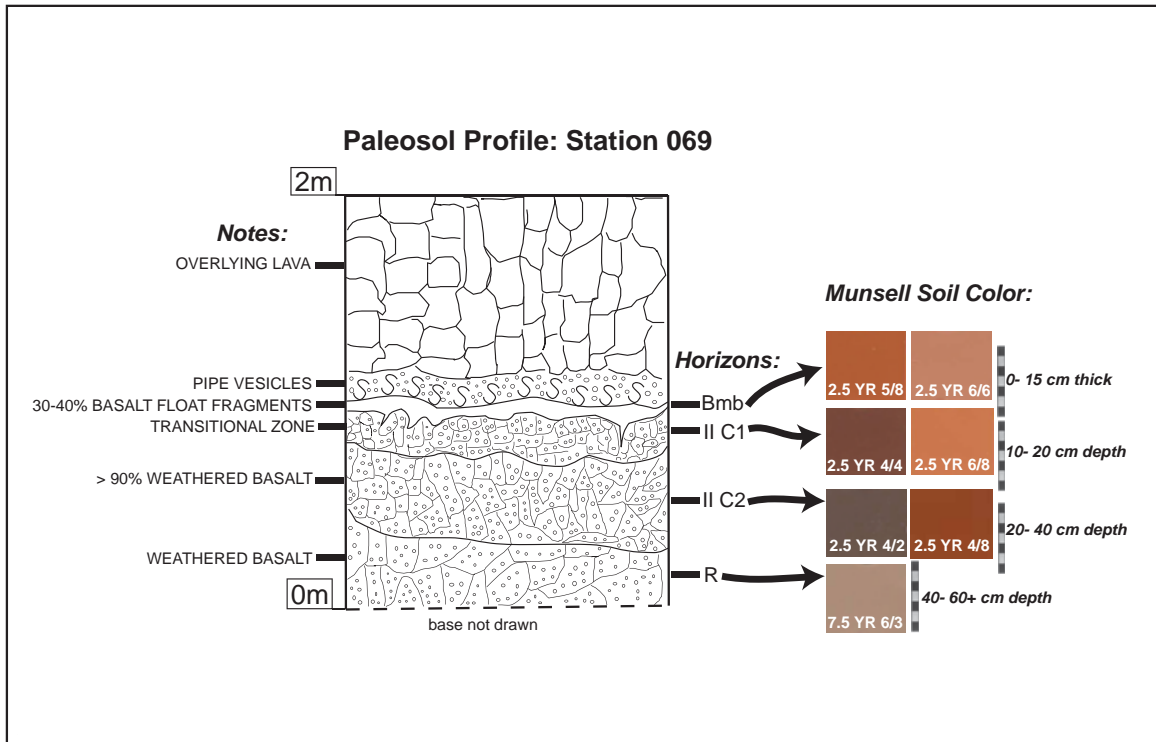


**Figure 4.5:** Paleosol profile at Station 069, Eastern Composite Log Section (Fig. 3.1). This profile is the typical paleosol found at Chasm. There is no O, A, or E horizon in this section. Horizon Bmb, means ‘B Horizon, ‘Bm’ is the subcategory delineating that the material has been altered from what the original material was to start with, and lowercase ‘b’ indicates that the paleosol is a buried paleosol. Roman numerals that are the same, in this case in the C Horizon, specifies that the material is the same, however the numbers 1 and 2 indicate that there are differences between the 2 layers, which separates them into 2 horizons (i.e. contact boundary, coloration, or other features). A C-horizon is weathered basalt; in this case, that has a hardness < 3 on the Mohs Hardness scale. The R horizon is unweathered or less weathered basalt, the only difference in the overlying lava in Stn 069, is that the R horizon is amygdaloidal. Note the Munsell colors combine hue, value, and chroma to define the soil color, which enables a standard for comparison of soil colors down the profile.



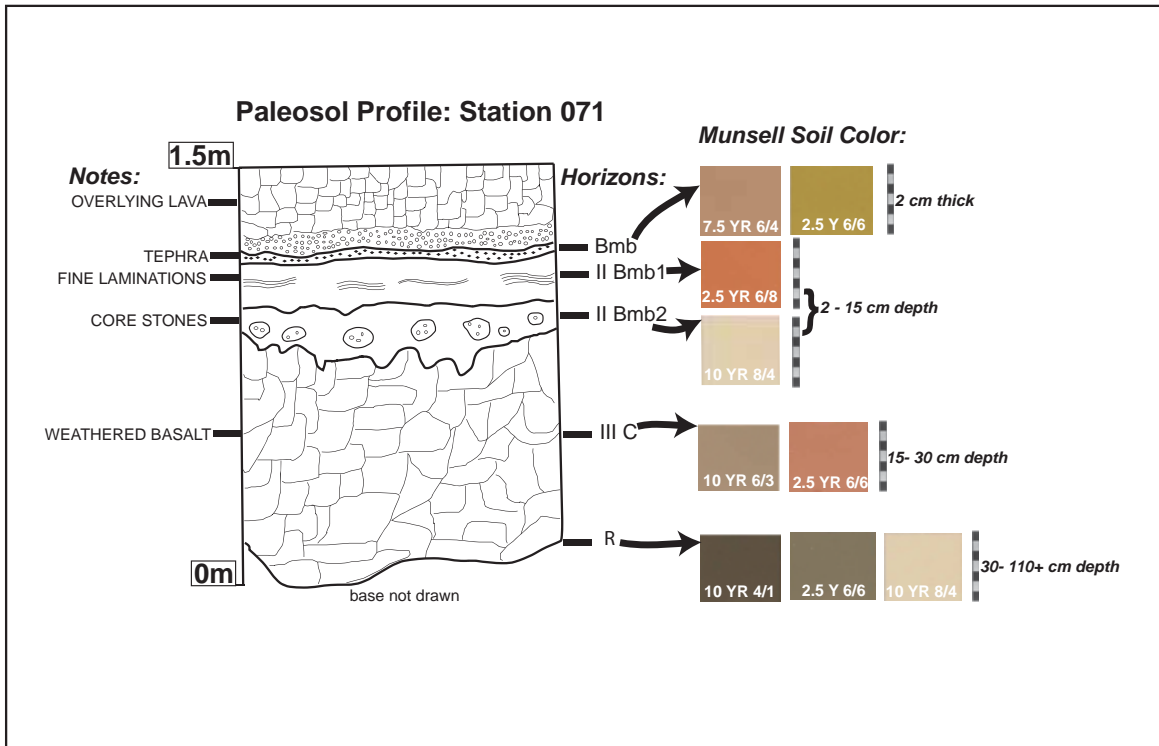


**Figure 4.6:** Paleosol profile at Station 071, in the Eastern Composite Log Section (Fig. 3.1) There is no O, A, or E horizon in this section (or in any section in Chasm) Horizon Bmb, means 'B Horizon, 'Bm' is the subcategory delineating that the material has been altered from what the original material was to start with, and lowercase 'b' indicates that the paleosol is a buried paleosol. Bmb in this profile is a tephra layer. Roman numerals that are the same, in this case in the IIBmb1 and IIBmb2 Horizon, specify that the material is the same, however the numbers 1 and 2 indicate that there are differences between the 2 layers, which separates them into 2 horizons (i.e. in this profile the 1st horizon has fine laminations whereas the 2nd horizon below has core stones). The C horizon is weathered basalt that has a hardness < 3 on the Mohs Hardness scale; it does not resemble the fine grained paleosol material of the overlying horizons, Roman numeral III denotes the different material. The R horizon is unweathered or less weathered basalt lava. Note the Munsell colors combine hue, value, and chroma to define the soil color, which enables a standard for comparison of soil colors down the profile.

## Station: 069

*Location: Chasm Provincial Park; eastern wall composite log section*

*Paleosol ID: P<sub>4</sub> (between lava 4 and 5)*

*Parent Material: Basalt (Miocene) & aeolian deposits including tephra*

*Soil Classification: Brunisol*

<i>Horizon (Sample)</i>	<i>Depth (cm)</i>	<i>Munsell Color</i>	<i>Description</i>
<b>Bmb</b> (RE-CH07-37) (RE-CH07-41)	0-15	Red (2.5 YR 5/8 d <sup>1</sup> ) Red (2.5 YR 6/6d)	very fine; grains: subrounded to rounded; 30-40% basalt float fragments; lower boundary broken ; friable
<b>IIC1</b> (RE-CH07-38) (RE-CH07-42)	10-25	Red (2.5 YR 6/8d) Dusky Red (2.5 YR 4/4d)	fine; grains: subangular to subrounded; 'transitional zone' from fine grained paleosol to weathered basalt. > 90% weathered basalt; friable
<b>IIC2</b> (RE-CH07-39) (RE-CH07-43)	25-50	Dusky Red (2.5 YR 4/2d) Dark Red (2.5 YR 4/8d)	fine; grains: subangular to subrounded; > 90% weathered basalt
<b>R</b> (RE-CH07-40) (RE-CH07-44)	40- 60+	Light Brown (7.5 YR 6/3d)	unweathered or less weathered basalt lava

<sup>1</sup> 'd' indicates a dry sample

**Table 4.1:** Paleosol samples from Station 069. This table accompanies Figure 4.5. In Bmb horizon a broken boundary means that the horizon is not laterally continuous, some parts of the horizon may be disjointed or disconnected (Soil Survey Staff, 1993).

## Station: 070

*Location: Chasm Provincial Park; eastern wall composite log section*

*Paleosol ID: (see Fig. 5)*

*Parent Material: Basalt (Miocene) & aeolian deposits including tephra*

*Soil Classification: Brunisol*

<i>Horizon (Sample)</i>	<i>Depth (cm)</i>	<i>Munsell Color</i>	<i>Description</i>
<b>Bmb</b> (RE-CH07-45) (RE-CH07-49)	0-15	Red (2.5 YR 6/6d) Red (2.5 YR 5/6d)	very fine; grains: subangular to subrounded; clear wavy boundary; core stones & basalt fragments common; friable
<b>IIC1</b> (RE-CH07-46) (RE-CH07-50)	15-30	Red (2.5 YR 6/6d) Weak red (2.5 YR 5/3d)	very fine; grains: rounded; core stones (cobble-sized); clear and broken lower boundary; weathered basalt; friable
<b>IIC2</b> (RE-CH07-47) (RE-CH07-51)	30-75	Dusky red (2.5 YR 4/3d)	fine; grains: subangular to subrounded; weathered basalt; friable
<b>IIC3</b> (RE-CH07-48) (RE-CH07-52)	75-150+	Greyish brown (10 YR 5/2d)	Weathered basalt; no "R" horizon present, since lower boundary is covered with taluvium

<sup>1</sup> 'd' indicates a dry sample

**Table 4.2:** Paleosol samples from Station 070. There is not a profile figure for this section, however it resembles Figure 4.5, which is the typical Chasm profile. In Horizon Bmb, the 'clear' boundary relates to the sharpness of the contact, which implies the thickness of the boundary to be 2-5 cm (Soil Survey Staff, 1993). The 'wavy' contact refers to the lateral continuity meaning that the crests and troughs of the contacts undulations are wider than they are deep.

## Station: 071

*Location: Chasm Provincial Park; eastern wall composite log section*

*Paleosol ID: (see fig. 5)*

*Parent Material: Basalt (Miocene) & aeolian deposits including tephra*

*Soil Classification: Brunisol*

<i>Horizon (Sample)</i>	<i>Depth (cm)</i>	<i>Munsell Color</i>	<i>Description</i>
<b>Bmb</b> (RE-CH07-53)	0-2	Light brown (7.5 YR 6/4d) Olive yellow (2.5 Y 6/6d)	tephra layer; very fine; grains: subangular to subrounded; laterally continuous for 7 m; retains uniform thickness; very fine gr., subangular to subrounded; possible platy structure; abrupt, smooth boundary
<b>II Bmb1</b> (RE-CH07-54) (RE-CH07-58)	2-15	Red (2.5 YR 6/8d)	very fine; grains: subangular to subrounded; abrupt; irregular boundary; very fine grained; subangular to subrounded; platy due to present-day weathering
<b>II Bmb2</b> (RE-CH07-55) (RE-CH07-59)	2-15	Very pale brown (10 YR 8/4d)	fine; strong; grains: subangular; medium platy; platy units aligned parallel to the face of exposure (due to present-day weathering), > 10% core stones (cobble-sized) gradational contact;
<b>IIIC</b> (RE-CH07-56) (RE-CH07-60)	15-30	Pale brown (10 YR 6/3d)	'Transistion zone' to weathered basalt; gradual; wavy boundary
<b>R</b> (RE-CH07-57) (RE-CH07-61)	30- 110+	Olive yellow (2.5 Y 6/6d) Dark grey (10 YR 4/1d) Very pale brown (10 YR 8/4d)	Coherent basalt

**Table 4.3:** Paleosol samples from Station 071. This table accompanies Figure 4.6. Horizon Bmb is an abrupt, smooth boundary.

4.6) to define horizon boundaries, establish the relative thickness of each horizon, describe the contact areas between horizons, and describe textures. Below, I review each step in the method and subsequently describe the results from each Chasm sampling/profile site.

Horizons are categorized into broader 'Major mineral horizons' and subordinate categories, denoted by a lowercased letter following the Master horizon (e.g., Xx), which adds pedogenic (soil-forming processes) information to the Master horizon (Retallack 2001).

The major horizons relevant to this study are: (A, Ae, B, C, R):

- 1) 'A' horizon (i.e., in Canadian soils either 'Ah' grassland soil with organic matter and roots or 'Ae' forest soils, which show the removal of clay and intensive weathering of primary minerals)
- 2) 'Ae' horizon (i.e., usually lighter in color, characterized by less organic matter, clays and iron and aluminum oxides)
- 3) 'B' horizon (i.e., the descriptive feature is the horizon does not resemble the rock structure, common ped structures can be present including granular, blocky or prismatic.
- 4) 'C' horizon (i.e., more weathered than bedrock, characterized by a hardness of 3 on the Mohs Hardness scale)
- 5) 'R' horizon (i.e., coherent bedrock).

Organic horizons (> 17% organic carbon) may or may not survive burial, and are often absent in paleosols. Different types of organic horizons are recognized depending on whether the original setting was either well-drained or subject to prolonged wet conditions. Soils that do not have all of these Master horizons can still be considered complete profiles, since diverse climates yield different soil profiles (Retallack 2001). In soil science methodology, a section is logged downward from the initial horizon.

Colour is categorized by using the Munsell Soil Color Chart (1994), and is commonly the first criterion used to assess the soil. The Munsell chart combines hue, value and chroma to develop a comprehensive range of colors to describe soils; the chart serves as a standard to relate color changes in the horizons. Importantly, colour distinctions serve as a method to differentiate between horizons.

For example for a reddish brown soil labelled 5 YR 4/3, the hue is 5YR, value is 4, and chroma is 3. With depth, elements are leached out and the coloration changes. For basaltic weathering, nearly all of Ca and Na, but less than half of Fe, K, and Al are leached out the rock (Bain et al. 1980). Ca and Na do not affect colour, soil colours usually are affected by the amount of organic matter present, redox (e.g., redding when soils oxidize), and addition of materials that coat primary grains.

### ***Textural analysis: micromorphology***

Micromorphology refers to microscopic observations, usually in thin sections. Micromorphology methods are useful in that they help identify fabrics and composition of soils, which may be used to distinguish one soil from another (Stoops 2003). Micromorphology is also used in conjunction with modeling to reconstruct climate. There are both qualitative and quantitative methods are that being developed (Kemp 1999; Sheldon 2003). Specific paleoclimatic information can be discerned only after an extensive study including the chemical weathering of the basalt and tephra deposits, microstructures, and other field features such as roots (Sheldon 2003). For a complete reconstruction, researchers have mostly used comparative biological data such as organic matter, fossil organisms or flora, to reconstruct paleo-climates. As no organic matter, roots, fossils, or flora have been observed at Chasm to date, a complete investigation was not attempted as part of this study. However, micromorphologies can be used to make preliminary climate interpretations (Kemp 1999; Kemp and Zarate 2000). In the macroscopic study of soil horizons at Chasm, there is insufficient field data to completely characterize the paleosols (e.g., the absence of roots or traces of roots in the profiles). Here, micromorphology methods are used to test whether the material in-between the Chasm basalts interpreted as lava flows are in fact paleosols.

### ***Methodology: 'fabric' studies***

The study of micromorphology is divided into two parts, fabric studies and compositional studies (Stoops 2003). In this study, I use fabric studies to evaluate the

micromorphologies of the Chasm suite of paleosols. The test of whether inter-flow layers are paleosols involved a micromorphological analysis of each horizon at all three sampling locations.

Fabric studies describe the different elements of the soil fabric. Bullock et al. (1985) define soil fabric as a comprehensive organization of the soil, not only an emphasis on the large grains, but the entire arrangement in the sample. Spatial relationships, frequency of elements, size, and shapes of features are all indicative of the processes that formed and weathered the soil. The field of fabric studies within micromorphology is complex and detail-specific, and hosts a variety of terms to describe all relevant features in the profile.

Soil science methods were followed for sampling and the preparation of thin sections, for optimal preservation of the microstratigraphy (Kemp 1999). Paleosols were sampled with known orientation and stratigraphic context in the soil profile. Each sample was taken from the middle of the defined horizon (Figs. 4.5 and 4.6) (Stoops 2003). A metal frame was inserted into the soil to keep the samples secure, oriented and the microstructures undisturbed. The microstratigraphic relationships are extremely fragile, and the paleosol material friable, especially the upper horizons. To preserve such fragile textures, the samples were impregnated with resin, and cut into lantern-sized thin sections at standard thin section thicknesses.

A total of sixteen Chasm samples were analyzed in the micromorphological study. The thin section analyses were carried out in the laboratory facilities at the University of Northern British Columbia. Components for the Chasm paleosols (Stations 069, 070, 071) are described using the Stoops (2003) reference collection of photographs illustrating the fabric complexities of paleosols (Table 4.4) For comparative purposes, slides from the stations were photographed at the same magnification (5x) to compare the types and relative abundances of the microstructures in each profile.

MICROMORPHOLOGY DATA		
Sample No.	Horizon	Summary of Observations:
<b>Station 069</b>		
RE-CH07-37	Bmb	~5% of quartz; Fe clay coating fragments; distinctive Mn rim around qtz crystal; granular clusters of Fe; accomodating planes; nodule of Mn with a hypo-coating of Fe; infilling of an Fe channel
RE-CH07-38	IIC1	similar to weathered basalt; basaltic clasts are vesicular; Fe clay coating fragments; Mn coating around the rim of the amygdules.
RE-CH07-39	IIC2	no soil textures preserved; weathered basalt
RE-CH07-40	R	no soil textures preserved; weathered basalt
<b>Station 070</b>		
RE-CH07-45	Bmb	Fe nodules (honey brown colour); laminations in Fe channel; Fe papules detached from original coating
<b>Station 071</b>		
RE-CH07-54	IIBmb1	platy structure; appears to have an alignment of clay coatings/nodules; ribbon-like (infilled channel) of the manganese coating; fragments of coatings observed; zonation in coating, light to dark honey brown colouration visible
RE-CH07-55	IIBmb2	platy strcuture; high % of quartz (~20%); sub-angular basalt fragments; olivine microphenocrysts; fragments of nodules and coatings; clusters of fe coating fragments; coating (rim) surrounding basalt clasts; fine laminations seen; example of micro-platy fabric
RE-CH07-56	IIIC	Fe coating fragments; Mn rims around vesicles in basalt clasts; accomodating planes; absence of quartz; showing typical weathered basalt (olivine, plag etc.)
RE-CH07-57	R	no soil textures preserved; weathered basalt

**Table 4.4:** Micromorphological data



#### **4.2.2 Horizon definition**

Horizons identification is key to analyzing modern soil profiles and paleosols. A horizon is a soil layer that is approximately parallel to the ground, and distinguished from overlying and underlying layers by physical, biological and chemical factors (Chesworth, 2008). The Canadian soil classification scheme (<http://sis.agr.gc.ca/cansis/taxa/cssc3/chpt2.html>), to define the soil horizons in the Chasm profiles. Using this scheme, I have defined soil horizons from all 3 sampling locations at Chasm (Figs. 4.5 and Fig. 4.6). At Chasm, because the O, A and E horizons are missing, the B-horizon is the initial horizon.

#### **4.2.3 Colour and thickness of horizons**

Colours for the paleosols observed at all 3 sampling locations are shown in Figures 4.5 and 4.6. In general, B-horizons range from red to purple; usually two different colors are described for this horizon. In all three Chasm stations, at least 1 Bmb horizon is described (Figs. 4.5, 4.6; Tables 4.1-4.3). The lowercase 'm' denotes that it is either has ped structures (i.e., an aggregate of grains that are separated from the adjacent ped based on a zone of weakness) or is colored appropriately for a B Horizon. The lowercase 'b' signifies that the soil is a buried soil. Once that is initially specified, all of the remaining horizons with depth are inferred to be 'buried' horizons.

Stations 069, 070, and 071 have single or multiple 'C' horizons (Figs. 4.5-4.6; Tables 4.1-4.3). The 'C' horizons are challenging to categorize on account of the differentiation between weathered basalt with unweathered basalt lava ('R'). These have been characterized as weathered basalt, which are distinguishable from the overlying basalt lava (above initial paleosol horizon, on the basis of the relative degree of weathering (Figs. 4.5-4.6; Tables 4.1-4.3). This interpretation of 'C' rather than 'R' is justified for the following reasons:

- 1) Hardness: 'C' horizons have a hardness value of less than 3 of the Mohs scale (i.e., calcite range), and can be sampled with a spade, whereas the underlying basalt lava that is less weathered and must be sampled with a rock hammer or a sledgehammer.

2) Fractures: There are numerous fractures in the Chasm 'C' horizons. The fractures are highly amygdaloidal, and coloration has a reddish hue compared to the grey-brown of the 'R' horizon.

3) Features: Rounded to sub-rounded basaltic core stones are common and are interpreted as basaltic fragments that have been ripped up from the underlying lava. Station 071 includes a tephra layer, which is the initial horizon, and then below it fine laminations are present, though larger-scale bedding is absent (Fig. 4.6; Table 4.3).

The 'R' horizon represents coherent rock, which must have hardness greater than 3 on the Mohs scale. The Chasm basalt is significantly harder than the 3 threshold, on account of the minerals olivine, pyroxene, and oxides, which all have a hardness greater than 6. These horizons are all varying percentages of vesicularity, however the vesicles have been in-filled (amygdales). There are less fractures in this final horizon, the basalt is cemented together, and no longer brittle. The coloration of this horizon is typically vastly different from the initial horizon (Figs. 4.5 and 4.6); there are no longer any 2.5 YR hues.

Providing that the initial materials were the same, and similar environments prevailed, older soils will have thicker A and B-horizons. The thickness of the horizons is relevant in describing soils; commonly B-horizons are <2 m (Retallack 2001), and the Chasm paleosols fit within this range. Each Chasm horizon ranges in thickness between 1- 40 cm. The total thickness of the paleosols range from <0.5-3 m. Soil profiles (Fig. 4.5 and 4.6) graphically show the thickness variations between stations 069 and 071.

#### **4.2.4 Horizon boundaries**

The nature of the contacts between the horizons is important, for these soil boundaries help interpretation of the soil-forming processes. The horizon boundary is always referring to the lower boundary. There are two broad categories within horizon boundaries: boundary sharpness and boundary lateral continuity (Retallack 2001).

Generally, the uppermost horizon has a sharp boundary, whereas the successive lower horizons have gradational contacts (Retallack 2001). All three of the study locations exhibit a relatively sharp boundary, which underlie the initial paleosol horizon (Tables 4.1-4.3).

Laterally contacts are typically undulating, irregular or broken and the paleosols commonly infill cracks within underlying lava units (Figs. 4.5 and 4.6). Texture (grain-size) follows the trend of finer grained at the initial horizon and coarser with depth. Two soil profiles (Figs. 4.5 and Fig 4.6) have been drawn to show the different types of profiles at Chasm, Station 69 is a typical profile, whereas Station 71 is a volcanic ash-rich paleosol.

Clastic dikes are a recurrent large-scale feature associated with the paleosols (Fig. 3.5c). The dikes are observed as vertical cracks that are in-filled with paleosol material. The dikes do not represent discrete features in time and space; rather, the dikes are commonly laterally connected with a paleosol horizon. Based on larger-scaled mapping, the Chasm paleosols are pockets which are commonly deeper than wide, and may be considered 'irregular' (e.g., Fig. 3.2.c). The pockets are approximately 1.5 to 5 m depth, however this is variable in the expanse of the canyon. The average depth of the pocket (clastic dike) is 2.2 m.

The three Chasm paleosol sites appear laterally uniform. However, additional fieldwork across the entire Chasm canyon reveals more complexity. When mapping the paleosols laterally, it is common for a paleosol to truncate (Figs. 5.2, 5.3 and 5.4), terminate, or show discontinuity at either the present day surface or mid-section. Moreover, paleosols appear locally 'welded', meaning there is a visible but blurred boundary where two separate paleosol profiles (older and younger soil profiles) are mixed together. Larger scale mapping of the paleosols reveals more lateral irregularities, and will be further discussed in Chapter 5.

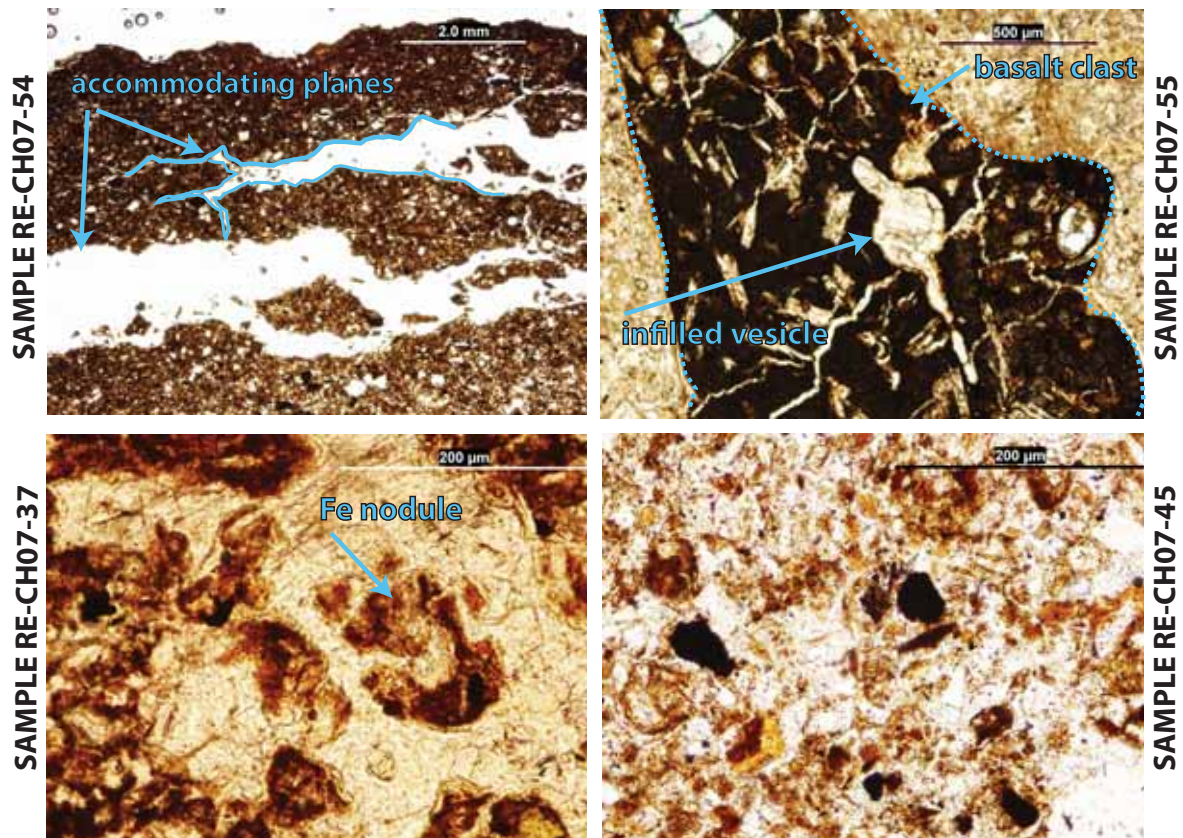


**Figure 4.7:** Summarizing the key soil micromorphology present in the Chasm paleosols. Four oriented thin sections showing the micromorphological diversity at Chasm. Sample RE-CH07-54 (stn. 071 / horizon IIBmb1) shows accommodating planes that are sub-parallel to the underlying basalt; RE-CH07-55 (stn. 71 / horizon IIBmb2) is an example of a corestone (vesicular basalt) set into the finer-grained matrix of the paleosol; RE-CH07-37 (stn. 069 / horizon Bmb) is a mixture of rod-like, globular, and blocky particles; RE-CH07-47 (stn. 70 / horizon Bmb) shows a poorly sorted sample, with Fe, Mn and clay coatings present.



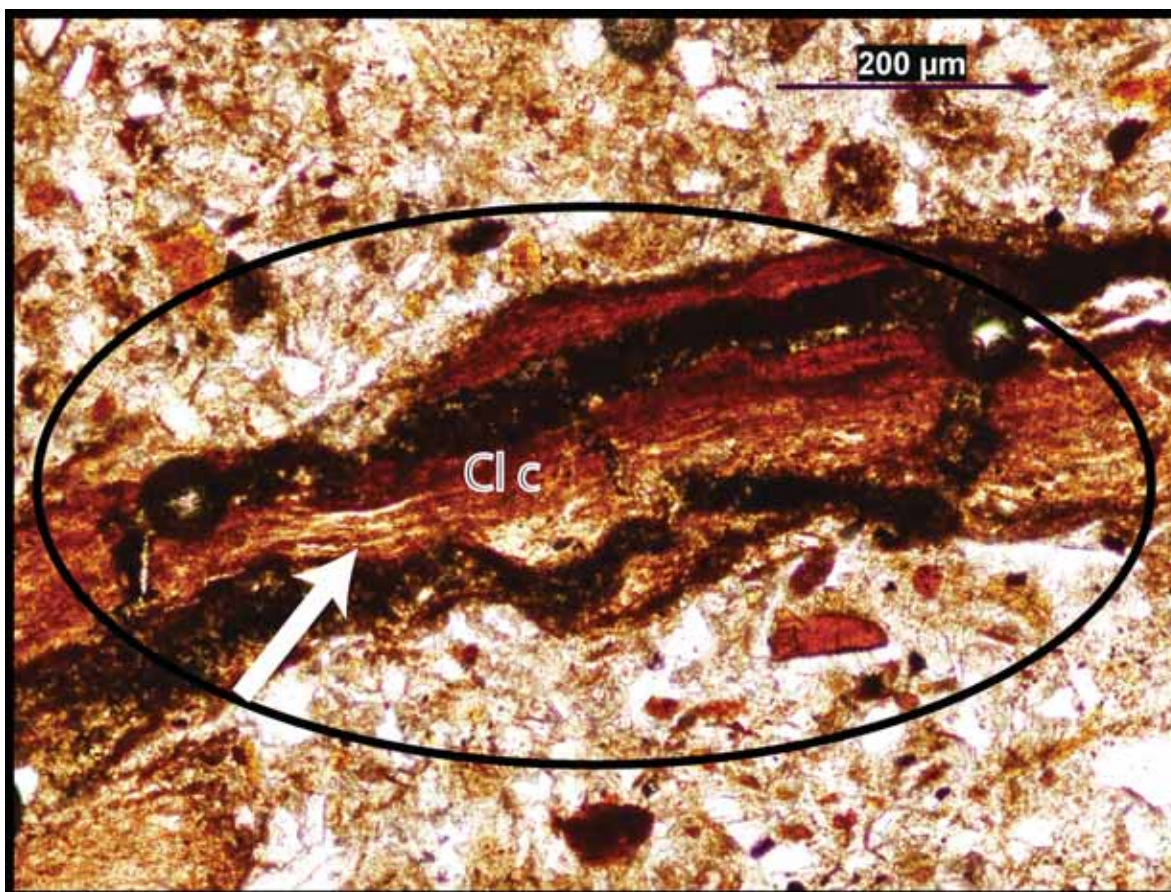


*Figure 4.8:* Clay coating (Cl c) with fine laminations visible. Sample RE-CH07-54.

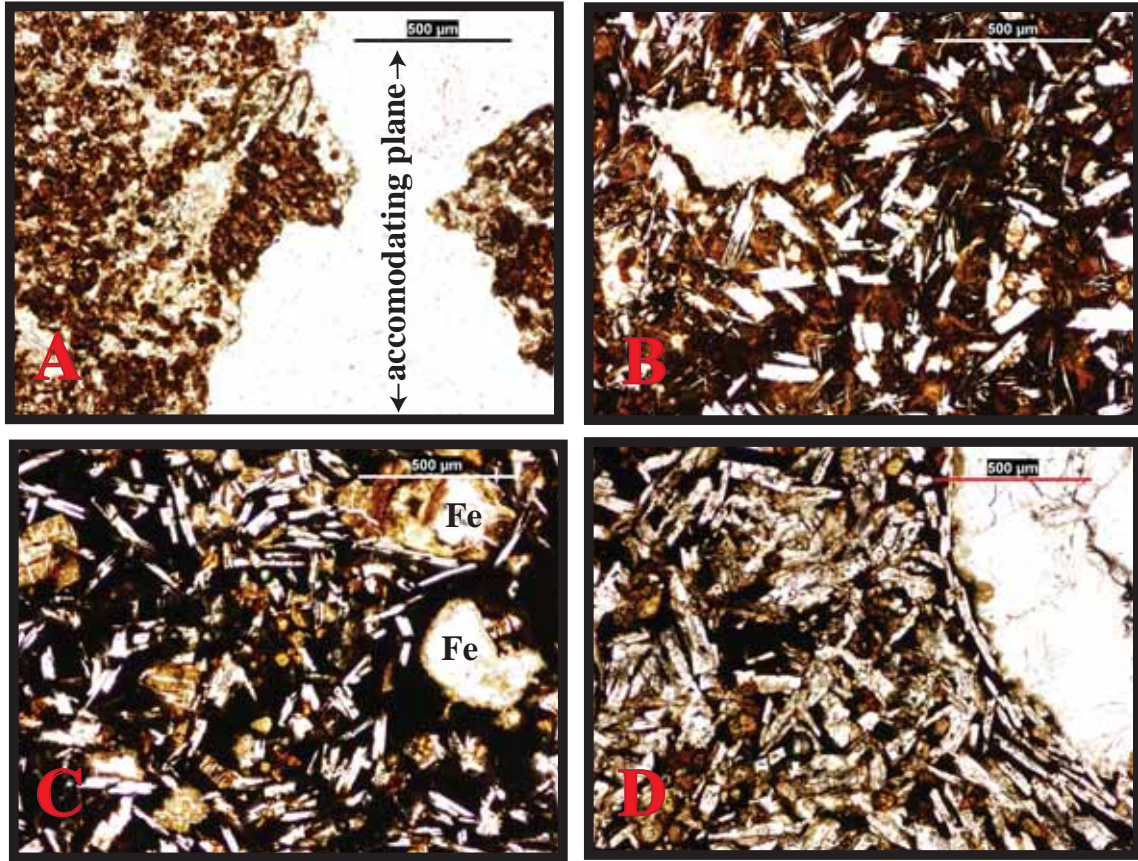


**Figure 4.9:** Micromorphology thin section plate at Station 69. All sections are taken from oriented samples. A is the Bmb horizon, B is the IIC1 Horizon, C is the IIC2 Horizon, and D is the R horizon; samples taken top to bottom in section profile. All photomicrographs at 5x magnification. A) A vertical accommodating plane (Sample: RE-CH07-37-A); B) Small Fe and Mn nodules make up the reddish brown and back globulars (Sample: RE-CH07-38-B); C) Weathered basalt with two prominent Fe coatings (Sample: RE-CH07-39-C), D) Weathered basalt, regolith, where the fabric of the basalt is present (Sample: RE-CH07-40-D).



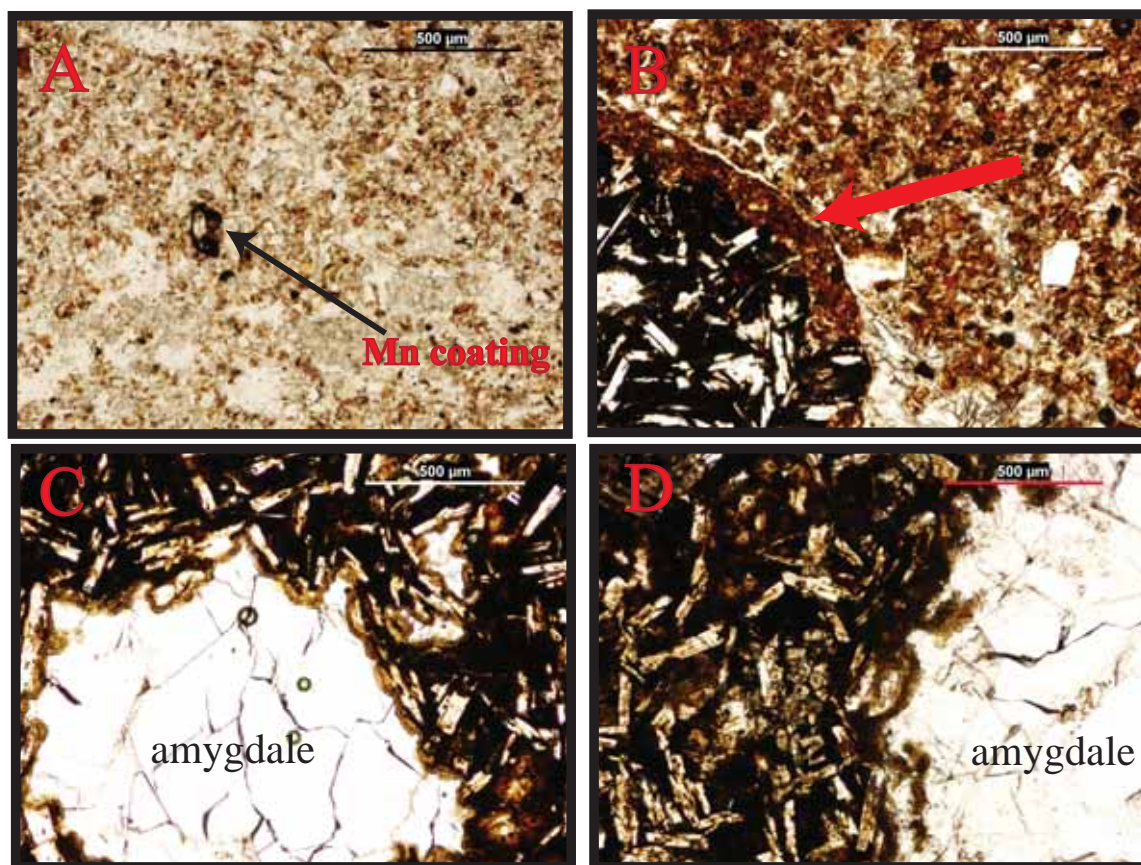


**Figure 4.10:** Micromorphology thin section plate at Station 70. All sections are taken from oriented samples. A is the Bmb horizon, B is the IIC1 Horizon, C is the IIC2 Horizon, and D is the IIC3 Horizon; samples taken top to bottom in section profile. All photomicrographs at 5x magnification. A) Shows a sub-rounded Mn coating (Sample: RE-CH07-45-A); B) Shows amygdale with a well-defined rim of Fe (Samples: RE-CH07-46-B); C) Weathered basalt with amygdale rimmed with an Fe coating (Sample: RE-CH07-47-C); D) Weathered basalt with amygdale (Samples: RE-CH07-48-D).

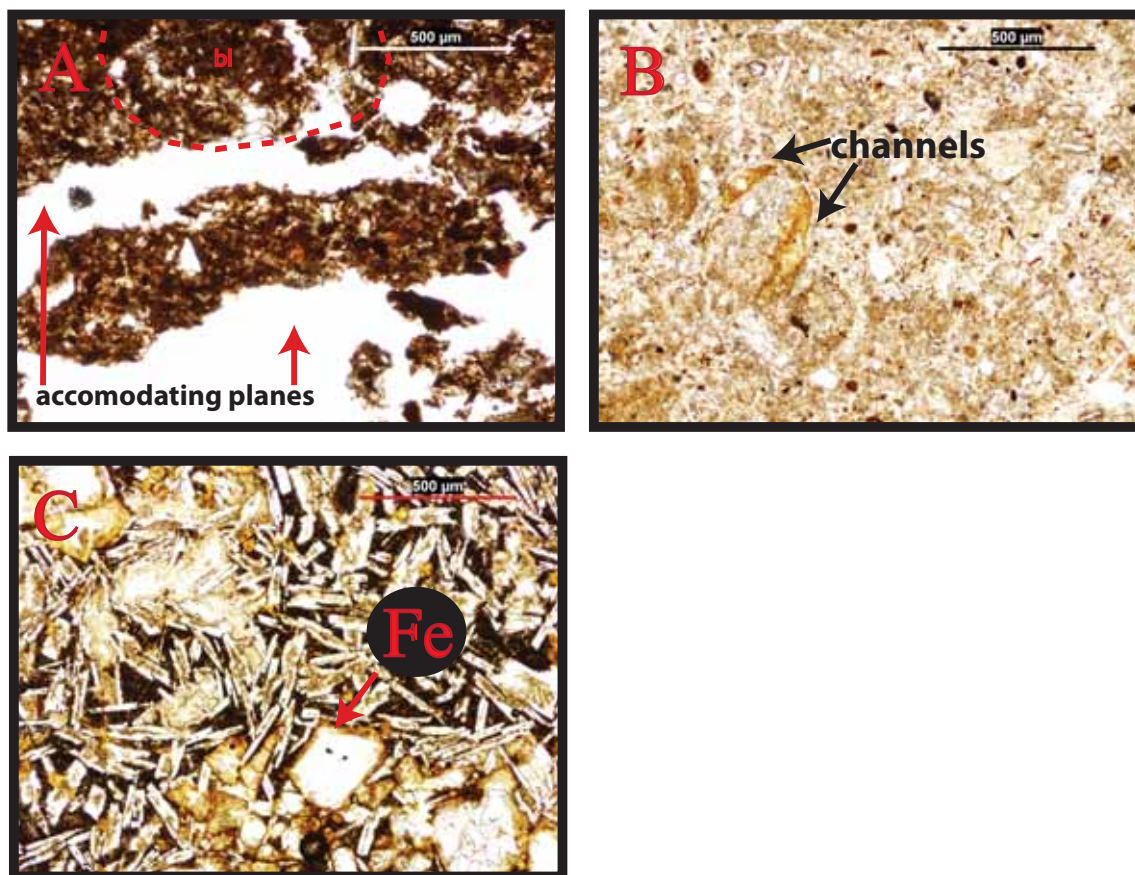


**Figure 4.11:** Micromorphology thin section plate at Station 71. All sections taken from oriented samples. A is the IIBmb1 horizon, B is the IIBmb2 Horizon, C is the IIIC Horizon; samples taken top to bottom in section profile. All photomicrographs at 5x magnification. A) Shows two accommodating planes sub-parallel to the horizon. Inside the dashed line is an example of blocky structure (Sample: RE-CH07-54-A); B) Two Fe channels are visible in this section. Darker sub-rounded particles are Mn coatings (Sample: RE-CH07-55-B); C) Predominately weathered basalt with Fe coatings surrounding many of the grains (Sample: RE-CH07-56-C).



#### **4.2.5 Results**

In this section, I will describe the aggregation, voids, microstructure, and pedofeatures of the horizons at Chasm (Stoops 2003). All of these terms will be defined, and described based on the findings within the Chasm paleosols.

##### ***Aggregation of Chasm paleosols***

Aggregation is how the soil partings create void spaces (i.e., peds); and are broken along areas of weakness in the ped (Stoops 2003). There can be granular peds, which are oval shaped and non-porous, or blocky peds (similar to larger-scaled blocky structure observed in the field (Stn. 068; Fig. 4.11a). These blocky peds are typical found lower in the soil profile in the B Horizon. This is observed at the horizon at station 068. The blocky peds are glued together by coatings that derive from the overlying horizon. These coatings are visible in thin sections (Fe and Mn) and fills in the voids in the pore spaces (Fig. 4.10a). At Chasm, angular to subangular blocky peds have been observed in thin-section (Fig. 4.11a), seen with angular edges of the blocks. Granular aggregates are more common and are common in the uppermost horizons (Figs. 4.9c, 4.9d, 4.11a and 4.11b). There are numerous ways that a soil can form differently shaped aggregates, from processes associated with amount of organic material, any microbial activity, freeze / thaw cycles and texture (grain-size). When the profile is devoid of aggregates, the horizon is deemed ‘massive.’ Observed soil peds at Chasm, expose a soil-forming process, confirming the classification of a paleosol.

##### ***Voids***

The voids observed in the Chasm samples, part of the fabric of the paleosol, yielded interesting features such as channels, vughs, and planes. Channels are ‘tubular smooth voids’ (Stoops 2003), and are commonly seen as channel fragments in the Chasm specimens (Fig. 4.8; Sample RE-CH07-37). These channels form shapes such as arches or cylinders, which help to discriminate channels from aggregates. Vesicles are seen where there are basaltic

clasts set into the paleosol matrix (Fig. 4.8; Sample RE-CH07-55). Typically, only there is only a 5% modal abundance of these basalt clasts, however when the abundance is higher the classification of a vesicular microstructure can be applied (Table 4.4).

X-ray diffraction methods helped identify the secondary mineralization infilling the vesicles as the zeolites chabazite-Ca and phillipsite (Appendix E). This occurred after burial, zeolites are unusual in soils, except where salinity is present.

### ***Microstructure***

There are two kinds of microstructures in the peds of Chasm: fractures and crumb microstructures.

Fractures in the soil are highlighted by a series/sequence of planes. If the observed planes can be hypothetically reassembled (puzzle-like), the planes are said to ‘accommodate’ one another. Accommodating planes are technically described as ‘elongated poroids’ (Stoops 2003) that have one or more sharp edges as the plane terminates in the section. These planes can form with the shrinking and swelling of clays in the horizons (usually the horizon with the highest clay content (Bt) horizons, however in our case, Bm horizons). Accommodating planes are typical in the Chasm suite (Fig. 4.8; Sample RE-CH07-54; Fig. 4.9a, Fig. 4.11aa). These planes are only identified in the initial horizon for each station.

Crumb microstructure is also recognized (Fig. 4.8; Sample RE-CH07-45). It comprises largely rounded aggregates, which lack accommodation structures, and locally some particles merge themselves together to form a rounded aggregate (Stoops 2003).

### ***Pedofeatures***

In paleosols, the most commonly documented micromorphological feature is clay coatings (pedofeatures; Kemp 1999). Iron and manganese coatings are observed in paleosols at every station in the Chasm suite, however clay coatings are less common. At Chasm, there are Fe and Mn coatings, where a rim is observed around the surface of the void (Stoops

2003). Clay coatings are birefringent under cross-polars and form through translocation of clay particles downward through the profile. Laminations are rare, but occur inside the clay coatings (Fig. 4.8: Station 71, Sample RE-CH07-54). Clay coatings are relict of soil processes, specifically the translocation of clay, forest settings need more water than grassland environments, clay coatings are suggestive a forest setting, however more work is necessary for a comprehensive classification.

### ***Parent Material***

The Chasm paleosol suite comprises a complex mix of two distinctive parent materials, mafic basalt and felsic tephra. Basaltic parent materials generally yield a higher clay content (Wilson 2006); clay minerals such as montmorillonite (smectite) become present in the post-burial alteration process. XRD analyses of sample RE-CH07-58 (Station 071; horizon IIBmb1) indicated dominant peaks of analcime (associated with zeolites), plagioclase, quartz, and zeolites (chabazite-Ca, phillipsite-K and tridymite). Smectite (montmorillonite), K-feldspar, muscovite, and grunerite are present in smaller proportions (Appendix E). With the higher clay content, this implies larger water retention, and studies have shown that basaltic soils hold 40% water content, compared to 17% for granitic soils (Olowolafe 2002), however water retention varies with the age of the soil. Water retention can expedite weathering of the basaltic minerals into soil. The parent material controls grain-size, and a basaltic parent will yield a finer-grained soil, opposed to a granitic parent (Wilson 2006). Basaltic weathering studies have measured the different rates of breakdown of the specific oxides, emphasizing the stages of weathering, which produce clay minerals (Bain et al. 1980; Eggleton et al. 1987; Wilson 2006).

The felsic ash component was identified in the field, incorporated into the soil profile, and confirmed as tephra in the laboratory using immersions oils, as a preliminary means of classifying the material. The ash component is found in all horizons down to the 'C' horizon of most Chasm profiles, and is inferred to the present in all P facies (refer to Chapter 3). The

Chasm paleosols are unique when compared to other Canadian soils due to the mixed nature of these parent materials. The smaller tephra fraction elicits a more complex classification and climatic interpretation. The Canadian soil classification does not have a separate classification for ash rich soils, however the US soil classification uses the term Andisols to name these soils. The US soil classification equivalent for a Brunisol is an Inceptisol.

Compositionally, the paleosols are predominately made up of weathered basalt (consistent mineralogy), however there are some non-basaltic minerals, such as quartz, which are interpreted to be introduced into the paleosols from a foreign location by wind or water. Chasm paleosols were chemically analyzed using citrate-dithionite-bicarbonate (CDB) extraction of Fe oxides. CDB extracts crystalline Fe oxides and hydroxides (hematite, goethite), non-crystalline Fe (ferrihydrite), and Fe (organically complexed). The paleosol chemistry is described in section 4.35.

## **4.3 DISCUSSION**

Horizon types, thicknesses, contacts, and textures in Chasm paleosols aid in interpreting the length of time between lava flows, soil maturity and paleo-climate.

### **4.3.1 Duration of hiatuses between lava flow fields**

The nature and the thicknesses of each horizon indicate the duration of time between lavas, however warmer climates accumulate soil faster and post-burial compaction with the overlying lava affects preserved thickness. The Chasm paleosols did not have adequate time to develop the soil before burial from the next lava flow. Age dates for lavas enclosing two paleosols provide minimum and maximum estimates for paleosol development for uppermost and lowest paleosols in the East Log section (Fig. 4.12). Development of the lowest exposed paleosol, occurred before the overlying lava (Sample: RE-CH06-12) dated at  $9.65 \pm 0.40$  Ma and after an underlying lava (Sample RE-CH08-1), dated at  $10.00 \pm 0.48$  Ma. The duration ranges between 0.35 m.y. and, 1.23 m.y. (Fig. 4.12).

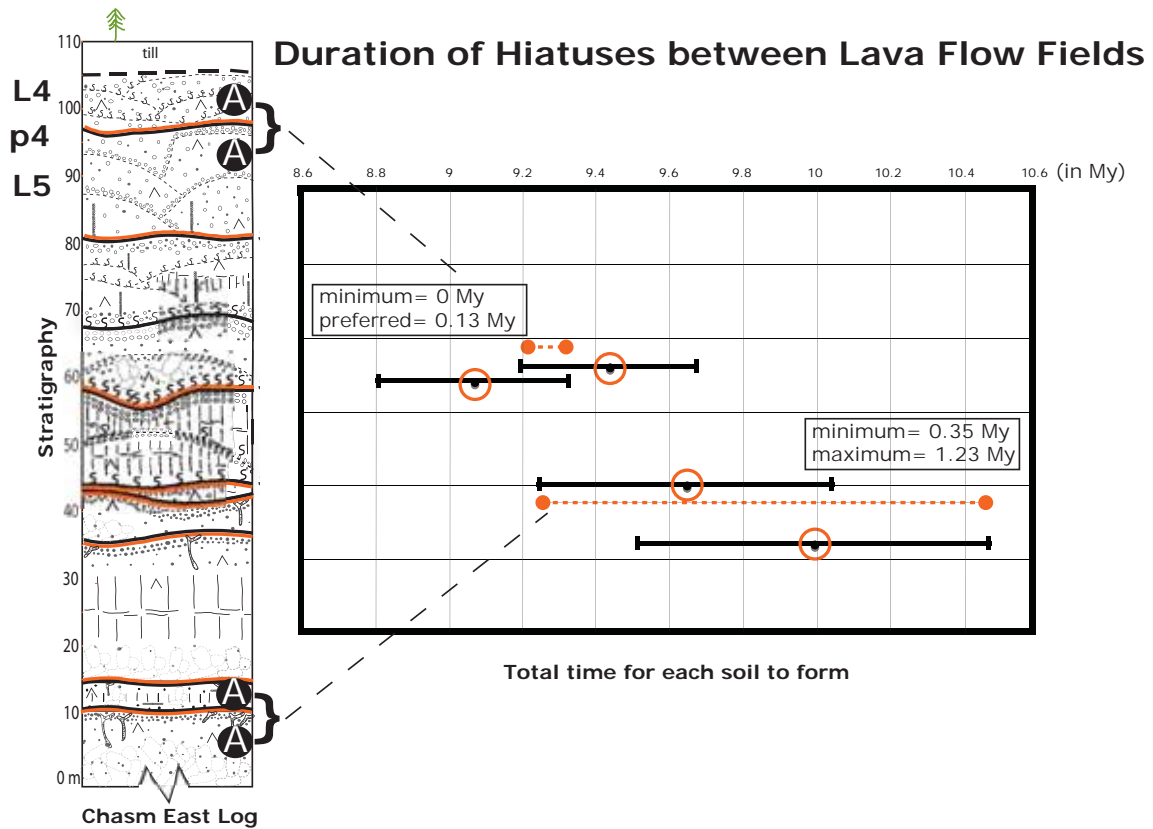


**Figure 4.12:** Stratigraphic context for Ar/Ar dates for basalt flows (A), which bracket the uppermost and lowest paleosols from the eastern composite stratigraphic log section. Results suggest the paleosols vary in the length of time it takes for each to accumulate, as the minimum value for the lowest paleosol is indicative of a formation period twice as long (270, 000 yrs) as the uppermost paleosol (130, 000 yrs).

In the case of formation of paleosol 4, involve dates on the uppermost lavas in the eastern stratigraphic log. The uppermost lava (Sample: RE-CH08-4) yielded an older age of  $9.44 \pm 0.24$  Ma than the lower lava (Sample: RE-CH06-4) dated at  $9.07 \pm 0.26$  Ma. The dates overlap in  $2\sigma$ -error. The minimum duration of hiatus between the two flow fields is 0 m.y. (since the older age is the uppermost lava) and the maximum is 0.13 m.y., deduced from the overlap of two errors on the ages, denoted with a dashed line on Figure 4.12. By age dating the bracketing flow fields for two paleosols, results suggest the paleosols vary in the length of time it takes for each to accumulate. Interpreting the minimum values of each, the stratigraphic lowest paleosol (350,000), potentially took more than twice as long to accumulate the soil opposed to p4, the uppermost paleosol (130, 000 yr or less). Our preferred duration time for the soil to form using this method is 0.13 m.y. Because of the short time inferred, the textures present in Chasm paleosols are not mature soils and duration of emplacement of the 10 flow fields in the canyon,  $1.28 \pm 0.61$  m.y., that for the soil development would be significantly less, perhaps in the range of 500-10,000 years (*pers. comm.* P. Sanborn) and due to the textures present in the Chasm paleosols, which are not mature soils.

Horizon contacts indicate that diffuse boundaries in the lower horizons of each of the 3 sites may be genetically related, since they are similar in composition and textural components. The term diffuse implies that the thickness of the contact is  $> 15$  cm (Retallack 2001). A long period of soil formation would promote horizons that are significantly different from each other, whereas at Chasm (Fig. 4.5 and 4.6), the horizons within a single sampling locality are generally similar to each other (minor differences denoted by numbers 1, 2 etc). Therefore these contacts require only a relatively short length of time to develop, based on the multitude of similarities horizon to horizon. Nazko cinder cone's 7,000 BP deposits, located west of Quesnel, B.C., have been classified as Orthic Eutric Brunisols (Sanborn 2010, *in prep*). Surveys of three sites (BC07-09, BC07-07, BC06-01) portray similar field characteristics in terms of horizon characteristics to Chasm, which indicate an immature soil. At Nazko, these sites show minor distinctions between horizons.

Horizon features indicate lack of preservation of structures due to post-burial breakdown, and the age of the paleosols. Blocky structure was observed at station 068, and the rest have been obliterated due to long time burial (~9 M.y.).

#### 4.3.2 Soil maturity

Horizons indicate a lack of soil maturity, since major horizons are similar to each other, whereas a mature soil would show vastly different horizons.

The Nazko soils, a more recent basaltic soil, with a parent material produced from Nazko Cone (deposits ~ 7,000 yrs BP; Souther and Clague 1987; Sanborn 2010 *in prep*), show similarities to the Chasm profiles. This young basaltic soil comprises an 'O' horizon, followed by a 'B' horizon, in this case horizons 'A' or 'E' do not exist. Because these are young soils therefore it is unlikely that they would have eroded away this rapidly, therefore it is concluded these horizons never existed, and by analogy, one possibility is that a similar profile may have existed at Chasm.

The Brunisolic environment for Chasm in the Miocene may be indicative of a forest environment, where originally the Chasm paleosols may have had an Ae horizon, which would be dark in color, rich in organic matter. Organic matter is not preserved in the Chasm paleosols, due to the emplacement of the capping lava, which would have burnt off the 'O' horizon, and any debris would not be preserved for ~ 9 Ma. The organic material, in an 'Ae' horizon, naturally decomposes with microbial activity, and therefore would be unlikely to be preserved at Chasm. Without fossil flora or organic matter, it is difficult to reconstruct the Miocene environmental habitat at the Chasm in the absence of fossil flora or organic matter, therefore this is a preliminary interpretation.

Horizon contacts indicate a lack of roots or root traces, which confirms an immature soil. One possibility of the origin of the clastic dikes, which are commonly joined to paleosol horizon boundary, could be a result of large roots (i.e., presently root casts) that had been growing into the weathered basalt. The preliminary interpretation **is an immature soil**,

however these dikes may have reused the root casts. These large cracks are suggestive of root development and have been observed in saprolites (pers. comm. P. Sanborn 2009). The dikes range in length, preserving the depth of the trace of the root. This depth distribution is observed at Nazko (~1.5 m depth), however these roots are considered taproots with small diameters, much larger root diameters would be necessary at Chasm to create these clastic dikes (Fig. 3.1; photo c). If the annual mean temperature (MAT) were warmer in the Miocene, then root development would increase with the warmer soil temperatures. This observation supports a milder MAT for the Miocene.

#### **4.3.3 Paleoclimate**

Several factors suggest paleosols in Chasm are Brunisols including absent horizons (O, A, E), and a shortened time for soil development due to the capping basaltic lava. A Brunisol is a young soil, which lacks soil horizon development and is suggestive of a forest environment for the Chasm during the Miocene. The Chasm paleosols are classified as Brunisols, by the Canadian soils classification scheme (Soil Classification Working Group 1998). For comparative purposes, the US classification scheme would yield the classification of an Inceptisol. The Brunisolic soil order is further organized into the '4 Great Groups,' however these categories refer to modern soils and Chasm paleosols cannot be classified further, because of the post-burial alteration processes.

Horizon textures may be suggestive of a forest environment, further micromorphological is necessary for a complete classification. The formation of Brunisolic soils can occur in an array of climates, ranging from tundra environment to a mixed forest (Soil Classification Working Group, 1998). The environmental scenarios include the following: sub-boreal forest, mixed forest, shrubs, grass, heath and tundra. Preliminary paleoclimatic interpretations for the Chasm would be mixed forest or shrubs.



#### **4.3.4 Comparative studies**

The purpose of describing the paleo-climates deduced at other locations (i.e., Porcupine Basalts and the Columbia River Flood basalts), is to compare the MAT values from each study, where the Chasm site fits geographically in-between these two cases. The two MAT's provide Miocene climate information north (Porcupine basalts; MAT 9°C; Smith 1994) and south (CRFB; MAT 12°C; Sheldon 2003) of the Chasm. Note that without organic material or fossil flora the goal of reconstructing a MAP (Mean Annual Precipitation) and MAT are not feasible (Sheldon 2002). There are not any organic matter nor fossil flora preserved at Chasm, however these case studies provide an MAT range for the Miocene Chasm climate.

#### ***Porcupine Basalts, Yukon-Alaska border***

A comparison of paleosols of the Porcupine River (Smith et al. 1994) from northeastern Alaska to the Chasm paleosols shows the scenarios are not identical, although methodology, parent material and mapping are comparable. The Porcupine River basalts are geochronologically well constrained with Ar-Ar isotopes with ages spanning between 14.4 and 16.8 Ma (Plumley et al. 1989; Kunk et al. 1994). The site comprises approximately 25 basaltic lavas with interstratified paleosols. The Porcupine River paleosols differ from the Chasm paleosols for they have components such as wood peat and organic materials. A combined interpretation, using the paleosols and the biological diversity in the sediments (i.e., palynology and fossils) is able to reconstruct the climate for the Miocene at the NE Alaska and Yukon border. Smith et al. (1994) provide the first paleoclimate reconstruction for the Miocene in this region. With each mapped paleosol profile, the horizons, fossil flora, palynological data and chemistry generate a pedoenvironmental interpretation such as 'swamp forest,' or regions that rich in elements to promote plant growth. Palynological data yields a climate with a MAT of 9°C, wet summers with milder winters (Wolfe 1978), and the cumulative paleosol results are in agreement with this climate interpretation.

### ***Columbia River Flood Basalt, Oregon USA***

In Oregon, Sheldon (2003) qualitatively and quantitatively delivers a paleoclimatic reconstruction of the Columbia River Flood basalt (CRFB) paleosols. Specifically, the Picture Gorge Subgroup is the focus of the study, which accumulated soil in the middle Miocene. The degree of chemical weathering in CRFB paleosols in the Bt (clay-rich) and Bw (Bm in Canadian soil classification) horizons provides data he uses to calculate mean annual precipitation (MAP). The MAT is derived from comparative modeling with modern soils (Sheldon, 2002). These two calculations, MAP and MAT, are based on data from three samples in the Bt horizon. The Miocene climate determined was a MAP of ~ 750 mm with a MAT of 12°C, Sheldon's results are in agreement with the fossil flora (Mascall flora).

#### **4.3.5 Soil geochemistry**

The objective in paleosol chemical analysis is two-fold, first it gleans the necessary evidence to consitutue as soil formation in regards to the Chasm paleosols, and secondly, it provides evidence for more than one parent material, a non-basaltic component, which can be observed chemically by the ratios of immobile elements (Table 4.6). The Chasm paleosol data is subsequently compared to Nazko cinder cone Brunisolic soil profile chemistry (Sanborn, 2010, *in prep*), which hosts weathered basalt as one of the parent materials, as is the case at Chasm.

In the field paleosols were tested for calcium carbonate, however concluded that the effervescent calcium carbonate on the surface of the paleosol results from the percolation of groundwater. In the chemical data, I test the hypothesis of how much organic C remains in the paleosols, as previously discussed all organic matter appears to have decomposed, however this is tested with calculating the amount of inorganic C from total C and  $\text{CaCO}_3$ . The inorganic C results are equal to or greater when compared to total C, therefore the amount of C is attributable to  $\text{CaCO}_3$  accounts for all C in the sample. An additional check is observing the N% data, which is basically zero, highlighting the fact that all organic materials have N

**Table 4.5: Paleosol chemistry****Chasm Station 069**

Sample No.	Horizon	SiO <sub>2</sub>	Al <sub>2</sub> O <sub>3</sub>	CaO	MgO	Na <sub>2</sub> O	K <sub>2</sub> O	Fe <sub>2</sub> O <sub>3</sub>	MnO	TiO <sub>2</sub>	P <sub>2</sub> O <sub>5</sub>	Cr <sub>2</sub> O <sub>3</sub>	SrO	BaO	LOI	Sum
RE-CH07-41	Bmb	48.1	16.6	4.45	3.74	5.52	0.79	8.29	0.12	1.06	0.15	0.02	0.03	0.05	10.3	99.22
RE-CH07-42	IIC1	45.4	14	8.02	6.12	2.83	0.4	11.4	0.14	1.57	0.3	0.04	0.05	0.02	8.55	98.84
RE-CH07-43	IIC2	44.9	13.3	9.5	6.13	2.57	0.23	12.85	0.15	1.74	0.46	0.05	0.05	0.01	7.59	99.53
RE-CH07-44	R	45.3	13.5	8.17	7.57	2.6	0.46	12.15	0.17	1.59	0.23	0.04	0.05	0.02	7.85	99.70

ppm					
Rb	Sr	Y	Zr	Nb	Ba
14.7	248	16.1	159	9	495
4.6	374	22.8	114	10.3	234
2.6	441	21.9	108	10.9	127
8.6	375	19.6	98	10.1	175

**Chasm Station 070**

Sample No.	Horizon	SiO <sub>2</sub>	Al <sub>2</sub> O <sub>3</sub>	CaO	MgO	Na <sub>2</sub> O	K <sub>2</sub> O	Fe <sub>2</sub> O <sub>3</sub>	MnO	TiO <sub>2</sub>	P <sub>2</sub> O <sub>5</sub>	Cr <sub>2</sub> O <sub>3</sub>	SrO	BaO	LOI	Sum
RE-CH07-49	Bmb	51.5	17.4	3.32	2.74	3.36	1.15	6.65	0.14	0.85	0.12	0.01	0.04	0.08	11.7	99.06
RE-CH07-50	IIC1	44.7	15.15	7.67	5.24	2.74	0.64	10.4	0.15	1.34	0.19	0.03	0.05	0.04	10.8	99.14
RE-CH07-51	IIC2	45.8	13.9	8.7	6.47	2.72	0.37	12.35	0.17	1.63	0.26	0.04	0.05	0.02	7.74	100.20
RE-CH07-52	IIC3	46.2	13.5	8.34	7.35	2.69	0.42	12.15	0.16	1.6	0.24	0.04	0.04	0.02	7.66	100.41

ppm					
Rb	Sr	Y	Zr	Nb	Ba
29.9	287	18.8	179	9.4	693
20.9	383	24.4	125	9.8	396
7	394	20.2	96	10.4	222
9.5	363	19.4	99	10.4	176

**Chasm Station 071**

Sample No.	Horizon	SiO <sub>2</sub>	Al <sub>2</sub> O <sub>3</sub>	CaO	MgO	Na <sub>2</sub> O	K <sub>2</sub> O	Fe <sub>2</sub> O <sub>3</sub>	MnO	TiO <sub>2</sub>	P <sub>2</sub> O <sub>5</sub>	Cr <sub>2</sub> O <sub>3</sub>	SrO	BaO	LOI	Sum
RE-CH07-53	Bmb	43.8	11.95	11.75	6.81	2.52	0.44	11.9	0.22	1.76	0.3	0.05	0.04	0.02	8.27	99.83
RE-CH07-58	IIBmb1	51.5	19.5	3.14	1.88	5.46	1.54	5.69	0.11	0.69	0.05	0.01	0.04	0.12	10.1	99.83
RE-CH07-59	IIBmb2	51.1	19.15	3.17	1.52	5.42	1.52	4.8	0.12	0.61	0.04	0.01	0.04	0.12	11.75	99.37
RE-CH07-60	IIIC	43.1	12.8	8.24	7.34	2.13	0.44	11.3	0.14	1.56	0.3	0.05	0.04	0.03	11.75	99.22
RE-CH07-61	R	45.1	12.95	7.17	9.1	2.57	0.76	12.05	0.16	1.66	0.31	0.05	0.04	0.02	8.06	100.00

ppm					
Rb	Sr	Y	Zr	Nb	Ba
9.5	289	22.8	120	14.3	174
33.1	329	16.1	203	13.3	1055
41.4	335	18	164	12.6	1100
7.6	347	21.7	109	15.4	298
8.8	366	18	111	16.4	213

**Fe Fraction, Ratios pH and Carbon Fraction, and N total****Chasm Station 069**

Sample No.	Fe <sub>t</sub>	Fe <sub>d</sub>	Fe <sub>d</sub> / Fe <sub>t</sub>	SiO <sub>2</sub> / Al <sub>2</sub> O <sub>3</sub>	CaO / TiO <sub>2</sub>	Na <sub>2</sub> O / TiO <sub>2</sub>	TiO <sub>2</sub> / Zr	pH (H <sub>2</sub> O 1:1)	C <sub>t</sub>	CaCO <sub>3</sub>	Inorganic C	N <sub>t</sub>
RE-CH07-41	5.8	1.983	0.342	2.898	4.198	5.208	66.67	9.01	0.211	2.83	0.34	0.007
RE-CH07-42	7.97	2.683	0.3366	3.243	5.108	1.803	137.7	9.54	0.158	2.027	0.24	0.004
RE-CH07-43	8.99	2.018	0.2245	3.376	5.46	1.477	161.1	9.66	0.182	2.191	0.26	0.005
RE-CH07-44	8.5	1.652	0.194	3.356	5.138	1.635	162.2	9.8	0.103	1.721	0.21	0.002

**Chasm Station 070**

Sample No.	Fe <sub>t</sub>	Fe <sub>d</sub>	Fe <sub>d</sub> / Fe <sub>t</sub>	SiO <sub>2</sub> / Al <sub>2</sub> O <sub>3</sub>	CaO / TiO <sub>2</sub>	Na <sub>2</sub> O / TiO <sub>2</sub>	TiO <sub>2</sub> / Zr	pH (H <sub>2</sub> O 1:1)	C <sub>t</sub>	CaCO <sub>3</sub>	Inorganic C	N <sub>t</sub>
RE-CH07-49	4.65	1.486	0.3196	2.96	3.906	3.953	47.49	8.76	0.266	2.827	0.34	0.013
RE-CH07-50	7.27	2.250	0.3095	2.95	5.724	2.045	107.2	9.71	0.375	3.47	0.42	0.005
RE-CH07-51	8.64	2.389	0.2765	3.295	5.337	1.669	169.8	9.17	0.135	1.916	0.23	0.009
RE-CH07-52	8.5	1.430	0.1683	3.422	5.213	1.681	161.6	9.85	0.113	2.075	0.25	0.004

**Chasm Station 071**

Sample No.	Fe <sub>t</sub>	Fe <sub>d</sub>	Fe <sub>d</sub> / Fe <sub>t</sub>	SiO <sub>2</sub> / Al <sub>2</sub> O <sub>3</sub>	CaO / TiO <sub>2</sub>	Na <sub>2</sub> O / TiO <sub>2</sub>	TiO <sub>2</sub> / Zr	pH (H <sub>2</sub> O 1:1)	C <sub>t</sub>	CaCO <sub>3</sub>	Inorganic C	N <sub>t</sub>
RE-CH07-53	8.32	0.803	0.097	3.665	6.676	1.432	146.7	8.25	0.804	4.881	0.58	0.031
RE-CH07-58	3.98	1.092	0.274	2.641	4.551	7.913	33.99	8.64	0.152	2.468	0.29	0.006
RE-CH07-59	3.36	0.727	0.216	2.668	5.197	8.885	37.2	9.22	0.193	2.553	0.3	0.004
RE-CH07-60	7.9	1.148	0.145	3.367	5.282	1.365	143.1	9.56	0.366	2.983	0.36	0.003
RE-CH07-61	8.43	1.812	0.215	3.483	4.319	1.548	149.5	9.8	0.12	2.068	0.25	0.004

in it, therefore it is the second line of evidence that no organic material has survived the ~9 m.y. burial. Basalts typically have higher calcium content, therefore it is not surprising that the pH data is alkaline. This data does not record information about the soils prior to burial, however shows that the succession was infused with calcium carbonate percolating by means of water down the rock/soil face. The Nazko data shows a comparable pH value, however does contain organic C, highest value in the first horizon (~ 50%), which comprises a typical forest floor such as L= fresh leaf litter, F= fermentation (moderate degree of decomposition), and H= hummus (unrecognizable organic matter) (LFH) (Sanborn 2010 *in prep*).

To assess the degree of weathering of the Chasm paleosols, I compare the elemental chemical analyses (majors and relevant traces) to the citrate-dithionite-bicarbonate Fe data. The citrate-dithionite-bicarbonate method is specifically designed to extract Fe oxides, and records the total amount of Fe present in the sample. The CDB method extracts Al, Mn, and Si, however is not specific to any form of these elements, therefore is not discussed in this study. The Fe indicates degree of weathering and includes crystalline Fe oxides and hydroxides (hematite, goethite), non-crystalline forms of Fe such as ferrihydrite, and Fe, which is organically complexed. Goethite is most common, and commonly hematite is produced in warmer climates within soil profiles. The Fe data confirms that the Chasm paleosols are soils. First, I observe the dithionite Fe is considerably less than the total Fe, and secondly, the  $Fe_d$  and  $Fe_t$  ratio tends to increase towards the top of the soil (1<sup>st</sup> horizon). These results are to be expected with soils, since the most intense weathering affects the surface and subsequently diminishes with depth, which is observed in station 069 and station 070. This is the best evidence to confirm that the Chasm paleosols are soils. The outlier station is station 071, which is the station where thin, however laterally continuous, tephra horizon is observed (RE-CH07-53). This sample must be regarded as complex, and consisting of a completely different parent material, while interpreting majors, traces and ratios. Sample RE-CH07-58 remains as representative of the first 'soil' horizon at station 071.

Using the  $SiO_2$ ,  $Al_2O_3$ , CaO and MgO major element data (Table 4.5), can grossly

indicate the presence of 1 or 2 parent materials. The  $\text{SiO}_2$  data yields the highest weight % in the 1<sup>st</sup> horizons (B horizons), confirming different parent materials in the profile. The  $\text{Al}_2\text{O}_3$  data yields the highest weight % in the 1<sup>st</sup> horizons (B horizons) and clay minerals (phyllosilicates) have a higher Al content, indicating the most intensely weathered horizon being the 1<sup>st</sup>, providing more evidence that Chasm paleosols are soils. In the cases of major elements CaO and MgO, the 1<sup>st</sup> horizon is half as much as the underlying horizons, implying 2 different parent materials since basalt is rich in Ca and Mg content, whereas other sediments (aeolian deposits etc) are not.

The  $\text{SiO}_2/\text{Al}_2\text{O}_3$  ratios are comparable between Chasm's Brunisolic paleosols and Nazko's Brunisolic soils, but both sites exhibit a decreasing value with depth (Sanborn 2010 *in prep*).  $\text{CaO}/\text{TiO}_2$  and  $\text{Na}_2\text{O}/\text{TiO}_2$  ratios increase with depth. Both Chasm and Nazko locales show a range in values of  $\text{TiO}_2/\text{Zr}$  ratio, where Chasm's values range between 37.2-162.2 differing from Nazko's range of 39.1-78.9 (Sanborn 2010 *in prep*). These higher values indicate multiple parent materials present, whereas consistent data near 20 wt % would be typical of 1 parent material.

To summarize, the paleosols, interstratified with basaltic lavas at Chasm, are soils because of their morphology and chemical composition.

#### **4.4 FUTURE WORK**

A reconstruction of the paleoclimate using microstratigraphic relationships, and depth trends of the micromorphological features (Kemp 1999), may render substantive climate information with Chasm's complexity of missing information such as organic material, comparative fossil flora, etc. Micromorphologists, such as Kemp and Zarate (2000), observe micro-laminated clay coatings, and disturbance in the coatings and are able to draw conclusions on transport, the processes used to produce the coating. Kemp et al. (2000) have developed semi-quantitative methods, such as organizing the varying abundances of micro-materials, placing them in a context of space and time (microstratigraphy) and applying a 'depth function.' This method in conjunction with additional fieldwork and chemistry would

yield a more comprehensive data suite for making paleoclimatic interpretations.

The second goal would be to determine to what proportion the Chasm Brunisolic soil has andic properties. An Andisol is a soil classification in the US soil classification scheme, which is generally refers to 'volcanic ash soil.' Additional chemistry is necessary for an accurate classification as an Andisol, which are the following: 1) ammonium oxalate-extractable Al, Fe, and Si; 2) phosphate retention; 3) bulk density; and 4) a determination of the volcanic glass content. Interpretation of laboratory work must consider the context that alteration occurs in the burial process of the paleosols, and Chasm paleosols have been buried since the Miocene. The chemical interpretation must be tailored to paleosols and comparative to other Andisols of similar age.

## **CHAPTER 5      VOLCANIC FACIES ARCHITECTURE**

---

### **5.1      INTRODUCTION**

Architectural Element Analysis (AEA) helps describe and interpret sequences of lavas and series of events. The facies architecture in the canyon was deduced from a combination of three approaches: 1) cross-sections, which map the CGB cliff exposures using photomosaics, 2) identification of the lava succession and their internal facies, and 3) mapping the spatial distribution of paleosols. The volcanic succession exposed in Chasm canyon comprises seven discrete facies and facies associations. The sequence of Chilcotin basalt lavas are numbered sequentially from the youngest, uppermost lava (Lava 1, L1) situated in the northern region of the Chasm canyon to the oldest dissected unit (Lava 10, L10) at the base of the canyon. Well-developed paleosols are preserved between some lavas; these paleosols are mapped and correlated laterally throughout Chasm canyon up to distances of 8 km. Paleosol 1 (p1) is the youngest paleosol observed and the oldest paleosol exposed is Paleosol 10 (p10). The volcanic facies architecture of Chasm canyon is subsequently classified, interpreted and compared with other relevant igneous provinces.

The concept of facies architecture and the method Architectural Element Analysis (AEA) originate in sedimentology where it is used to target exploration initiatives in sedimentary basins (i.e., coal, petroleum, placer minerals, and epigenetic ore deposits; (Miall 2000)). The overall objective of AEA is to identify and describe individual facies and understand their origins. The architectural elements defined for Chasm incorporate two additional objectives: 1) the environment where the eruption(s) are occurring; and 2) the environment of final deposition (McPhie and Allen 1992).

Volcanic facies architecture has been applied to Large Igneous Provinces (LIPS) (e.g., Mangan 1986; Self et al. 1996; Self et al. 1997; Hooper 1997; Jerram et al. 1999; Jerram 2002; Jerram and Widdowson, 2004; Bondre et al. 2004; Passey & Bell 2007; Elliot and Fleming 2008;) and ancient volcanic successions (marine and subaerial) (Cas et

al. 1989; McPhie and Allen 1992; Paulick and McPhie 1999; Simpson and McPhie 2000; Moore et al. 2000). The volcanic architecture can provide insight on volcanic style, eruptive volume, duration, and periodicity of the succession (Jerram 2004).

### **5.1.1 Methodology**

A modified version of the sedimentological AEA, developed by Miall (1985) has been utilized here to define the volcanic facies architecture. The AEA method at Chasm identifies four architectural elements as defined by Allen (1983) to include descriptions of: 1) the upper and lower bounding surface, 2) the geometry of the unit, 3) the scale of the unit, and 4) the internal geometry (e.g., facies) (Miall 1985; Miall 2000; Gilley 2003).

Miall (1985) specifies the importance of the outcrop quality, noting the outcrop lateral size must be at a minimum of 30 m in order to see the geometry of the units (specific to sedimentology), and there is no maximum lateral extent given, however the lateral range is typically less than 2 km. Continuous exposure is critical for this method; therefore a study area with minor structural disturbance is ideal. Chasm canyon meets the minimum criterion and represents a suitable study area for the AEA method, though Chasm's lateral extent is considerably larger than traditionally selected sites. The modified method of AEA used at Chasm is found in Appendix A.

The western canyon walls were mapped using two photomosaics: i) Lookout Panorama (Fig. 5.2), and ii) Liden Panorama (Fig. 5.3). The Lookout Panorama extends along the western canyon wall from the head of the canyon, at the Chasm Provincial Park lookout site. The Liden Panorama extends from a midpoint in the western walls to a point near Liden Pond. Beyond the most southerly point in the mosaic, the valley widens and the walls curve to the SW and SE respectively out of the plane of the mosaic. For specific lateral extents of the mosaics, refer to Figure 5.1. The walls range in height from approximately 10 to 120 meters, and consist of subhorizontal basalt lavas that are commonly interstratified by red paleosols.



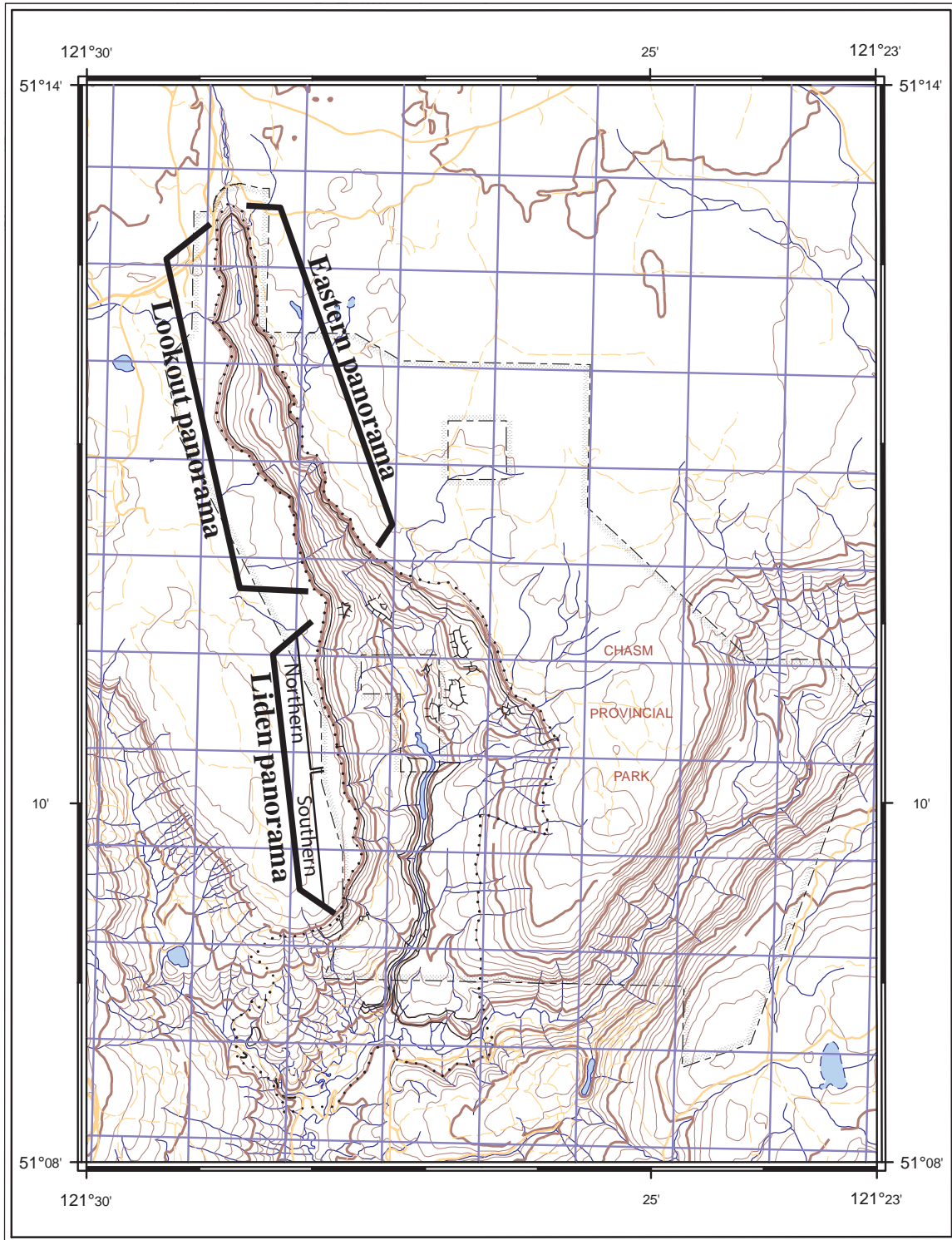


**Figure 5.1:** Inset Map showing the lateral extents of the cross sections modified from publish map (2010; Fig. 2.2). A 1: 50 000 scale map is shown. Extents are approximate.

**Figure 5.2:** Lookout Panorama, view to the west. Photomosaic illustrating the stratigraphic relationships on the western wall of the Chasm canyon, beginning at the head of the canyon near the Provincial Park Lookout. The approximate length of this section is 4.5 km. There is no vertical exaggeration. There is some exaggeration inevitably introduced in the production of the photomosaic as a consequence of the location that the panoramic photograph was made with a conventional camera. The walls range in height from approximately 40 to 120 meters and expose subhorizontal basalt lavas that are underlain by red paleosols. Lavas and paleosols vary in thickness and internal texture. The sequence dips gently to the north, where the youngest lava (Lava 1) on this canyon wall is exposed. Moving south along the canyon exposes older lavas. Circles areas are reference points between the image and the line drawing. Brown line is the top surface of the section. A, B, C, D, E on the photomosaic correspond with A, B, C, D, E on the line-diagram. Note: Projections may or may not line up due to perspective differences in this panorama. Actual figure available at the UBC Library.

**Figure 5.3:** Liden Panorama, view to the southwest. Photomosaic illustrating the stratigraphic relationships on the western wall of the Chasm canyon, terminating near Liden Pond. The approximate length of this section is 3 km. This panorama has been spliced into two panoramas (southern and northern) due to perspective. The northern panorama is enlarged 66 times the size of the southern panorama, using the 'C' control point as reference. Letters B and C are control points across the two panoramas. Lava 2 is circled highlighting an identifiable feature in the exposed lavas. The abbreviation 'R.C.' indicates the southernmost exposure of the red colouration of the paleosols. There is no vertical exaggeration. There is some exaggeration inevitably introduced in the production of the photomosaic as a consequence of the location that the panoramic photograph was made with a conventional camera. The walls range in height from approximately 40 to 120 meters and expose sub-horizontal basalt lavas that are underlain by red paleosols. The view ends at the northern end of the "west composite graphic log" (Figure 3.2). Lavas and paleosols vary in thickness and internal texture. Moving south along the canyon exposes older lavas. Circles areas are reference points between the image and the line drawing.

Lava 3/4 and paleosol 4 have been correlated across an area of no exposure. The stratigraphic correlation is made on the basis of colour and texture of the paleosol horizon, the blocky to massive character of the columnar-jointed lava, and the clear association of the Lava 3/4 to paleosol 4, where there is exposure. A, B, C, D on the photomosaic correspond with A, B, C, D on the line-diagram. Actual figure available at the UBC Library.

**Figure 5.4:** Eastern Panorama, view to the east. Photomosaic illustrating the stratigraphic relationships on the eastern wall of the Chasm canyon. The approximate length of this section is 4 km. There is no vertical exaggeration. There is some exaggeration inevitably introduced in the production of the photomosaic as a consequence of the location that the panoramic photograph was made with a conventional camera. The walls range in height from approximately 40 to 120 meters and expose subhorizontal basalt lavas that are underlain by red paleosols. The view begins at the head of the canyon, which is visible from the Chasm Provincial Park lookout site, and ends at a location of the northern end of the “East composite graphic log” (Figure 3.1). Lavas and paleosols vary in thickness and internal texture. The sequence dips gently to the north, where the youngest lava (Lava 1) on this canyon wall is exposed. Moving south along the canyon exposes older lavas. Circles areas are reference points between the image and the line drawing. Brown line is the top surface of the section. A, B, C on the photomosaic correspond with A, B, C on the line-diagram. Actual figure available at the UBC Library.

The southernmost point on the Liden panorama includes part of the subaqueous succession, and overlaps with a portion of the western composite graphic log (Fig. 3.2). There is nearly continuous exposure except in the area ~ 4.5 km southward away from the head of the canyon, on the western wall. Lavas and paleosols vary in geometry, thickness and internal lobe textures. The western sequence dips gently to the north, where Lava 2 is the uppermost lava, however the azimuth. To the south, the sequence dips due to the presence of a paleodepression where Lava 1 is first exposed within this depression on the western canyon walls (Figs. 5.2 and 5.3). About ~ 2.5 km to the south away from the head of the canyon, the oldest lavas occur at the base of the exposed sequence (Lava 10).

The Eastern Panorama is a photomosaic (Fig. 5.4), which includes the stratigraphic relationships on the eastern wall of the Chasm canyon. The walls range in height from approximately 40 to 120 meters and are underlain by intercalated subhorizontal basalt lavas and red paleosols. The mosaic comprises a 4 km extent of the canyon (Fig. 5.4) starting at the head of the canyon, visible from the Chasm Provincial Park lookout site, to the location of the northern end of the composite graphic log (Fig. 3.3), the extent is shown on Figure 5.4. The lavas and paleosols are continuously exposed and vary in thickness, geometry and internal texture within the lobes (see section 5.2). The sequence dips gently to the north, where the uppermost lava (Lava 1) occurs. Lavas are seen farther south within the canyon walls and at the ~2.5 km point in the mosaic the oldest lava (Lava 10) is observed in the sequence. The generalized stratigraphy at Chasm is summarized in Figure 5.5.

Following the basalt terminology of Self et al. (1997), a *lava flow* is the product of a single outpouring of lava, and comprises many flow lobes. A *flow lobe* is one succinct package of lava, which is distinguished by a chilled margin around the outer rim of the lobe. A *sheet lobe* shows the complexity involved in discerning the flow lobe and the lava flow; it is observed as a sheet-like or tabular single lobe, as no chilled margins or smaller lobes are visible. A *compound lobe* is the combination of two or more flow lobes, which

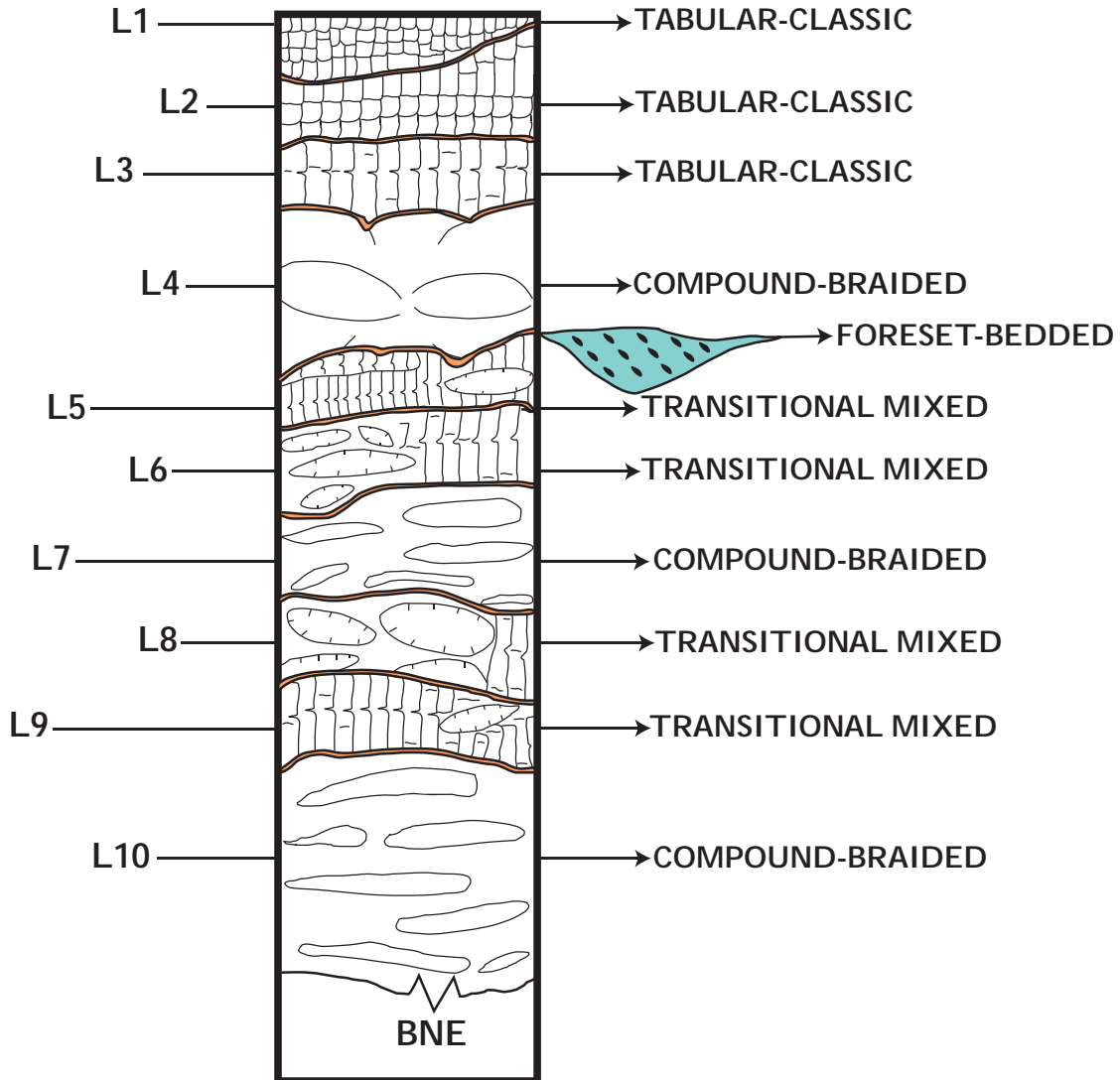


**Figure 5.5:** Generalized schematic Chasm canyon stratigraphic log illustrating volcanic facies architecture. Four architectural elements are represented: 1) Tabular-classic, 2) Compound-braided, 3) Foreset-bedded, and 4) Transitional-mixed. The transitional-mixed type is the dominant volcanic facies architecture at Chasm. 'BNE' refers to 'base not exposed'.



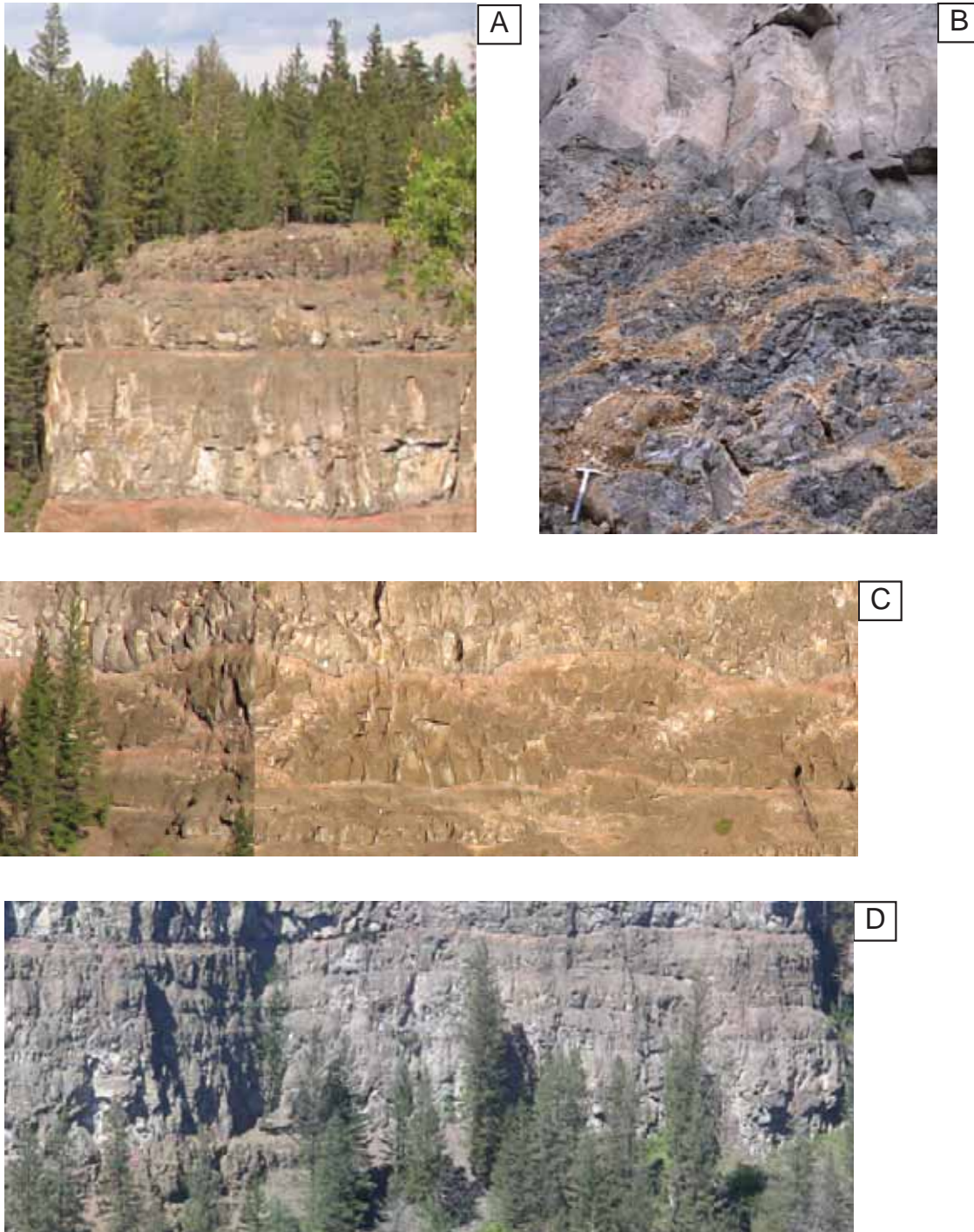


**Figure 5.6:** Field photographs illustrating volcanic facies architecture. A) Tabular-classic (L1, L2, L3). Trees for scale range from 3-6 m, B) Foreset-bedded. Hammer for scale is 30 cm, C) Compound-braided (L9). Trees for scale range from 3-6 m. Average lobe is 3 m in height, and D) Transitional-mixed (L5). Trees for scale range from 3-6 m.



**Figure 5.7:** A photomosaic of a section of the western wall to Chasm canyon illustrating the irregular, non-linear geometry of the canyon wall; locally the wall forms concave outward embayments that result from a post-glacial outburst flooding event. The glacial deluge exhumed the canyon in likely a matter of hours (pers. comm. J.K. Russell, 2009). This is a mosaic comprised of 4 photographs, which is part of the larger profile of Fig. 5.2



can be any shape or size (Walker 1972). A *flow field* is one or more lavas resulting from a single eruption or pulse of volcanism (Pinkerton and Sparks 1976; Kilburn and Lopes 1991; Mattox et al. 1993).

The lavas provide the geometry of the flow fields, distinctively marked by the presence of the red paleosols (Figs. 5.1, 5.2 and 5.3). Details such as lobe boundaries, paleosols, jointing patterns, evidence of structural disturbance (i.e., landslides) are obvious in the lateral profiles.

The photomosaics provide a unique opportunity to map the lateral variability of the paleosols over the length of the canyon. The total number of flow fields in the canyon are marked by the paleosols, because they represent distinct hiatuses in the volcanism. Without the paleosols, identification of individual lava flow fields would be less precise due to the difficulty in delineating the lobe boundaries in the photomosaics (Fig. 5.6). Typically paleosols are assessed laterally within a 1-2 m extent, therefore a 5 to 8 km mapped cross section is unusual, highlighting ample lateral variability (Fig. 5.7).

At Chasm, the paleosols have been classified as truncated paleosols, merged paleosols (this study), or a combination of both. Truncated paleosols terminate or are discontinuous in the lateral profile due to erosion or as a result of the lava morphology (i.e., abut against a flow lobe boundary). Merged paleosols refers to locales where the boundary between upper and lower paleosols cannot be distinguished and the soil profiles are merged together (Schaetzl and Anderson 2005). Symbols for these elements are labeled on the mosaics.

Due to the complex lateral behaviour of the paleosols (Fig. 5.7), a descriptive model was established to ensure consistency in the mapping and accurate classification of lavas and paleosols. The model is straightforward, using the geologic principle of superposition, and is abbreviated in the following list:

### ***Descriptive model for lateral mapping of paleosols***

- 1) The modern soil horizon is p0, and the descending sequence continues as paleosols (p1, p2, p3...pn)
- 2) A paleosol, higher in the stratigraphic profile, must be younger than a lower stratigraphic paleosol.
- 3) Identify continuous, truncated paleosols vs. merged paleosols.
- 4) In the circumstance of complex paleosols (Fig. 5.6), note the areas where paleosols merge (i.e., merged) and consider the upper bounding surface younger, with the lower bounding surface as an older paleosol. Refer to Figure 5.6 (section B) for one explanation of how these vertical paleosols could have formed.
- 5) Discontinuous paleosols are treated as follows: they are always overlain by younger lava and underlain by older lava. This applies even where the paleosol has only a few meters of strike length and cannot be laterally connected with an adjacent paleosol (Figs. 5.8 and 5.9).

### **5.1.2 Volcanic facies architecture**

Facies architecture is reliant on the geometry and lateral variability of the lavas. Multiple facies can be observed in one architectural element. Each architectural element is coded (i.e., TC= tabular-classic) after Jerram (2002) to provide a volcanological terminology used specifically in volcanic facies architecture (also referred to as ‘stacking patterns’) to specifically target the processes pronounced at the study area. A number of researchers, working on igneous provinces or continental flood basalts, have used these types defined by Jerram (2002) (Passey and Bell 2007; Elliot and Fleming 2008). Modifications to the architectural-types have been applied, specifically thickness. The following descriptions are tailored to be Chasm-specific.

The facies architecture is shown schematically in Figure 5.7, and in the mosaic figures (5.2, 5.3, and 5.4). The architectural elements described by Jerram (2002) are listed below:

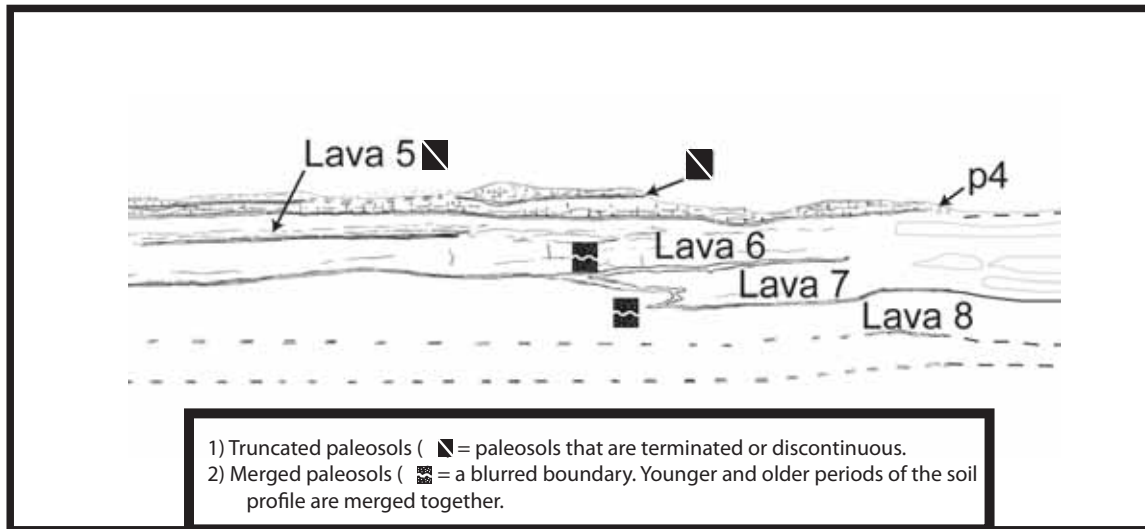


**Figure 5.8:** Detailed view of interpreted line-diagram of a section of the eastern wall illustrating the stratigraphic complexity of the paleosols. Truncated and merged paleosols are illustrated in the figure. Scale is approximately 10 m.

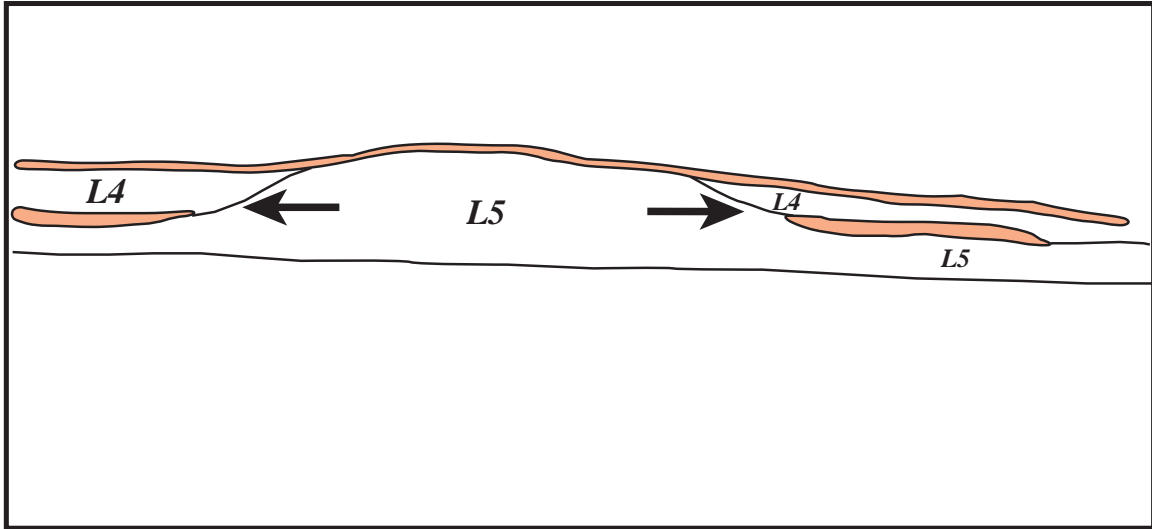


**Figure 5.9:** Paleosol truncates against local paleo-topographic high formed by pre-existing lobe of lava. Scale is approximately 5 m for this schematic diagram.

### ***Facies Architecture***

**TC= Tabular-classic facies architecture:** (i.e. thick flows (~50 m thick) with massive core and vesicular tops and bases. Columnar-joints ranging from poorly developed to well-developed.

**CB= Compound-braided facies architecture:** thin anastomizing pahoehoe lava flows, with the maximum thickness of each lobe at 3 m. Subsequent lavas can in-fill the ‘accomodation space’ located in between the flow lobes (eg., crevices).

**TR= Transitional mixed facies architecture (TC + CB):** tabular-clasic and compound-braided architecture are observed in the same flow field. The tabular-classic sheet lobes may fill-in depressions resulting from CB-type, creating a relatively planar surface (Jerram 2002). This is equivalent to the element ‘Combination’ of Jerram (2002) and ‘mixed sheet flows and compound flows’ (Passey and Bell 2007).

**FB= Foreset-bedded facies architecture:** This represents lava flowing into lakes or seawater. A delta accumulates at the margin of a lake and can be observed as building bars across the embayment (Reading and Collinson 1996). In volcanology, these bars are the foreset-beds. The foreset-beds are created when lava flows down steep, high angled slopes, which produce a pahoehoe basaltic lava-fed delta (Skilling 2002). FB is equivalent to Jerram’s (2002) ‘Dipping hyaloclastite.’ The foresets ranging from a few to tens of thousands of meters thick in flood basalts.

#### **5.1.3 Stratigraphic Analysis of Chasm Lavas**

Ten discrete paleosols and lava flow fields were identified in the canyon, correlated in the western and eastern walls, and the laterally variability of each flow field determined. Field descriptions and hand samples were cross-correlated in the canyon for Lava 1 and Lava 2, older lavas proved more difficult with this method, and reliance on lobe geometry and thickness of the lava were used for correlation. An objective in tracing the lateral extent of the profiles was to correlate them with the eastern and western composite log extents,

in which the small-scale physical volcanological features within each flow field and facies classification were determined. West Mosaic Liden overlaps with the western composite log, and East Mosaic overlaps with the eastern composite log. A composite log resulted, which illustrates the generalized ‘Chasm stratigraphy’ for the canyon lava succession (Fig. 5.5). The east and west canyon walls mirror each other for approximately 2 km from the apex except for Lava 1 which is not present of the western wall. The thickness of the lavas changes laterally, but the internal geometry (e.g., facies) is consistent. Generally, the colour and degree of weathering is identical for both sides of the canyon. Where accessible, the walls were checked and correlated across the canyon with hand samples.

The internal geometry (facies) have been determined for each lava flow field at Chasm (Fig. 5.5). Uppermost lavas, L1, L2, and L3, are classified as ‘aphyric columnar-jointed facies’ (acB). L4 is ‘vesicular basaltic pahoehoe lobe facies’ (vIB), whereas L5 and L6 are a combination of acB and vIB facies. L7 and L10 are characterized as vIB facies, where an increase in flow lobe size is observed. Lastly, L8 and L9 are recognized as the combination of acB and vIB facies, which is the most prevalent flow field facies at Chasm.

#### **Chasm canyon descriptions: 4 architectural elements**

The volcanic facies architecture is summarized in the schematic composite section (Fig. 5.5) and the four architectural elements are individually illustrated in Figure 5.6.

##### ***Tabular-classic facies architecture***

This element is recognized at Chasm by a flat upper bounding surface, a lack of recognizable lobes, but not thickness. It is stratigraphically uppermost in the top three flow fields in the canyon. The thickness of these TC-type flow fields ranges between ~2 to 10 meters. Paleosols are observed between flow fields. The ‘aphyric columnar-jointed’ facies (acB) comprises this architectural element. The columnar-joints are moderate to well-developed columns, and colouration of the two flow fields that makes up this type, appear

to be less oxidized ranging from dark grey to dark brown. These flow fields have a massive, non-vesicular interiors, with highly vesiculated lava tops and bases. Vesicle sheets and chimneys (cylinders) are visible in the massive interiors of these sheet-like flow fields.

### ***Compound-braided facies architecture***

The CB element is characterized by overlapping pahoehoe flow lobes. The CB-type is medial and basal in the three flow fields in the Chasm canyon stratigraphy. The geometry is lobate, and the thickness of the flow lobes ranges from 10 cm to 2 m. The flow field thickness varies significantly ~8-15 m, and represents the thickest architectural type in the canyon. The quantity and size of flow lobes in any flow field varies. Paleosols are interstratified between the flow fields. The ‘vesicular basaltic pahoehoe lobe’ (vLB) facies is the constituent of this architectural-type. There is an absence of columnar-joints. Flow lobes are 2-40% vesicular and pipe vesicles or pipe amygdales are observed along the lobe boundaries, classifying these features as p-type pahoehoe (Self et al. 1998) at Chasm.

### ***Transitional mixed facies architecture***

This TR-type, a mix of non-lobate TC-type with the CB-type, is the dominant architectural element of the Chasm canyon, where multiple flow lobes are observed in a single flow field. There is not a consistent observed trend of one type morphologically changing into the other, therefore the architectural element is defined as a mixed sequence, whereby the oscillation between the elements may occur multiple times over the length of the canyon. One architectural element can consist of 1 or multiple facies, and in this case both acB and vLB are observed in the TR-type. Stratigraphically, the TR-type occurs in four of the middle flow fields in the canyon walls. Commonly, paleosols bracket the flow fields. The thickness range for this architectural-type is ~0.5 m to 8 m.

### ***Foreset-bedded facies architecture***

FB-type architecture is observed in the southwest section of the western canyon wall. Four discrete subaqueous units are exposed, each exhibiting classic foreset-bedding. Upper and lower bounding surfaces of these units are sharp with the interstratified subaerial

lavas (Fig. 3.2). The following facies are observed: 'intact-pillow basalt' (ipB), 'pillow-fragment breccia' (pfB), 'hyaloclastite' (hB), and 'lacustrine sandstone' (lsS). The FB-type element occurs in the middle of the succession, however it is restricted to the southern most western wall. The thickness of the forest-bedded units varies throughout section, from ~8 to 22 m.

The subaqueous to subaerial succession is classified as a Gilbert-type basaltic lava-fed deltaic sequence (Skilling 2002) is summarized below and illustrated in Figures 5.8 and 5.9. Delta set-1 is the oldest sequence exposed.

***Delta set-1*** represents the basal delta unit observed at Chasm and is 12 m thick. The unit comprises foreset-beds that dip about 40° to the south (estimate from two planar pillow measurements). The dominant facies is intact pillow basalt facies (ipB), with minor pillow-fragment breccia (pfB) facies. A pillow pile is located at the base of this unit. The foresets are abruptly truncated at the base of approximately 12 meters of overlying subhorizontal coherent basalt (vlB and acB facies), which constitutes the topset. The bottomset is not exposed in the section. This Delta-set 1 is interpreted to reflect lava flowing south into the initial standing body of water.

***Delta set-2a*** has a thickness of 7.5 m. Five planar pillow measurements (volcanic layering) record an average dip of 34° to the south. The foresets are dipping approximately to the southwest, and a pillow pile is observed at the base of the unit. The dominant facies represented is intact pillow basalt facies (ipB), with minor pillow-fragment breccia facies (pfB). The average size of the intact pillows in this section is 0.67 m. The basal contact of the topset, approximately 10 m of basalt (vlB, acB, vlB facies sequence), abruptly truncates the Delta set-2a.



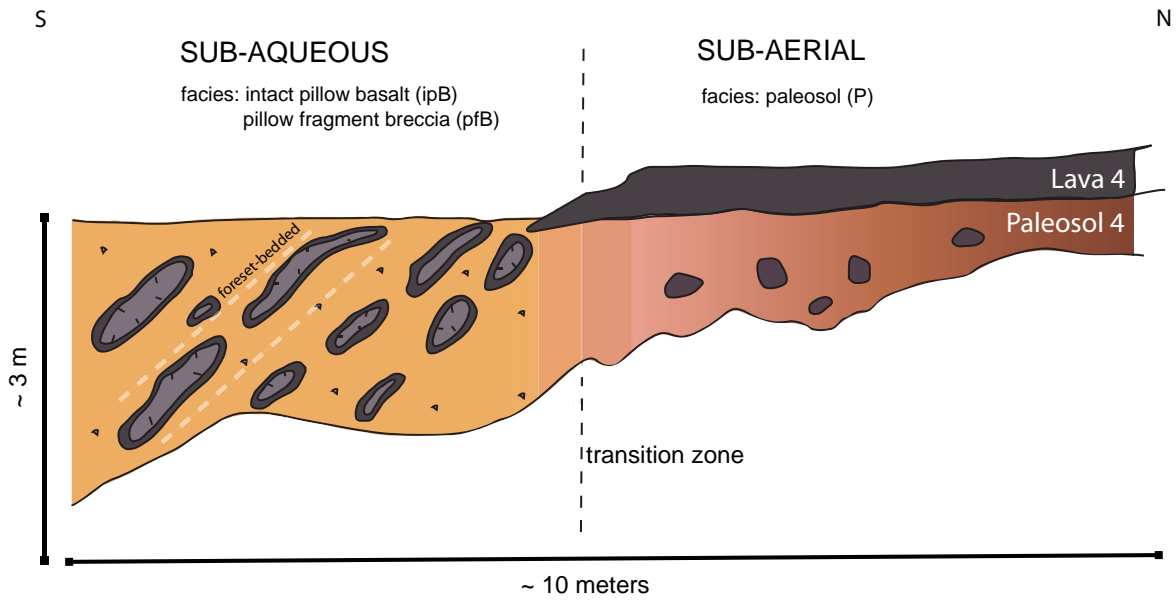


**Figure 5.10:** Schematic diagram illustrating the transition from the intact pillow basalt (ipB) and pillow fragment breccia (pfB) facies transitioning into the paleosol (P) facies. Note the paleosol facies consists of vesicular basaltic core stones. The interpretation is that ipB and pfB were emplaced into a temporary lake, deep enough to accommodate foreset beds (> 10 m minimum depth, Pedersen 1998).

# SCHEMATIC CROSS-SECTION OF WESTERN COMPOSITE LOG AREA

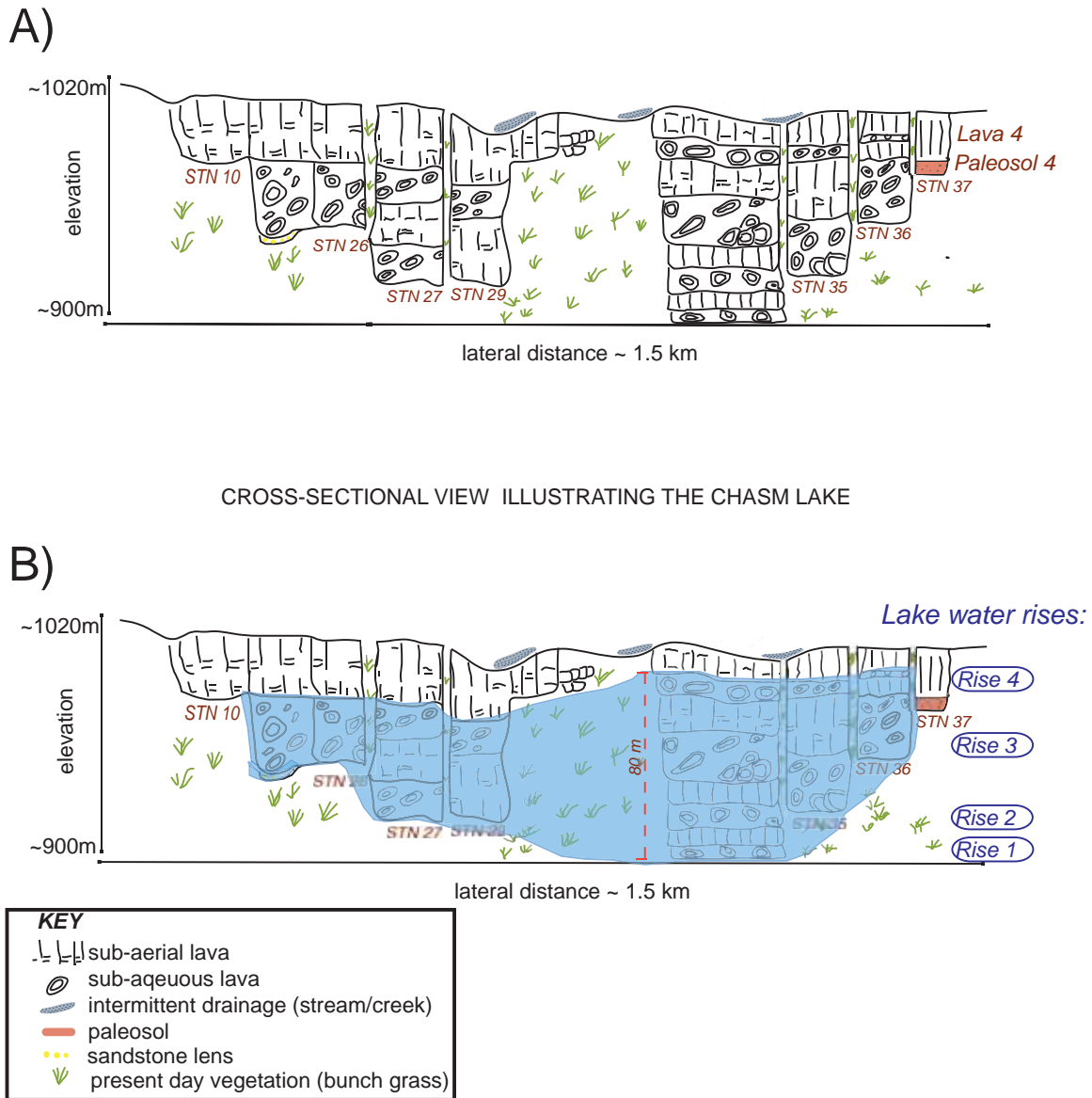


**Figure 5.11:** Schematic representation of stratigraphic relationships in a portion of western canyon wall. A) Stratigraphic relationships in transition zone from subaerial (right) to sub-aqueous (left) facies. Station numbers correspond to numbers on western composite graphic log (Figure 3.2). B) Interpretation cross-section of exposed stratigraphic units illustrating the extent of a temporary lake formed by rapid emplacement of Chasm lavas. The maximum water depth is inferred to be ~80m, based on the height of the foreset beds in pillow breccia deposits (Pedersen, 1998).

***Delta set-2b*** contains the thickest subaqueous sequence observed at Chasm at ~25 m thick. Delta set-2a and 2b are part of the same sequence, but are separate by an interval of no exposure between them (Fig. 5.10). The foreset beds are dipping approximately 34° to the southwest. Intact pillows basalt (ipB) facies is observed and clusters of intact pillows are mapped in the set, less dominant pillow-fragment breccia (pfB) represents the remainder of inter-pillow space. Both the largest pillows and the hyaloclastite facies (hB) are confined to the base of the section, and the hyaloclastite is a rare occurrence at Chasm. The overlying subaerial lava sharply truncates the Delta set-2b, and is approximately 9 m thick. Delta set-2ab is interpreted to represent the second water rise of the temporary Chasm Lake.

***Delta set-3*** is 16 m thick with foreset-beds dipping approximately 36° to the southwest. The base of the unit is a localized lens of coarse-grained quartz-sandstone overlain by packed pillow lava, deposited in a pillow pile. The overlying subaerial lava is 8m thick and truncates the set, visible as a sharp, planar contact. Along its northern extent, the Delta set-3 includes a record of the subaqueous to subaerial transition. An important shift is observed as Delta set-3 transitions laterally into Paleosol 4 (Fig. 5.8). This is interpreted to represent the shoreline of the temporary Chasm Lake, where the overlying Lava 4 supplied the lava lobes, which subsequently flowed down and south westwards, driven by gravity, illustrated by the driving ‘nose’ and ‘tail’ of the lobe (Jones & Nelson, 1970). Delta set- 3 is interpreted as the record of the third water rise of the Chasm Lake.

***Delta set-4*** is the final set of the delta progradation. This set is truncated by the uppermost subaerial lava unit (~5 m? thick). Delta set 4 is crudely estimated to range between 5 and 8 m. This set is inaccessible, due to exposure height in the cliff, and no pillow structure data were obtained. Through lateral profile mapping, Delta set-4 is interpreted as the fourth water rise of the temporary lake, and suggests correlation with Paleosol 3, a post-subaqueous to subaerial transition (Fig. 5.2).

## 5.2 VOLCANIC INTERPRETATION

The Chasm canyon sequence provides the record of: 1) the architecture of volcanic facies and facies associations, 2) a mappable transition from subaqueous interstratified coherent and volcanoclastic deposits to subaerial lavas and paleosols, 3) the variation visible in the laterally-continuous paleosols and the implied paleotopographic landscape, and 4) the directions of transport and deposition.

### 5.2.1 Subaqueous to subaerial succession

There is an important transition within the Chasm study area, between subaqueously deposited clastic rocks and subaerially emplaced lava flows. On the basis of facies associations, the hypothesis is that the source vent(s) was subaerial and that the subaqueous deposits formed when subaerial lava flowed into a standing body of water. Temporary lakes, affiliated with basaltic systems, are not an uncommon occurrence such as the Laki basaltic deposits in Iceland, which are very similar to the Chasm sequence (*pers. comm.* T. Thordarson 2007), and these types of deposits were first described in Antarctica by Jones and Nelson (1970), with subsequent studies in Greenland (Pedersen 1973; Clarke and Pedersen 1976; and Pedersen et al. 1998) and further Antarctic reviews by Porebski and Gradzinski (1990). Englacial and subglacial basaltic pahoehoe lava-fed deltas, host similar products to Chasm, and are described by Smellie (2001, 2005) and Skilling (2002).

Upon closer examination of the subaqueous – subaerial succession (Figs. 3.2, 5.8 and 5.9), the interstratified subaerial lava flows, not sills, due to field observed textures of pahoehoe ropes and wrinkles, and an absence of black, glassy chilled margins. Using the schematic cross-section of these units as a reference (Fig. 5.9), the basal exposure is subaqueous, indicating that the body of water existed prior to the emplacement of the oldest exposed lava in the sequence. It is possible that earlier lavas dammed a stream (Jones and Nelson 1970), which created the temporary ‘Chasm Lake,’ however, neither older coherent lava flows nor the basal contact with the pre-volcanic landscape are exposed. Therefore

the formation of 'Chasm Lake' may or may not be the result of the CGB volcanism in the Neogene; lakes do occur in volcanic environments without direct association to a volcanic process (White and Riggs, 2001). Field observations and the cross-sectional view (Fig. 5.9) support the hypothesis of Chasm Lake originating prior to volcanism in a paleodepression.

Chasm Lake is interpreted as terrestrial in origin based upon the lacustrine lava-fed delta sequence, and siliciclastic deposits, and defined as the lsS facies (described in Chapter 3). No ripples, laminations or any other sedimentary structures are observed in this localized quartz sandstone lens. Therefore, the present interpretation for the coarse grained deposit is a channelized flow in the lake or the shoreline of the lake. With this coarse-grained steep delta, the shoreline would have little sediment transport, and ripples or gravel lags can be a by-product (Orton and Reading, 1993); however, these are not observed at Chasm, perhaps due to cliff inaccessibility for sampling and describing the width of the quartz-sandstone lens. Grains are subangular to subrounded, indicating some transport, however the unit is massive, therefore could have been transported all at once in a flooding event. Lakes are affiliated with a low-energy environment. Peperite was not observed at the contact with the quartz-sandstone lens. The upper and lower contacts of this material were not accessible to retrieve any further information.

The Chasm deltaic sequence is analogous to the sedimentary coarse-grained Gilbert-type deltas. A Gilbert-type delta is defined as a three-part stacked sequence including a topset, dipping foreset, and bottomset (Postma 1990; van der Straaten 1990). The sequence may or may not comprise a topset. The term 'topset' may be interchangeable with 'bottomset' of the next deltaic sequence pending the sequence continues. Each stacked sequence is a 'set', for example 'delta set-1...delta set-n,' according to the protocol outlined in van der Straaten (1990).

***A basaltic lava-fed deltaic sequence must incorporate the components listed below:***

- 1) A basal unit comprised of course-grained breccia, which is foreset-bedded typically at 30,° however can exhibit dips greater than 40°.
- 2) Basaltic lava caps the clastic sequence; the contact between the units is sharp and abrupt and defined as the passage zone (Jones and Nelson 1970; Skilling 2002). These lavas are often referred to as ‘drowned lavas’ (Pedersen 1998). The top surfaces of the coherent interstratified lavas show sharp contacts, which are depositional features.

The height of the foresets relative to the basement rocks permit an estimate of the total water depth; an 80 m accumulation described in the Chasm section. For the formation of foresets to occur, there is a required water depth of ~10 m (Skilling 2002). In circumstances where the water depth is shallower, a broad inclined delta front is deposited caused by the underlying friction of the basal sediment, which produces a gently dipping slope, opposed to the steeply dipping foresets, and is defined as a Hjulström-type delta (Skilling 2002). There are no known basaltic lava-fed Hjulström-type deltas (Skilling 2002). The geometry of Chasm Lake cannot be determined nor a plan-view map due to an absence of bounding points on the opposing canyon wall.

Paleosols are not part of the delta sequence, they are part of the laterally equivalent subaerial succession. The transition, from foreset-bedded pillow-breccia to the subaerial lava (i.e. paleosol), is illustrated in Figure 5.8. Heading northwest up-section, the canyon walls comprise exclusively subaerial lava flow fields (vIB and acB facies) (Fig 5.3).

### **5.2.2 Lateral mapping of the paleosols**

A key relationship is observed between the paleosols and the underlying lava flow field morphology (i.e., architecture), whereby there is a direct correlation between the thickness of the paleosol and the underlying lava flow field architectural type (Fig. 5.10). Tabular-classic facies architecture produces an upper surface, which is sheet-like

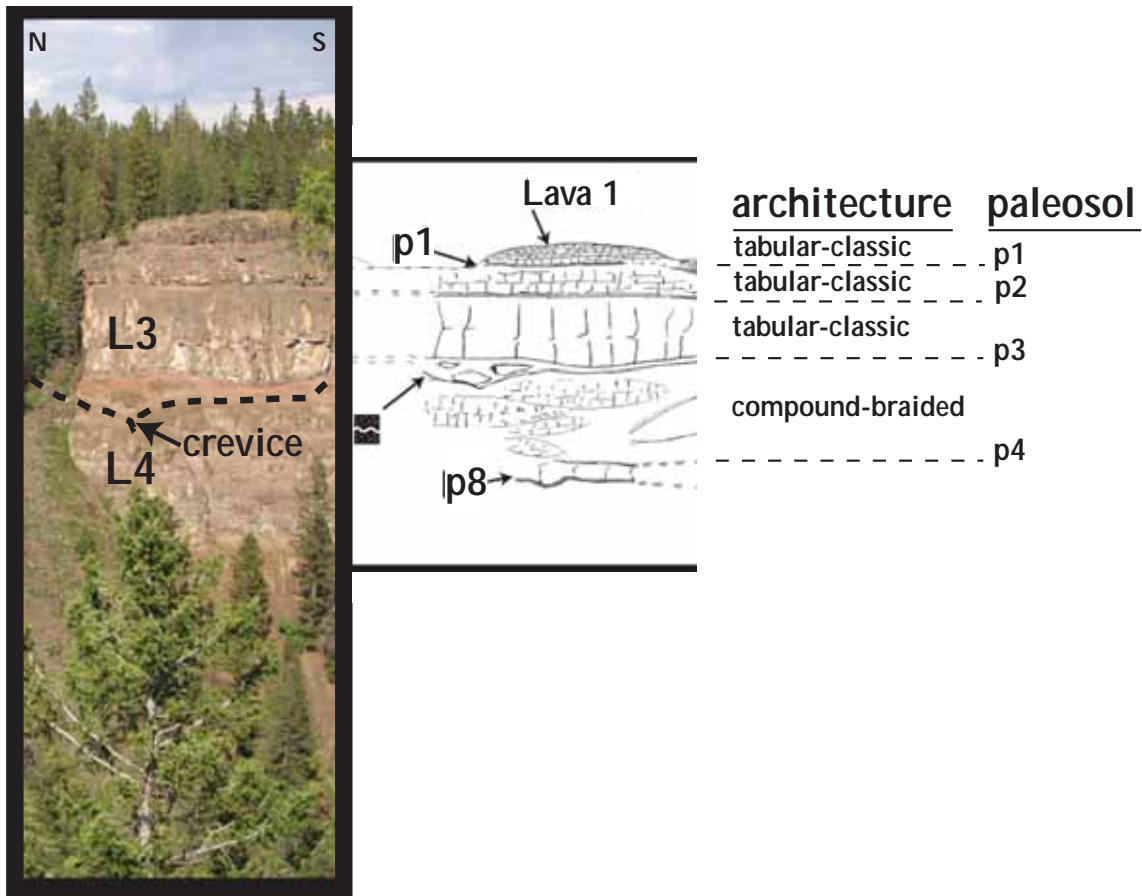


**Figure 5.12:** A field photograph and interpreted line diagram showing relationship between paleosol thickness and lava architecture. P3 paleosol is particularly thick and this is a reflection of the nature of the surface of the underlying lava (L4). Lava 4 is Transitional-mixed architecture, opposed to the tabular-classic type of L1, L2, and L3, whereby the lobate geometry promotes crevices, which subsequently stimulates soil development. The crevice highlighted in photograph results from intersection of two pahoehoe flow lobes. This crevice contains the thickest paleosol in the Chasm sequence. This photo is a section of the Eastern panorama (Figure 5.4). The lavas are approximately 45 m thick.

and homogeneous. The weathering of the basalt is fairly uniform over the surface. At Chasm, the paleosols overlying a TC-type architectural component, shows an evenly distributed, relatively thinner paleosol (~0.3 m to 0.5 thickness) (Figs. 5.2, 5.3 and 5.4) due to a homogenous surface for soil development. The CB-type and TR-type architectural elements have a heterogeneous, irregular upper surfaces and abundant crevices (not cracks), which allow for an increase in soil development and vegetation situated in these paleotopographic depressions. The CB and TR-types display a paleosol thickness ranging from approximately 0.5 to 2 m (Fig. 5.10).

Pahoehoe lava flow surfaces have been known to yield more vegetation, compared to a'a flow surfaces (Vaughan and McDaniel 2009). The crevices in between the pahoehoe lobes create very favourable environment for soil development, acting like a catchment system where tephra, other aeolian deposits and water accumulate in the crevice. There are no a'a flow fields observed at Chasm. Cracks, not crevices, are prominent in a'a flows, whereby the water is not retained, but instead percolates through the rock sequence, and soil development is hindered and delayed (Vaughan and McDaniel 2009). The Chasm paleosols are tephra-rich paleosols, where the tephra acted as a catalyst promoting soil development. The tephra is inferred to be distal from its source, supplied from felsic volcanism, composed of felsic glasses and hydrous micro-phenocrysts, opposed to a product CGB Chasm's eruptive centre(s). The source of the felsic volcanism is unknown.

Distal tephra is more fine-grained and retains water, like silt, which aids the weathering and erosion of the underlying basalt and supports soil development and plant growth (Ugolini and Dahlgren 2002). While plants and small shrubs localize in the crevices, litter is collected beneath the vegetation, stimulating more plant growth, and larger shrubbery and trees. Proximal tephra may not promote as much soil development as distal tephra due to increased porosity, therefore limiting water retention (*pers. comm.* P. Sanborn 2010). The tephra contributes to recognizing the lateral continuity of the lavas independent of the architectural-type of the underlying lava flow field. Truncated, welded, and other



paleosol complexities are observed, however lateral profile mapping of the paleosols extends over distances of 5 to 8 km (east and western walls, respectively) in the canyon providing precise correlations within the main composite graphic logs (Fig 5.7 and 5.10).

Each of the paleosols represents a preservation of a paleotopographic surface. The uppermost topographic surface (depicted with a brown line; Figs. 5.1-5.3), is underneath the current vegetation (P0). This surface is p0, which is the modern soil surface and modern topographic profile.

### **5.2.3 Locating eruptive centre(s)**

Source vents for the lavas at Chasm Provincial Park have not been identified. Inflated pahoehoe lavas are thought to be capable of flowing for tens of kilometers during emplacement, and it is possible that the source vents were a considerable distance away (Self et al. 1998). The absence of proximal features such as spatter deposits (i.e., formed from spatter cones on the boundary of the fissure (Greeley 1977)), volcanic bombs (i.e., ejecta from a shield volcano (Greeley 1977)), or volcanic edifices is consistent with the Chasm flows being distal from their sources. A series of enigmatic gabbroic plugs have been identified approximately 30 km to the north as possible lava sources (e.g. Mount Begbie; Farquharson and Stipp 1969; Bevier 1983; Matthews 1989). The paleosols imply a periodic emplacement of the Chasm lavas (Andrews and Russell 2008). The lavas are suggestive of low mean effusion rates (Andrews and Russell 2008).

This geochronological study tested this hypothesis, yielding a result of a complex chrono-stratigraphy, as discussed in Chapter 3. A slight younging trend in age dates occurs to the north on Highway 99, towards Mount Begbie, however a minima age of the uppermost lava in the canyon (L1: 08REF003A01; run B) is 7.44 Ma, and the Mount Begbie sample (JD-MB07-01; run B) results in a minima of 7.77 Ma; the geochronological data does not provide a clear correlation or trace to specific eruptive centre(s).

The lateral mapping of the lavas, which delineate the lava sequence at Chasm,

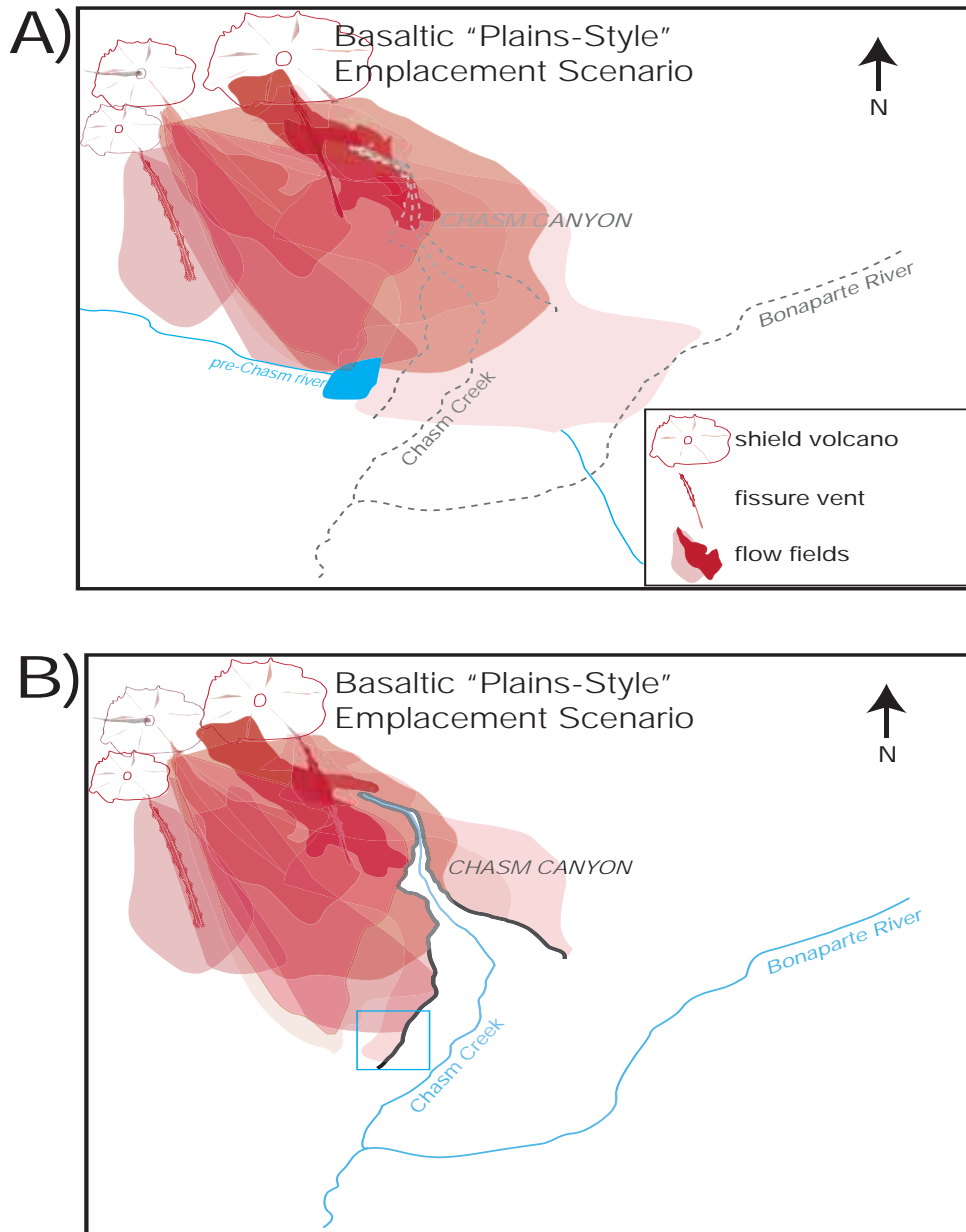


**Figure 5.13:** A) Emplacement model for Chasm Canyon showing a modern trace of the Chasm canyon and associated drainages, denoted by gray dotted lines. This figure illustrates multiple source vents including coalescing shield volcanoes and flank fissures. A pre-Chasm river was dammed by a flow field, creating the temporary Chasm Lake. Note different flow fields, representing distinct volcanic pulses, yielding a complex geochronological history. The model is schematic and the entire lava succession is not represented. B) Chasm canyon exhumed by a glacial deluge, with the CGB lavas outskirting the canyon walls. The modern trace of the canyon and present-day Chasm Creek and Bonaparte River are noted in bold. Blue box shows the approximate location of facies association, Mcb2, which represents interstratified subaqueous and subaerial facies.

provide further insight on direction of flow, and eruptive centre(s) (Fig. 5.11). There is a general northerly flow direction, with a localized northwesterly flow direction where the paleo-depression is located on the western wall, approximately 4.5 km south from the head of the canyon. The Chasm dominant architectural-type is 'Transitional mixed' facies architecture, which favors the Plains-style of volcanism (Greeley 1977), therefore one eruptive centre is not the likely source for the entire sequence. The duration of volcanism is calculated as  $1.28 \pm 0.61$  Ma, and architectural assessment is indicative of shield volcano and small fissure, point source, eruptions with a northerly transport direction. This is discussed further in the next section.

#### **5.2.4 Emplacement model at Chasm canyon**

The emplacement of the CGB lavas within Chasm Provincial Park can be explained in this descriptive volcanological model, which encompasses geological mapping, facies associations, geochronology, and architectural element analysis (AEA).

Facies architecture, when combined with vertical graphic logs, provides insight on the lateral variability of the facies and paleosols representing the complex age relationships between flow fields. These changes and complex age relationships have been recorded in other volcanic and sedimentary regimes, and are a factor in assessing the three-dimensional emplacement history (Cas and Wright 1990; Miall 2000). Chasm canyon extends approximately 8 km to the south and ranging between 500-3000m wide, and 300 m deep. The dominant facies architecture is 'Transitional mixed' (TR), characterized by the changeover between the TC and CB architectural-types (or vice a versa), which suggests basaltic 'plains-type' volcanism (Greeley 1976, 1977, 1982) also observed at the Snake River Plain, Idaho, and in Iceland (Rossi and Gudmundsson, 1996). Bevier (1982) classified the regional CGB as a product of plains-style volcanism, however, detailed stratigraphy and geological mapping were not a part of her study. Recent detailed physical volcanology at Chasm, which dissects and interprets the architectural complexity, supports

Relevant Volcanic Provinces	Summary of Characteristics:
<b>Chilcotin Group Basalt (CGB)</b>	<p><i>Type:</i> Medium-sized igneous province</p> <p><i>Aerial extent:</i> 17,000km<sup>2</sup> (total CGB)</p> <p><i>Architecture:</i> Chasm canyon = 1) Tabular-Classic (~2-10m thick), 2) Compound-braided (~10cm-2m), 3) Transitional-mixed (~0.5-8m thick), 4) Foreset-bedded (~ 10m avg.)</p> <p>Paleosols often observed between lava flow fields.</p> <p><i>Age:</i> 38.3-1Ma (Chasm: 9Ma)</p>
<b>Columbia River Basalt (CRFB)</b>	<p><i>Type:</i> Continental flood basalt (CRBG)</p> <p><i>Aerial extent:</i> 160,000km<sup>2</sup></p> <p><i>Architecture:</i> Compound pahoehoe lavas inflated by SWELL hypothesis and dominantly fissure-fed. Sheet lobes range from 20-50m thick. Paleosols often observed between flow fields observed.</p> <p><i>Age:</i> 16Ma</p>
<b>Faroe Islands Basalt Group (FIBG)</b>	<p><i>Type:</i> Continental flood basalt (North Atlantic Igneous Province; NAIP)</p> <p><i>Aerial extent:</i> 1,300,000km<sup>2</sup></p> <p><i>Total stratigraphic thickness:</i> ~ 6.6km (7 formations: Faroe Islands Basalt Group; FIBG)</p> <p><i>Architecture:</i> 1) Tabular-Classic for the Beinissvørð Fm. (~300m thick), 2) Compound-braided for the Malinstindur Fm. (~30m thick), and 3) A 'mixture of simple and compound flows' for the Enni Fm. (~70m thick). Paleosols often observed between flow fields.</p> <p><i>Age:</i> 62-54Ma</p>
<b>Snake River Plain (SRP)</b>	<p><i>Type:</i> "Plains" Volcanism (intermediary scale between shield volcano output and flood basalts)</p> <p><i>Aerial extent:</i> 49,200km<sup>2</sup></p> <p><i>Total stratigraphic thickness:</i> ranging between 300-1500m</p> <p><i>Architecture:</i> Mixture of sheet lobes and compound flows resulting from coalescing shield volcanoes and flank fissure systems. Lava thickness ranges from 3-18m. Shield height ranges from 16-30km. Paleosols often observed between flow fields.</p> <p><i>Age:</i> 17-6Ma</p>
<i>Data Sourced from:</i>	Dohaney, 2009; Farrell et al., 2007; Self et al., 1996; Passey & Bell, 2007; Greeley, 1977; Hooper, 2000 ; White,2006

**Table 5.1:** Architectural-type Comparison to relevant volcanic provinces

the previous classification. Refer to Table 5.1, a table of comparative provinces. Continental flood basalts differ from the Chasm area in that the TC- type is generally significantly thicker than the CB-type.

Greeley (1976) defined the basaltic plains-style volcanism as a combination of coalescing broad shield volcanoes and smaller fissures with intermediary scale lava flow thicknesses between a flood basalt and hawaiian-type eruption (i.e., ~ 10 m/ flow field). The coalescing of the shield volcanoes, often termed 'low shields,' creates a plateau landscape (Greeley, 1976, 1977). At Chasm, the youngest lavas are located on the eastern canyon wall situated adjacent to the apex of the canyon, however are immediately absent on the western walls mirroring the east wall exposure. Lateral cross-sectional mapping (AEA) provides an explanation, whereby identifying a large paleodepression (~500 m)

The paleodepression heads south along the western canyon wall (Figs. 5.2 and 5.3). The western wall exposure of the youngest lavas suggests an onlapping of the lavas at this topographic low-point. In addition to AEA, field descriptions and samples were used to confirm these youngest flows. Pahoehoe basaltic flows succumb to barriers, with heights as little as 30 cm, can redirect the flow and continue, gravity-controlled, towards the paleotopographic low areas (Hon et al. 1994). Either the flow was redirected to this paleodepression at Chasm, from the main vent, or a smaller fissure, point-source, supplied the lava. Small fissure systems have been recorded on Mauna Loa, Hawaii and King's Bowl, Idaho (Greeley 1977). Illustrated by the western composite log section, there is a sub-aqueous to subaerial succession where an existent lake, was subsequently lava-fed creating a delta lake over a period of time. The eruptive style of volcanism at Chasm is reflected in the defined facies architectural-type. The sequence from the exposed base (L10) of the canyon to the uppermost flow field (L1) consists of the following facies architecture (Fig. 5.5):

***CB(L10) ->TR(L9)->TR(L8)->CB(L7) ->TR(L6) ->TR(L5) ->( +/- FB) ->CB(L4)  
->TC(L3) ->TC(L2)->TC(L1)***

### ***Tabular-classic interpretation***

A tabular-classic facies architecture comprises the stratigraphic upper three flow fields (L1 through L3), and is interpreted to have been emplaced by subaerial effusive basaltic lavas, with a more continuous, steady supply rate of lava, which is likely to have inflated the lobe (i.e., SWELL hypothesis; Self et al., 1998). After the lobe is inflated, lobe boundaries are indistinguishable, and the flow field resembles a sheet-like flow with characteristic poorly to moderately columnar-joints. There is no colonnade and entablature sequence observed at Chasm. Sheet lobes are inferred to have been emplaced from a fissure vent, however at Chasm, there is no indication of proximity to the source vent.

### ***Compound-braided interpretation***

Interspersed within the sequence compound-braided facies are found (L10, L7 and L4). Compound-braided facies architecture suggests effusive basaltic volcanism, represented by pahoehoe non-channelized flows. CB-type architecture is likely emplaced from a low shield volcano where anatomising, branching lobes occur. A pahoehoe lobe, likely initially 10-50 cm thick, can inflate to a size of 4 m as calculated by Kilauea field observations by Hon et al (1994). There is a relationship between the size of the individual lobes and the supply rate of the incoming lava (Hon et al. 1994). Pahoehoe toes are at the flow front in the CB-type, and with a low dip, the toes are predicted to have equant toe widths opposed to elongated toes found with emplacement on steeper surfaces (Crown and Baloga; 1999). There are no observed spatter or bombs, indicating Chasm to be distal to the eruptive centre(s).

### ***Transitional mixed interpretation***

Transitional mixed facies architecture is a mixture of TC- and CB-architectural types, and the morphology of the flow fields suggests a bimodal emplacement. The TR-

type represents the quintessential Snake River Plain type volcanism, interpreted to have erupted from coalescing low shield volcanoes, emplacing the CB-type, in addition to fissure eruptions (often on the flanks of the shields), which emplaces the TC-type that subsequently fills in the topographic irregularities (i.e., plateau landscape) (Greeley 1976, 1977, 1982; Jerram 2002; Passey and Bell 2007). Another hypothesis for this changeover between architectural types in a single flow field, could be a result of inflation. Jerram (2002) interprets the shift as a beginning with CB-type, and through continual supply of lava, and inflation the TC-type is formed. At Chasm, the changeover between types can occur in both directions within one flow field, illustrated in Figures 5.1 through 5.3.

### ***Foreset-bedded interpretation***

Foreset-bedded facies architecture is spatially positioned on the southern end of the western canyon wall. FB-type indicates subaqueous lavas representing the relict bars of the delta sequence. A subaerial vent is interpreted to have supplied the lava of the pillow lavas. Further discussion and interpretations regarding the temporary Chasm Lake are found in section 5.2.1 of this chapter.

The sequence of L10 to L1 is indicative of evolution of the volcanic history through time (Fig. 5.11). It is observed that there are changes in the eruptive style, which suggests a progression of volcanism that may indicate different eruption rates. Roughly, the same phenocrysts are present in the Chasm succession as well as a fairly static landscape during emplacement, therefore the changes observed in the architecture reflects different fluxes of magma. The viscosity of the magma could change the style of the flow field. These observations imply a similar cooling history for each of the 10 flow fields. The tabular-classic architectural type has been inferred to be a product of a continuous supply of lava, whereas the compound-braided type can indicate early stages of the eruption where there may be intermittent breaks in the supply of lava (Jerram, 2002). The presence of CB-type at the base of the sequence (L10) suggests the early stages of the eruption from low-angle shield volcanoes (perhaps coalescing), prominent with pahoehoe lobes. The next two

episodes of volcanism are observed as the TR-type, a mixture of TC and CB, emulating the ‘Plains-style’ of volcanism, which may indicate an irregular supply of lava or sources from multiple sources, such as a shield volcano and a flank fissure. The uppermost lavas are classified as TC-type, which implies a constant supply of lava for the final 3 volcanic episodes, capping the emplacement history of Chasm. There are no field observations to suggest proximity to a vent in the volcanic sequence.

The Chilcotin Group basalts at Chasm are laterally confined to a broad valley between basement highs to the east and west. The lavas are inferred to fill and bury a long-lived paleochannel, which cuts into the early Miocene Deadman Formation, which itself filled a paleochannel cut into the pre-Miocene basement rocks (Farrell et al., 2007). This suggests that there is a persistent drainage system in Chasm Provincial Park area that has been able to re-establish itself several times in the past 15My.

### **5.3 IMPLICATIONS FOR REGIONAL CHILCOTIN GROUP**

This section provides insight on the relevance of the Chasm detailed physical volcanology in relation to the regional CGB, which spans the interior of British Columbia from Kamloops to Prince George totaling 17,000km<sup>3</sup> (Dohaney, 2009). A suggested field-based approach is presented for future needs of mapping and interpreting CGB exposures. This is useful and can be modified for detailed mapping, reconnaissance-scale mapping, and mineral exploration potentials.

Implications derived from the volcanic facies architecture can be applied regionally to see if there is a regional correlation of the CGB. The mapping of Chasm study area is consistent with the Andrews and Russell model (2008), which states that the thickest successions of the CGB such as Chasm, Dog Creek and Bull Canyon are situated in ‘paleo-lows’ (Matthews 1989) and the areas between these thick successions can be considered ‘paleo-highs’ with basalt thicknesses ranging between 0- 30 meters. The areas surrounding the Chasm canyon can be considered a ‘paleo-high’, where the thickness of the basalt



rapidly diminishes.

The possibility of multiple source vents must be examined in future studies, and whether the lava was sourced from a low-angle shield volcano or a fissure. Attention to lavas and volcanic textures is imperative, as proximity to the vent can be determined if spatter or bombs are observed. Distal flows may be suggestive of inflated pahoehoe. Chasm boasts a volcanic sequence with ten distinctive volcanic episodes, whereby future regional studies can map paleosols indicative of volcanic hiatuses, and are able to constrain flow fields. The implications of multiple eruptive events and periods of quiescence emphasizing that the emplacement is not one large outpour. Lastly, the flow-type changed with time (CB-TR-TR-CB-TR-TR-CB-TC-TC-TC; L10 to L1), and potentially regional trends could be recognized.

## **REFERENCES**

---

- Allen, J.R.L., 1983: Studies in fluvial sedimentation: bars, bar-complexes and sandstone sheets (low-sinuosity braided streams) in the Brownstones (L. Devonian), Welsh Borders. *Sediment. Geol.*, 33: 237-293.
- Anand, R.R., and Butt, C.R.M., 1988: The Terminology and Classification of the Deeply Weathered Regolith. Division of Exploration Geoscience, CSIRO, Perth
- Anderson, R.G., Resnick, J., Russell, J.K., Woodsworth, G.J., Villeneuve, M.E., Grainger, N.C., 2001: The Cheslatta Lake suite: Miocene mafic alkaline magmatism in central BC. *Canadian Journal of Earth Sciences*, 38: 697-717.
- Andrews, G.D.M., Russell, J.K., 2007: What is the mineral exploration potential beneath the Chilcotin Group basalts?: Preliminary insights from volcanic facies analysis. *British Columbia Geological Survey, Geological Fieldwork Reports 2007-1*, p.229-238.
- Andrews, G.D.M., Russell, J.K., 2008: Cover thicknesses across the southern Interior Plateau, British Columbia (NTS 092, P; 093A, B, C, F): Constraints from water-well records. *Geoscience BC Summary of Activities 2007, Report 2008-1*, p.11-20.
- Bain, D.C., Ritchie, P.F.S., Clark, D.R., and Duthie, D.M.L., 1980: Geochemistry and Mineralogy of weathered basalt from Morvern, Scotland. *Mineralogical Magazine*, 43: 865-72.
- Bevier, M.L., 1982: Geology and Petrogenesis of Mio-Pliocene Chilcotin Group basalts, British Columbia. Ph.D thesis, The University of Santa Barbara, Santa Barbara, California: 110pp.
- Bevier, M.L., 1983a: Regional stratigraphy and age of Chilcotin Group basalts, south-central BC. *Canadian Journal of Earth Sciences*, 20: 515-524.
- Bevier, M.L., 1983b: Implications of Chemical and Isotopic Composition for Petrogenesis of Chilcotin Group Basalts, British Columbia. *Journal of Petrology*, Vol. 24, Part 2, pp. 207-226.
- Bevier, M.L., Armstrong, R.L., and Souther, J.G., 1979: Miocene peralkaline volcanism in west-central British Columbia- Its temporal and plate-tectonic setting. *Geology*. Vol. 7, p. 389-392.
- Bondre, N.R., Duraiswami, R.A., Dole, G., 2004: Morphology and emplacement of flows from the Deccan Volcanic Province, India. *Bull Volcanol.* Vol. 66, p. 29-45.

- Brown, M., and D. Lowe, D., 2007: Automatic Panoramic Image Stitching using Invariant Features. *International Journal of Computer Vision*, 74(1), p.59-73.
- Bullock, P., Fedoroff, N., Jongerius, A., Stoops, G., Tursina, T., Babel, U., 1985: Handbook for soil thin section description. Waine Research Publications, Wolverhampton, U.K.
- Campbell, R.B., and Tipper, H.W., 1965: Geology of Bonaparte Lake Map-Area, British Columbia. Geological Survey of Canada, Memoir 363.
- Carlisle, D., 1963: Pillow breccias and their aquagene tuffs, Quadra Island, British Columbia. *The Journal of Geology*, vol 71, p.48-71.
- Cas, R.A.F., Landis, C.A., Fordyce, R.E., 1989: A monogenetic, Surtla-type, Surtseyan volcano from the Eocene-Oligocene Waiareka-Deborah volcanics, Otago, New Zealand: A model. *Bulletin of Volcanology*, vol 51, no 4, p. 281-298.
- Cas, R.A.F., and Wright, J.V., 1995: *Volcanic Successions*. 2<sup>nd</sup> ed. Allen and Unwin. London. 528p.
- Cas, R.A.F., Porritt, L., Pittari, A., and Hayman, P., 2008: A new approach to kimberlite facies terminology using a revised general approach to the nomenclature of all volcanic rocks and deposits: Descriptive to genetic. *Journal of Volcanology and Geothermal Research*. Vol. 174, p. 226-240.
- Chesworth, W., 2008: *Encyclopedia of Soil Science*. Springer. The Netherlands. 849p.
- Clarke, D.B., and Pedersen, A.K., 1976: Tertiary volcanic province of West Greenland. In: Escher, A., Watt, W.S. (Eds.), *Geology of Greenland*. Geol. Surv. Greenland, Copenhagen. p. 365-385.
- Cockfield, W.E., 1948: Geology and mineral deposits of the Nicola map-area, British Columbia. Geological Survey of Canada, Memoir 249.
- Crown, D.A., and Baloga, S.M., 1999: Pahoehoe toe dimensions, morphology, and branching relationships at Mauna Ulu, Kilauea Volcano, Hawai'i. *Bull Volcanol*. Vol. 61, p. 288-305.
- Dawson, G.M., 1879: Report on exploration of the southern portion of British Columbia. Geological Survey of Canada. Progress Report, 1877-1878, p. 1-186B.
- Dawson, G.M., 1895: Economic Minerals of the Kamloops Sheet, British Columbia, Geological Survey of Canada, Map 557.

- Dohaney, J., 2009: Distribution of the Chilcotin Group basalts, British Columbia. M.Sc. Thesis, The University of British Columbia, Vancouver, B.C. 125p
- Dohaney, J., Joseph, J., & Andrews, G. D. (2010). Interactive Bibliography and Database for the Chilcotin Group Basalts (NTS 82E, L, M; 83D; 92H, I, J, O, P; 93A, B, C, F, G, J, K, L), south-central British Columbia. Open File 6286. Vancouver, British Columbia: Geological Survey of Canada.
- Dostal, J., Hamilton, T.S., Church, B.N., 1996: The Chilcotin basalts, British Columbia. *Neus Jahrbuch fuer Geologie und Palaeontologie, Abhandlungen. Stuttgart (Abh)*, 170: 207-229.
- Eggleton, R.A., Foudoulis, C., Varkevisser, D., 1987: Weathering of Basalt: Changes in Rock Chemistry and Mineralogy. *Clays and Clay Minerals*. Vol. 35, No. 3, 161-169.
- Elliot, D.H., and Fleming, T.H., 2007: Physical volcanology and geological relationships of the Jurassic Ferrar Large Igneous Province, Antarctica. *Journal of Volcanology and Geothermal Research*. p.20-37.
- Enkin, R.J., Vidal, B.S., Baker, J., Struyk, N.M., 2008: Physical Properties and Paleomagnetic Database for South-Central British Columbia. *Geological Fieldwork 2007*, B.C. Ministry of Energy, Mines and Petroleum Resources, Paper 2008-1, pp. 5-8.
- Expert Committee on Soil Survey, 1983: The Canadian soil information system (CanSIS) manual for describing soils in the field. Revised ed. Agriculture Canada, Ottawa. 164p.
- Evans, S.G., 1983: Landslides in layered volcanic successions with particular reference to the Tertiary rocks of south central British Columbia. Ph.D. Thesis. The University of Alberta, AB.
- Farrell, R.-E. Andrews, G.D.M., Russell, J.K., Anderson, R.G., 2007: Chasm and Dog Creek lithofacies, Chilcotin Group basalt, Bonaparte Lake map area, British Columbia. *Geological Survey of Canada Current Research*, A5: 11p.
- Farrell, R.-E., Simpson, K.A., Andrews, G.D.M., Russell, J.K., and Anderson, R.G., 2008: Preliminary interpretations of detailed mapping in the Chilcotin Group. Chasm Provincial Park, British Columbia. *Geological Survey of Canada: Current Research Paper 2008-13*, 11pp.
- Farrell, R.-E., Anderson, R.G., Simpson, K.A., Andrews, G.D.M., and Russell, J.K. 2010: Geology, Chasm Provincial Park and vicinity, British Columbia; Geological Survey of Canada Open File 6230 and Geoscience BC Map 2009-16-1; 1 sheet, scale 1:20 000.

- Farquharson, R.B., Stipp, J.J., 1969: Potassium-argon ages of dolerite plugs in the South Cariboo region, BC. *Canadian Journal of Earth Sciences*, 6: 1468-1470.
- Fink, J.H., and Fletcher, R.C., 1978: Ropy pahoehoe: surface folding of a viscous fluid. *J Volcanol Geotherm Res.*, Vol 4, 151-170.
- Gilbert, G.K., 1885: The topographic features of lake shores. *Ann. Rep. US. Geol. Surv.*, 5, 75-123.
- Gilley, B.H.T., 2003: Facies architecture and stratigraphy of the Paleogene Huntingdon Formation at Abbotsford, British Columbia. M.Sc. Thesis. Simon Fraser University, Burnaby, B.C. 152p.
- Gordee, S.M., Andrews, G.D.M., Simpson, K.A., Russell, J.K., 2007: Sub-aqueous, channel-confined volcanism: Bull Canyon Provincial Park, British Columbia, British Columbia Geological Survey, Geological Fieldwork Reports 2007-1, p.285-290.
- Greeley, R., 1982: The Snake River Plain, Idaho: Representative of a new category of volcanism. *Journal of Geophysical Research*, Vol. 87, pp. 2705-2712.
- Greeley, R., and King, S., 1977: Volcanism of the Eastern Snake River Plain, Idaho: A comparative Planetary Geology Guidebook. NASA CR-154621, Guidebook (Arizona State University), 308pp.
- Hon, K., Kauahikaua, J., Denlinger, R., and Mackay, K., 1994: Emplacement and inflation of pahoehoe sheet flows: observations and measurements of active lava flows on Kilauea volcano, Hawaii. *Geol. Soc. Am. Bull.* Vol. 106, p. 351-370.
- Hooper, P.R., Conrey, R.M., 1989: A model for the tectonic setting of the Columbia River Basalt eruptions. *Geological Society of America Special Paper*, 239: 293-306.
- Hooper, P.R., 1997: The Columbia River Flood Basalt Province: Current Status. *Large Igneous Provinces: continental, oceanic, and planetary flood volcanism eds.* Mahoney, J.J., and Coffin, M.F. American Geophysical Union. Washington, D.C.
- Jerram, D.A., 2002: Volcanology and facies architecture of flood basalts. *Geological Society of America Special Paper* 362: 119-132.
- Jerram, D.A., Mountney, N., Holzforster, F., and Stollhofen, H., 1999b: Internal stratigraphic relationships in the Etendeka Group in the Huab Basin, NW Namibia: Understanding the onset of flood volcanism. *Journal of Geodynamics*, Vol. 28, p. 393-418.

- Jerram, D.A., and Widdowson, M., 2004: The anatomy of Continental Flood Basalt Provinces: geological constraints on the processes and products of flood volcanism. *Lithos*. 79, p-385-405.
- Jones, J.G., and Nelson P.H.H., 1970: The flow of basalt lava from air into water- its structural expression and stratigraphic significance. *Geol. Mag.* 107, 1. p.13-21.
- Keller, G., Adatte, T., Gardin, S., Bartolini, A., and Bajpai, S., 2008: Main Deccan volcanism phase ends near the K-T boundary: Evidence from the Krishna-Godavari Basin, SE India. *Earth and Planetary Science Letters* 268. Issues 3-4, p. 293-311.
- Kemp, R.A., 1999: Micromorphology of loess-paleosol sequences: a record of paleoenvironmental change. *Catena* 35. 179-196/
- Kemp, R.A., Zarate, M., Espinosa, M., and Ferrero, L., 2000: Pedosedimentary and palaeoenvironmental significance of a Holocene alluvial sequence in the southern Pampas, Argentina. *The Holocene*, vol 10, issue 4, p 481
- Kilburn, C.R.J., and Luongo, G., 1993: *Active Lavas: monitoring and modeling*. London: UCL Press 287 p.
- Kunk, M.J., Reich, H., Fouch, T.D., and Carter, L.D., 1994:  $^{40}\text{Ar}/^{39}\text{Ar}$  age constraints on Neogene sedimentary beds, Upper Ramparts, Half-way Pillar and Canyon Village Sites, Porcupine River, east-central Alaska. *Quaternary International*. Vol. 22/23: p-11-29.
- Le Maitre, R.W., 2002: *Igneous Rocks. A Classification and Glossary of Terms. Recommendations of the International Union of Geological Sciences Subcommission on the Systematics of Igneous Rocks*, 2<sup>nd</sup> ed. Cambridge, New York, Melbourne: Cambridge University Press. 236pp.
- Long, P.E., Wood, B.J., 1986: Structures, textures, and cooling histories of Columbia River Basalt flows. *Geological Society of America Bulletin*, 97: 1144-1155.
- Mack, G.H., James, W.C., and Monger, H.C., 1993: Classification of Paleosols. *GSA Bulletin*. Vol. 105, p. 129-136.
- Mangan, M.T., Wright, T.L., Swanson, D.A., Byerly, G.R., 1986: Regional correlation of Grande Ronde Basalt flows, Columbia River Basalt Group, Washington, Oregon and Idaho. *Geol. Soc. Am. Bull.* 97: 1300-18p
- Mathews, W.H., Rouse, G.E., 1961: Radioactive dating of Tertiary plant-bearing deposits. *Science*, 133: 101-116.

- Mathews, W.H., Rouse, G.E., 1963: Late Tertiary volcanic rocks and plant-bearing deposits in British Columbia. *Geological Society of America Bulletin*, 74: 55-60.
- Mathews, W.H., Rouse, G.E., 1986: An Early Pleistocene pro-glacial succession in south-central BC. *Canadian Journal of Earth Sciences*, 23: 1796-1803.
- Mathews, W.H., 1989: Neogene Chilcotin basalts in south-central BC. *Canadian Journal of Earth Sciences*, 26: 969-982.
- Mattox, T.N., Heliker, C., Kauahikaua J., Hon, K., 1993: Development of the 1990 Kalapana Flow Field, Kilauea Volcano, Hawaii. *Bull Volc.* 55: 407-13
- McDougall, I., and Harrison, T.M., 1999: *Geochronology and Thermochronology by the  $^{40}\text{Ar}/^{39}\text{Ar}$  Method*, 2<sup>nd</sup> ed. Oxford University Press: New York Oxford: 269pp.
- McPhie, J., and Allen R.L., 1992: Facies architecture of mineralized submarine volcanic sequences: Cambrian Mount Read volcanics, Western Tasmania. *Economic Geology*, vol. 87, p. 587-596.
- McPhie, J., Doyle, M., Allen, R.L., 1993: *Volcanic Textures*. University of Tasmania. 198p.
- Miall, A.D., 1985: Architectural-Element Analysis: A New Method of Facies Analysis Applied to Fluvial Deposits. *Earth-Science Reviews*, 22: 261-308.
- Miall, A.D., 2000: *Principles of Sedimentary Basin Analysis*, 3<sup>rd</sup> ed. Springer-Verlag Heidelberg New York, 616pp.
- Mihalynuk, M.G., 2007: Neogene and Quaternary Chilcotin Group cover rocks in the Interior Plateau, south-central British Columbia: A preliminary thickness model. *BC Geological Survey Geological Fieldwork 2007-1*, p. 1-5.
- Munsell Color (firm), 1994: *Munsell soil color charts*. Baltimore, MD. 1 vol.
- Olowolafe, E.A., 2002: Soil parent material and soil properties in two separate catchment areas on the Jos Plateau, Nigeria. *GeoJournal*, vol. 56, no. 3, p. 201-212.
- Orton, G.J., and Reading, H.G., 1993: Variability of deltaic processes in terms of sediment supply, with particular emphasis on grain size. *Sedimentology*. 40. 475-512.
- Paton, T.R., Humphreys, G.S., Mitchell, P.B., 1995: *Soils: A new global view*. University College London Press. 213pp.
- Paulick, H., and McPhie, J., 1999: Facies architecture of the felsic lava dominated host sequence to the Thalanga Massive Sulfide Deposit, Lower Ordovician, Northern Queensland. *Australian Journal of Earth Sciences*, vol. 46, p. 391-405.



- Passey, S.R., & Bell, B.R., 2007: Morphologies and emplacement mechanisms of the lava flows of the Faroe Islands Basalt Group, Faroe Islands, NE Atlantic Ocean. *Bull Volcanol.*, Vol. 70, p. 139-156.
- Pedersen, A.K., 1973: Report on field work along the north coast of Disko, 1971. *Rapp. Gronl. Geol. Unders.* 53, 21-27
- Pedersen, A.K., Larsen, L.M., Pedersen, A.K., and Hjortkjar, B.F., 1998: The syn-volcanic Naajaat lake, Paleocene of West Greenland. *Palaeogeography, Palaeoclimatology, Palaeoecology*. Vol. 140. P. 271-287.
- Pinkerton, H., and Wilson, L., 1994: Factors controlling the length of channel-fed lava flows. *Bull Volc.* 56: 109-20
- Plouffe, A., and Levson, V.M., 2001: Late Quaternary glacial and interglacial environments of the Nechako River- Cheslatte Lake area, British Columbia. *Can. J. Earth. Sci.* 38 p 719-731
- Plumley, P.W., Vance, M.S., Milazzo, G., 1989: Structural and paleomagnetic evidence for Tertiary bending of the astern Brooks Range flexure, Alaska. In: Hillhouse, J.W. (ed) *Deep structure and past kinematics of accreted terranes*. AGU, *Geophys Monograph* 50, 127-150.
- Porebski, S.J., and Gradzinski, R., 1990: Lava-fed delta in the Polonez Cove Formation (Lower Oligocene), King George Island, West Antarctica. *Spec. Publs int. Ass. Sediment.* 10 p-335-351.
- Postma, G., 1990: Depositional architecture and facies of river and fan deltas: a synthesis. In: Colella, A. & Prior, D.B. (eds) *Coarse-grained deltas*. International Association of Sedimentologists. *Special Publications*, 10, 13-27.
- Read, P.B., 1989: Miocene stratigraphy and industrial minerals, Bonaparte to Deadman River area, southern BC (92I/14, 15; 92P/2, 3). *Ministry of Energy, Mines and Petroleum Resources Paper*, 1989, 1: 515-518.
- Reading, H.G., and Collinson, J.D., 1996: *Sedimentary Environments: Processes, Facies and Stratigraphy*. 3<sup>rd</sup> ed. Blackwell Science. Oxford. 688pp.
- Retallack, G.J., 2001: *Soils of the Past: An Introduction to paleopedology*. 2<sup>nd</sup> ed. Blackwell Science. Oxford. 404pp.
- Reynolds, J.M., 1997: *An introduction to applied and environmental geophysics*. John Wiley & Sons. New York. 796pp.



- Rice, H.M.A., 1947: Geology and mineral deposits of the Princeton map area, British Columbia. Geological Survey of Canada, Memoir 243.
- Sanborn, P., (*in prep.*) Soil Formation on Holocene Basaltic Lava and Tephra, Nazko Cinder Cone, Central Interior British Columbia.
- Sayyed, M.R.G., and Hundekari, S.M., 2006: Preliminary comparison of ancient bole beds and modern soils developed upon the Deccan volcanic basalts around Pune (India): Potential for palaeoenvironmental reconstruction. *Quaternary International*. Vol. 156/157, p. 189-199.
- Schaetzl, R.J., and Anderson, S., 2005: Soils: genesis and geomorphology. Cambridge University Press, New York, 817p.
- Self, S., Thordarson, Th., Keszthelyi, L., Walker, G.P.L., Hon., K., Murphy, M.T., Long, P., and Finnemore, S., 1996a: A new model for the emplacement of the Columbia River Basalts as large inflated pahoehoe lava flow fields. *Geophysical Research Letters*. Vol. 23, No. 19, p. 2689-2692.
- Self, S., Keszthelyi, L., and Thordarson, T., 1998: The importance of pahoehoe. *Annual Reviews of Earth and Planetary Sciences*, 26: 81-110.
- Self, S., Thordarson, T., and Keszthelyi, L., 1997: Emplacement of Continental Flood Basalt Lava Flows. *AGU Geophysical Monograph* 100, p. 381-409.
- Sheldon, N.D., 2003: Pedogenesis and geochemical alteration of the Picture Gorge subgroup, Columbia River Basalt, Oregon. *Geol. Soc. Am. Bull.*, Vol. 115, p. 1377-1387.
- Sheldon, N.D., 2006: Quaternary Glacial-Interglacial Climate Cycles in Hawaii. *Journal of Geology*. Vol. 114, p. 367-376
- Simpson, K., and McPhie, J., 2000: Fluidal-clast breccia generated by submarine fire fountaining Trooper Creek Formation, Queensland, Australia. *Journal of Volcanology and Geothermal Research*. 109, p. 339-355.
- Single, R.T., and Jerram, D.A., 2004: The 3D facies architecture of flood basalt provinces and their internal heterogeneity: examples from the Palaeogene Skye Lava Field. *Journal of the Geological Society*, London. Vol. 161, p. 911-926.
- Skilling, I.P., 2002: Basaltic pahoehoe lava-fed deltas: large-scale characteristics, clast generation, emplacement processes and environmental discrimination. Smellie, J.L & Chapman, M.G. (eds) *Volcano-Ice Interaction on Earth and Mars*. Geological Society, London, Special Publications, 202, 91-113.

- Smellie, J.L., 2001: Lithofacies architecture and construction of volcanoes erupted in englacial lakes: Icefall Nunatak, Mount Murphy, eastern Marie Byrd Land, Antarctica. *Spec. Publs int. Ass. Sediment.*, Vol. 30: pp. 9-34.
- Smellie, J.L., 2006: The relative importance of supraglacial versus subglacial meltwater escape in basaltic subglacial tuya eruptions: An important unresolved conundrum. *Earth Science Reviews* 74, 241-268.
- Smith, R.M.H., 1990: Alluvial Paleosols and Pedofacies sequences in the Permian Lower Beaufort of the Southwestern Karoo Basin, South Africa. *Journal of Sedimentary Petrology*. Vol. 60. No. 2. P. 258-276.
- Smith, C.A.S., Fox, C.A,m and Kodama, H., 1994: Paleosols associated with Miocene Basalts, Porcupine River, Northeastern Alaska: Implications for Regional Paleoclimates. *Quaternary International*. Vol. 22/23: pp 79-90.
- Soil Classification Working Group, 1998: The Canadian System of Soil Classification, 3<sup>rd</sup> ed. Pub. 1646. Research Branch, Agriculture and Agri-Food Canada, 187p.
- Souther, J.G., and Clague, J.J., 1987: Nazko cone: a Quaternary volcano in the eastern Anahim Belt. *Canadian Journal of Earth Sciences*, Vol. 24, pp. 2477-2485.
- Stoops, G., 2003: Guidelines for Analysis and Description of Soil and Regolith Thin Sections. Soil Science Society of America, Inc., Madison, Wisconsin. 184pp.
- Tipper, H.W., 1971a: Surficial Geology of Bonaparte Lake (NTS 92P), Geological Survey of Canada, Map 1202A, Scale 1:250,000.
- Tipper, H.W., 1978: Taseko Lakes map-area. Geological Survey of Canada, Open File 534.
- Uglolini, F.C., and Dahlgren, R.A., 2002: Soil development in volcanic ash. *Global Environmental Research*. Vol. 6, Issue 2, p 69-81.
- Uglow, W.L., 1922: Geology of the North Thompson Valley map-area, B.C.; Geological Survey of Canada, Summary Report, 1921, Pt. A: 72-106.
- Van der Straaten, H.C., 1990: Stacked Gilbert-type deltas in the marine pull-apart basin of Abaran, late Serravallian-early Tortonian, southeastern Spain. *Spec. Publs int Ass. Sediment.*, Vol. 10: 199-222.
- Vaughan, K.L., and McDaniel, P.A., 2009: Organic Soils on Basaltic Lava Flows in a Cool, Arid Environment. *Soil Sci. Soc. Am. J.* Vol. 73, No. 5, 1510-1518p.

- Vitousek, P.M., Chadwick, O.A., Crews, T.E., Fownes, J.H., and Hendricks, D.M., 1997: Soil and ecosystem development across the Hawaiian Islands. *GSA Today*, Vol. 7, p. 1-8.
- Walker, G.P.L., 1971: Compound and simple lava flows and flood basalts. *Bull Volc.* 35: 579-90.
- White, J.D.L., and Riggs, N.R., 2001: Introduction: styles and significance of lacustrine volcanoclastic sedimentation. *Spec. Publs int. Ass. Sediment.*, Vol 30: pp. 1-6.
- Wilson, M.J., 2006: Factors of soil formation: parent material. As exemplified by a comparison of granitic and basaltic soils. *Soils: Basic concepts and future challenges*, ed. Cambridge University Press. Ch 9. 113-129.
- Wolfe, J.M., 1978: A palaeobotanical interpretation of Tertiary climates in the northern hemisphere. *American Scientist*. Vol. 66: p. 694-703.
- Yamagishi, H., 1979: Classification and features of subaqueous volcanoclastic rocks of Neogene age in Southwest Hokkaido, Japan. *Rep. Geol. Surv. Hokkaido*, 51: 1-20
- Yamagishi, H., 1983: Surface structures on pillow lobes. *Bull Volcanol. Soc. Jpn.*, Ser. 2, 28: 233-243.
- Yamagishi, H., 1985: Growth of pillow lobes-evidence from pillow lavas of Hokkaido, Japan and North Island, New Zealand. *Geology*, 13: 499-502

## **APPENDIX A**

### **FIELD METHODOLOGY**

*The modified method of AEA used at Chasm is abbreviated in the following list:*

#### ***Field Method***

*Step 1:* Assess study area, and choose outcrop suitable for AEA

*Step 2:* Plan traverses. Develop a photographic method to execute the lateral mapping of the canyon.

*Step 3:* Traverse the canyon, and use a digital camera to photograph the opposing walls of the canyon using the photographic method.

*Step 4:* Stitch the digital photos together in a graphics program (i.e., Adobe Illustrator).

Note: Autostitch (Brown and Lowe 2007) or camera photo stitching program cannot be used, if the curves/ undulations in the canyon are observed. These programs cannot normalize the curves. If you have a small lateral extent (500 m-1 km), autostitch is the preferred method.

*Step 5:* Print using field printer, and attach overlays (vellum) on top of the mosaic.

*Step 6:* Map directly onto the overlays, noting the external geometry (i.e., sheet, lens, lobate, wedge, scoop, or u-shaped). Describe the contact boundaries of the flow lobes and the flow field.

#### ***Post-field analysis***

*Step 7:* Assimilate all photos into two lateral profiles, one for each wall of the canyon.

*Step 8:* Finalize the mosaics in graphics program, and scan the overlays, then digitize the mapping linework and produce the working draft of the lateral profile.

*Step 9:* Print the mosaics and linework, and identify the succession of lava flows (youngest to oldest), and paleosols for the canyon.

*Step 10:* Correlate the lava and paleosols with the graphic logs ensuring a context of space and time.

*Step 11:* Define the architectural elements. Note these elements may comprise multiple facies. Laterally variability must be incorporated into the assessment and classification of the architectural elements.

The photographing method is specific to Chasm due to the significant number of undulations of the canyon walls; four type panorama sequences are taken at each station. Additional sketches and notes are made at each station, for systematic purposes since the length of the canyon walls yields three long lateral profiles, where the collation of photographs can prove complex in certain junctures.

### **Magnetic susceptibility**

Magnetic susceptibility (MS) measurements were taken using a KT-9 Kappameter during field seasons from 2006 through 2008 (Figs. 2.2, 3.6, 3.7; Table 3.3) in Chasm. The objective was to compare values between different lavas in our stratigraphic sections, and/or identify an overarching trend in the Chasm canyon. Fifty-eight measurements were recorded from the Chasm study area, and the measurement type is either a field measurement or a laboratory measurement, where samples uncut or cored were tested with the hand-held KT-9 Kappameter. The number of measurements at each field station was typically 10 (minimum of 3 measurements are required at each station), which have subsequently been averaged into the recorded MS value. Data is recorded in  $10^{-3}$  SI units (Table 3.3). For CGB paleomagnetism data, including the Chasm study area, refer to Enkin et al. (2008).

### **Structural measurements:**

Structural data of the CGB comprises planar pillow measurements (volcanic layering) (Appendix D; Fig. 2.2). Planar measurements of the Deadman Formation bedding is recorded (Appendix D; Fig. 2.2). The structure data is plotted on the Chasm Map (Fig. 2.2).

A scheme was developed to address the level of certainty for the structure data in the study area, which is outlined below. Measurements assigned a 1 or 2 level are plotted on the Chasm Map (Fig. 2.2) and used for interpretation. Recordings of a 3 or 4 level are discarded.

***Level of certainty for the structure data***

1. *3D pillow / highest level of certainty*
2. *Estimating plane*
3. *Crude estimate of plane*
4. *Uncertain*

**Chasm Samples:**

All CGB samples are in the regional CGB Database (Dohaney et al. 2010)

## APPENDIX B

### AR<sup>40</sup>/AR<sup>39</sup> SAMPLE PREPARATION

#### *Sample Preparation*

The geochronological data set for the Chasm Provincial Park and immediately adjacent areas is extensive for a canyon of this size. Typically only the lowest and highest lava would be sampled, therefore giving a result of the duration of volcanism for the lavas exposed inside the canyon. The rationale in deciding which basalts to date was based on 3 factors: 1) volcanic stratigraphy (the length of time for the eastern log succession to have been emplaced); 2) constraint of the duration of soil development using the lavas immediately above and below a paleosol; and 3) the aim of determining the duration of volcanism for Chasm Canyon.

Two different batches of geochronological samples were prepared for the CGB (Chasm specific and regional) and are separated into categories of 2007 and 2009. Forty-one samples in total (Chasm and regional) were analysed for Ar<sup>40</sup>/Ar<sup>39</sup>. The analyst for the 2007 ages was T. Ullrich and for 2009 ages J. Gabites. All samples were analyzed at Pacific Centre for Isotopic and Geochemical Research at UBC). The methodology for the sample preparation for both sample sets is identical. First, the basalt samples are cut using a standard rock saw into approximately 8 x 8 x 8 cm sized sections, which are then crushed to gravel size using a Rhino Jaw Crusher. A 10 g split of the crushed basalt sample is then subjected to leaching, to clean the samples before picking the freshest gravel-sized basalt fragments. The sample is rinsed multiple times in deionized water until the water runs clear with the decanting. Approximately 10 ml of 5% nitric acid is then added to the sample and allowed to saturate for five minutes. Deionized water (~150 ml) is added, and the samples are placed in an ultrasonic bath for 5 minutes, and then drained onto filter paper. Once the samples have dried, the individual grains are picked using a binocular microscope, with the freshest basalt grains selected. Grains are picked that are representative of the whole rock

basalt samples, and 10-15 grains of basalt were selected for each sample. This final picking step is critical for locations where a high degree of alteration has taken place, such as at Chasm, and only the freshest grains were selected for analysis. In many cases, the grains are highly oxidized, with a range of colours red to orange, microvesicular with infilled vesicles, and brittle, following this observation these grains are discarded. As mentioned previously, two separate batches of whole rock CGB were submitted and these batches are distinguished by the year (i.e., 2007 or 2009 ages).

An ideal plateau would have contiguous steps within the 2 sigma error, use 50-100% of the  $^{39}\text{Ar}$  gas, have a MSWD value near 1, and a low error value. The plateau shown on the plots (Figs. 3.8-3.13; and in Appendix C) show the width of each square (step) as the amount of gas released and the height of each square as the error associated with the specific step. The statistical error resides in each individual heating step, therefore the final plateau age combines the error of each step. Error increases based on the stability of the mass spectrometer, the J factor (irradiation parameter), and the accuracy and precision blanks used.

As shown on the table, samples analysed by T. Ullrich were analysed once, therefore recorded a single age result, whereas the samples analysed by J. Gabites each sample was analysed twice, therefore, there are two ages recorded for each sample. When two ages resulted from the same sample number, the addition in quadrature statistical method was used to provide a  $2\sigma$  weighted average for the error (internal error) using Isoplot.



## **APPENDIX C**

**REGIONAL GEOCHRONOLOGICAL DATA:** see included cd

GEOCHRONOLOGY OF CHILCOTIN GROUP BASALTS: REGIONAL <sup>a</sup>							
Sample Number <sup>b</sup>	AGE (Ma)	System	UTM Easting (NAD83)	UTM Northing (NAD83)	LOCATION	Context	Analytical Notes
RE-AF06-53	9.0 ± 1.4	Ar-Ar	487708	5764223	Anahim Flats	Lava 1: basal lava	
RE-AR06-8	9.64 ± 0.35	Ar-Ar	641623	5649526	Arrowstone Hills	Top lava	
RE-AR06-10	11.04 ± 0.14	Ar-Ar	642074	5648949	Arrowstone Hills	Basal lava	
RE-AR06-13	DISCARDED	Ar-Ar	642116	5649056	Arrowstone Hills	Middle lava	excessive amts of excess Ar gas-NO DATE
RE-BC-214E*	5.32 ± 0.80	Ar-Ar	474286	5771309	Bull Canyon	Middle lava	forced plateau; 61.6% of 39Ar; steps 7-10
RE-CD06-66*	6.21 ± 0.30	Ar-Ar	446246	5704620	Cardiff Mountain	Basal lava: BC telephone	forced plateau; 82.7% of 39Ar; steps 1-5
RE-CD06-74	DISCARDED	Ar-Ar	446451	5704530	Cardiff Mountain	Middle lava: colonnade	humped plateau; possibility a result of 39Ar recoil in sample
RE-CH06-4	9.07 ± 0.26	Ar-Ar	608609	5671735	Chasm East Composite Log	Lava 9	
RE-CH06-12*	9.65 ± 0.40	Ar-Ar	609057	5671112	Chasm East Composite Log	Lava 2	poor isochron (low initial 40/36); 70.9% of 39Ar; steps 5-9
RE-CH06-18	9.86 ± 0.30	Ar-Ar	609006	5671220	Chasm East Composite Log	Lava 6	
RE-CH06-92	9.83 ± 0.31	Ar-Ar	607730	5668821	Western Chasm wall	No strat. Reference	
RE-DC06-32*	1.162 ± 0.057	Ar-Ar	555488	5716721	Dog Creek	Top lava	forced plateau; 91.3% of 39Ar; steps 3-8
RE-DC06-36*	2.89 ± 0.42	Ar-Ar	555012	5716235	Dog Creek	Middle lava	forced plateau; re-test; 60.1% of 39Ar; steps 7-9
RE-DM06-2 <sup>1"</sup>	17.33 ± 0.28	Ar-Ar	647894	5667970	Deadman Falls	Basal lava	
RE-DM06-2 <sup>2"</sup>	17.43 ± 0.16	Ar-Ar	647894	5667970	Deadman Falls	Basal lava	
RE-HA06-45	DISCARDED	Ar-Ar	492172	5756349	Hanceville	Top lava	saddle shaped plateau; possibly a result of excessive amts of Ar gas
RE-SK06-60	2.78 ± 0.21	Ar-Ar	481886	5771101	Stum Road	Basal lava	analyst's notes: very low atmos. for high steps
RE-SK06-64	2.17 ± 0.26	Ar-Ar	481886	5771101	Stum Road	Top lava	
RE-VK06-79	8.24 ± 0.58	Ar-Ar	444047	5710329	Vedan Lake	Lava 1: basal lava	
RE-VK06-86	7.27 ± 0.35	Ar-Ar	444200	5710432	Vedan Lake	Lava 17: middle lava	98.9% of 39Ar; steps 2-8
RE-VK06-89	6.61 ± 0.36	Ar-Ar	444254	5710436	Vedan Lake	Lava 24: top lava	
<sup>a</sup> UBC, T. Ullrich, analyst. Unpublished preliminary results.							
<sup>b</sup> All samples are whole rocks.							
* Forced Age plateau: not complete step spectrum (1-9). At least 3 steps are used, and at 50-100% of the gas for these samples.							

Table C1: Regional geochronology

## **APPENDIX D**

### **Structure Data**

## Chasm Structure Measurements for Map

STATION	EASTING	NORTHING	STRIKE	DIP	NOTES*
<b>PLANAR PILLOW MEASUREMENTS (VOLCANIC LAYERING)</b>					
08REF34	607675	5669360	56	30	Certainty 2
08REF34	607675	5669360	62	30	Certainty 2
08REF34	607675	5669360	40	34	Certainty 2
08REF34	607675	5669360	32	40	Certainty 2
<b>REF34_AVG</b>	<b>607675</b>	<b>5669360</b>	<b>48</b>	<b>34</b>	<b>AVG</b>
08REF079	607434	5670258	90	45	Certainty 2
08REF079	607434	5670258	92	32	Certainty 2
<b>REF079_AVG</b>	<b>607434</b>	<b>5670258</b>	<b>91</b>	<b>39</b>	<b>AVG</b>
08REF006	607788	5669179	29	35	Certainty 2
08REF006	607788	5669179	61	29	Certainty 2
08REF006	607788	5669179	27	51	Certainty 2
08REF006	607788	5669179	26	36	Certainty 2
08REF006	607788	5669179	40	30	Certainty 2
<b>REF006_AVG</b>	<b>607788</b>	<b>5669179</b>	<b>37</b>	<b>36</b>	<b>AVG</b>
08REF005	607769	5669348	52	38	Certainty 2
08REF005	607769	5669348	53	48	Certainty 2
<b>REF005_AVG</b>	<b>607769</b>	<b>5669348</b>	<b>53</b>	<b>43</b>	<b>AVG</b>
08REF010	607682	5668454	127	35	Certainty 2-
08REF010	607682	5668454	98	36	Certainty 2-
08REF010	607682	5668454	105	36	Certainty 2-
08REF010	607682	5668454	134	28	Certainty 2-
<b>REF010_AVG</b>	<b>607682</b>	<b>5668454</b>	<b>116</b>	<b>34</b>	<b>AVG</b>

### \* Level of Certainty

1= 3D pillow or highest level of certainty

2= Estimating plane

3= Crude estimate of plane

4= Uncertain

### PLANAR BEDDING MEASUREMENTS

STATION	EASTING	NORTHING	STRIKE	DIP	NOTES
08REF023	608188	5667679	154	13	Certainty 1
08REF025	608205	5667984	217	20	Certainty 1
08REF025	608205	5667984	218	30	Certainty 1

**Table D1:** Chasm structure measurements for map

## **APPENDIX E**

### **XRD RESULTS: MATERIAL INFILLING THE VESICLES AT CHASM**

*Analyses run by Jenny Lai (UBC)*

#### **EXPERIMENTAL METHOD**

The five samples were ground into fine powder with a corundum mortar and smeared on to a glass slide with ethanol. Step-scan X-ray powder-diffraction data were collected over a range  $3-80^{\circ}2\theta$  with CoK $\alpha$  radiation on a Bruker D8 Focus Bragg-Brentano diffractometer equipped with an Fe monochromator foil, 0.6 mm ( $0.3^{\circ}$ ) divergence slit, incident- and diffracted-beam Soller slits and a LynxEye detector. The long fine-focus Co X-ray tube was operated at 35 kV and 40 mA, using a take-off angle of  $6^{\circ}$ .

#### **RESULTS**

Mineral identification was done using the International Centre for Diffraction Database PDF-4 and Search-Match software by Siemens (Bruker). The results are shown in Table 1. The X-ray diffractograms are shown in Figures 1 – 5. The presence of montmorillonite in samples 08REF030A01, RE-CH07-53, and RE-CH07-58 is confirmed by glycolation. The fit of the montmorillonite pattern varies between samples due to different amounts of hydration within each sample.

## Summary of Results:

*XRD qualitative results from Jenny Lai (UBC)*

### ***Mineralization in the Pillow Breccia***

***West Chasm Composite Stratigraphic Log- all samples have a stratigraphic reference***

1) 08REF030A02

Possible zeolites found in the matrix clastic material found at contact between WL2 and WC2

Rationale= confirm the zeolite composition, with additional classifying of the type of zeolite.

**Result: Yes, these are zeolites. Specifically, chabazite-Ca and Phillipsite-K, both in the Zeolite Group.**

2) 08REF034A01

Possible chalcedony. Sampled from WC3

Rationale = confirm the mineral composition, and classify the material

**Result: Major peak of analcime (associated with zeolites), and zeolite (phillipsite-K). Montmorillonite (Smectite Gr.) present, in addition to plagioclase (albite) and Qtz.**

3) 08REF030A01

chalky material interstitial with pillows in WC2.

Rationale= classify this material, what kind of secondary mineralization is this?

**Result: Major peak of analcime (assoc. with zeolites), and zeolite (wairakite). Montmorillonite (Smectite Gr.) present, calcite, clinochore, plag., k-feldspar, and qtz.**

### ***XRD of complete soil profile: Station 071***

***(all samples have stratigraphic reference: refer to soil profile & table for this stn)***

4) RE-CH07-53 Tephra layer

Rationale: identify and classify the different minerals in this 1<sup>st</sup> horizon (Bmb)

**Result: Zeolite (chabazite-Ca), Smectite (Montmorillonite), Plag., Cpx., Clinochore, Gypsum, Calcite. Plagioclase and cpx are the dominant peaks, also montmorillonite.**

5) RE-CH07-58 Clastic finely laminated paleosol

Rationale: identify and classify the different minerals in this 2nd horizon (IIBmb1)

**Result: Major peaks = analcime (assoc. w/ zeolites), plag and quartz- which makes sense. Zeolites (chabazite-Ca, phillipsite-K and tridymite) are also present. Smectite Gr. montmorillonite is present. K-feldspar, muscovite, and grunerite.**

Mineral	Ideal Formula	08REF030A02	08REF034A01	08REF030A01	RE-CH07-53	RE-CH07-58
Chabazite-Ca	$(\text{Ca}, \text{K}_2, \text{Na}_2)_2(\text{Al}_2\text{Si}_4\text{O}_{12})_2 \cdot 12\text{H}_2\text{O}$	X			X	X
Phillipsite-K	$(\text{K}_2)_{0.48}\text{Ca}_{0.52}\text{Al}_2\text{Si}_4\text{O}_{12} \cdot x\text{H}_2\text{O}$	X	X			X
Analcime	$\text{NaAlSi}_2\text{O}_6 \cdot \text{H}_2\text{O}$		X	X		X
Wairakite	$\text{CaAl}_2\text{Si}_4\text{O}_{12} \cdot 2\text{H}_2\text{O}$			X		
Plagioclase	$\text{NaAlSi}_3\text{O}_8 - \text{CaAl}_2\text{Si}_2\text{O}_8$		X	X	X	X
K-Feldspar	$\text{KAlSi}_3\text{O}_8$			X		X
Quartz	$\text{SiO}_2$		X	X		X
Calcite	$\text{CaCO}_3$			X	X	
Clinochlore	$(\text{Mg}, \text{Fe}^{2+})_5\text{Al}(\text{Si}_3\text{Al})\text{O}_{10}(\text{OH})_8$			X	X	
Gypsum	$\text{CaSO}_4 \cdot 2\text{H}_2\text{O}$				X	
Augite	$(\text{Ca}, \text{Na})(\text{Mg}, \text{Fe}, \text{Al}, \text{Ti})(\text{Si}, \text{Al})_2\text{O}_6$				X	
Muscovite	$\text{KAl}_2(\text{AlSi}_3\text{O}_{10})(\text{OH})_2$					X
Tridymite	$\text{SiO}_2$					X
Montmorillonite	$(\text{Na}, \text{Ca})_{0.3}(\text{Al}, \text{Mg})_2\text{Si}_4\text{O}_{10}(\text{OH})_2 \cdot n\text{H}_2\text{O}$		X	X	X	X
Grunerite	$\text{Fe}^{2+}_7\text{Si}_8\text{O}_{22}(\text{OH})_2$					X

*Table E1: Results of qualitative analysis*

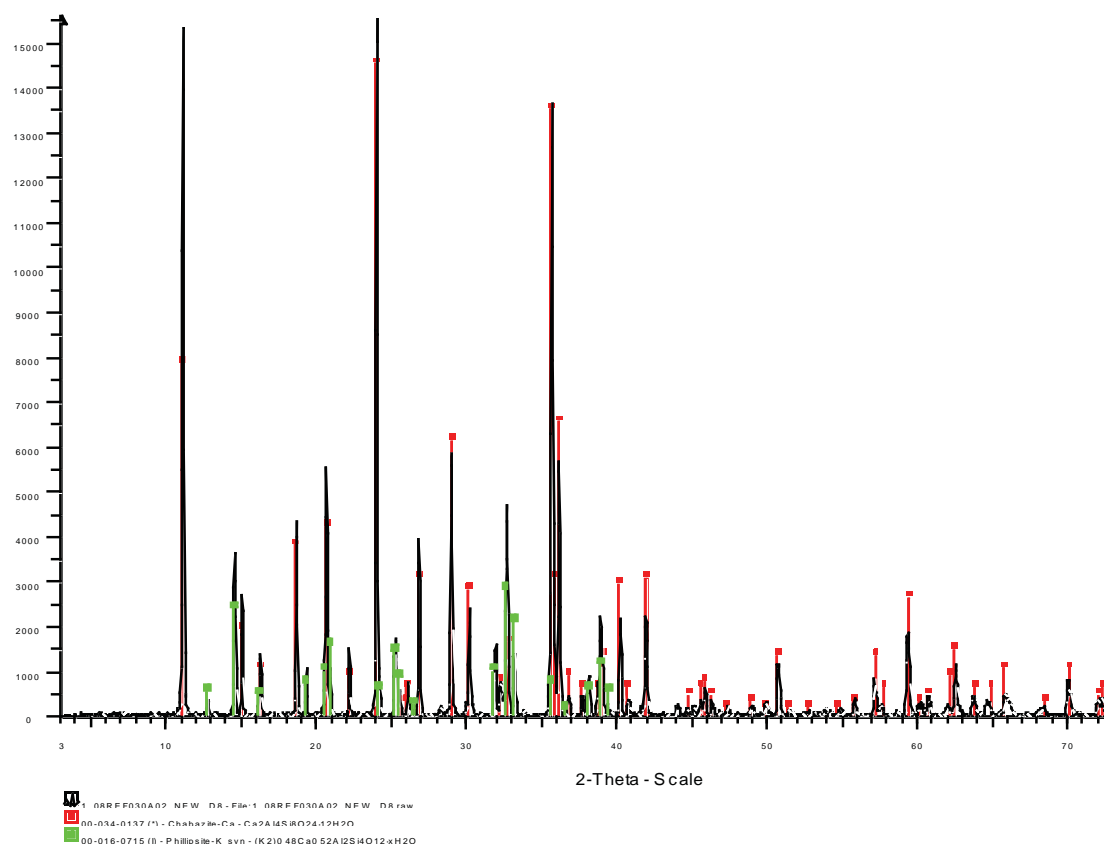


**Figure E1:** X-ray diffractogram of sample 08REF03A02



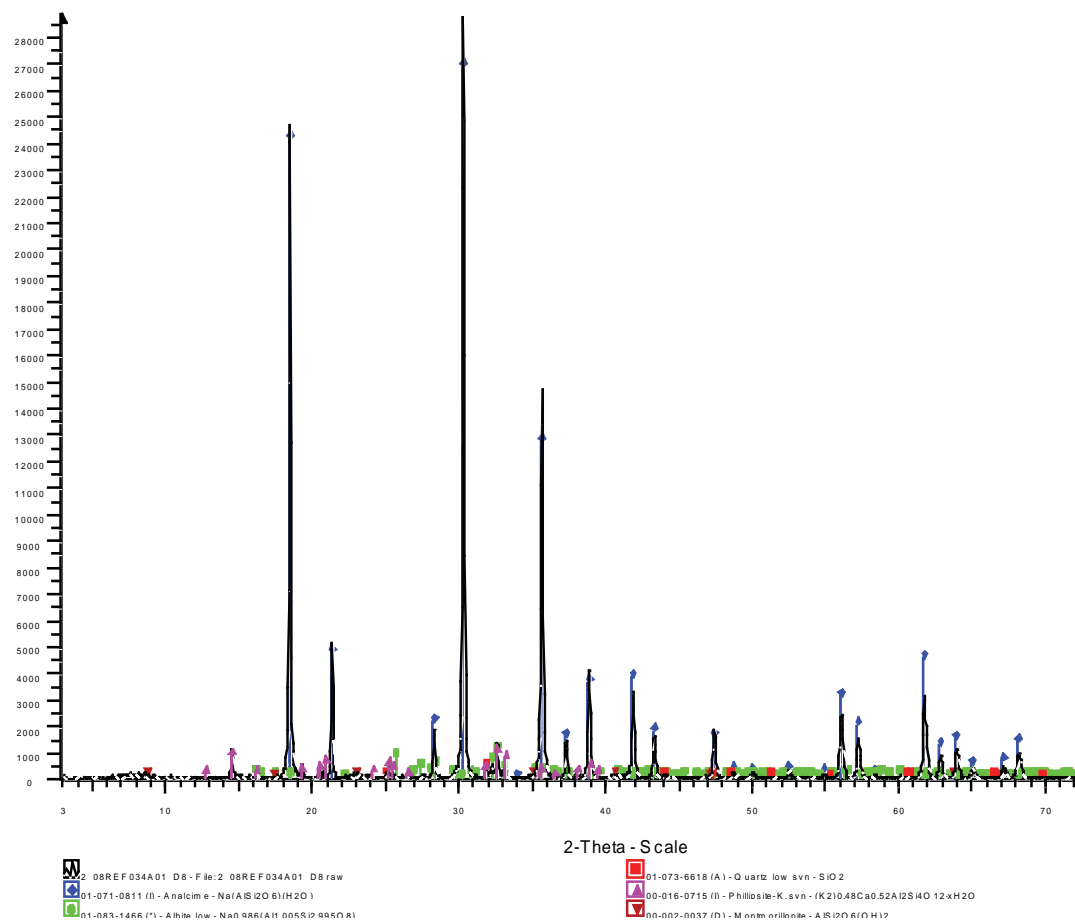


**Figure E2:** X-ray diffractogram of sample 08REF034A01

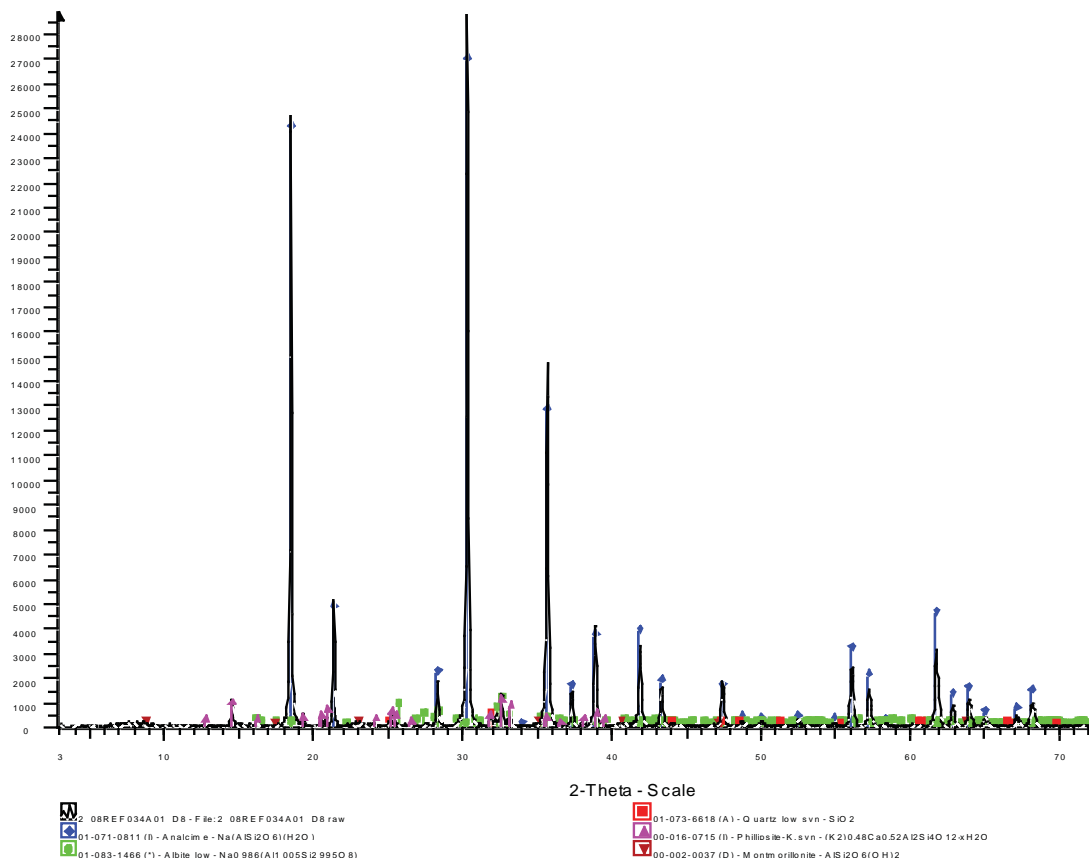


**Figure E3:** X-ray diffractogram of sample 08REF030A01

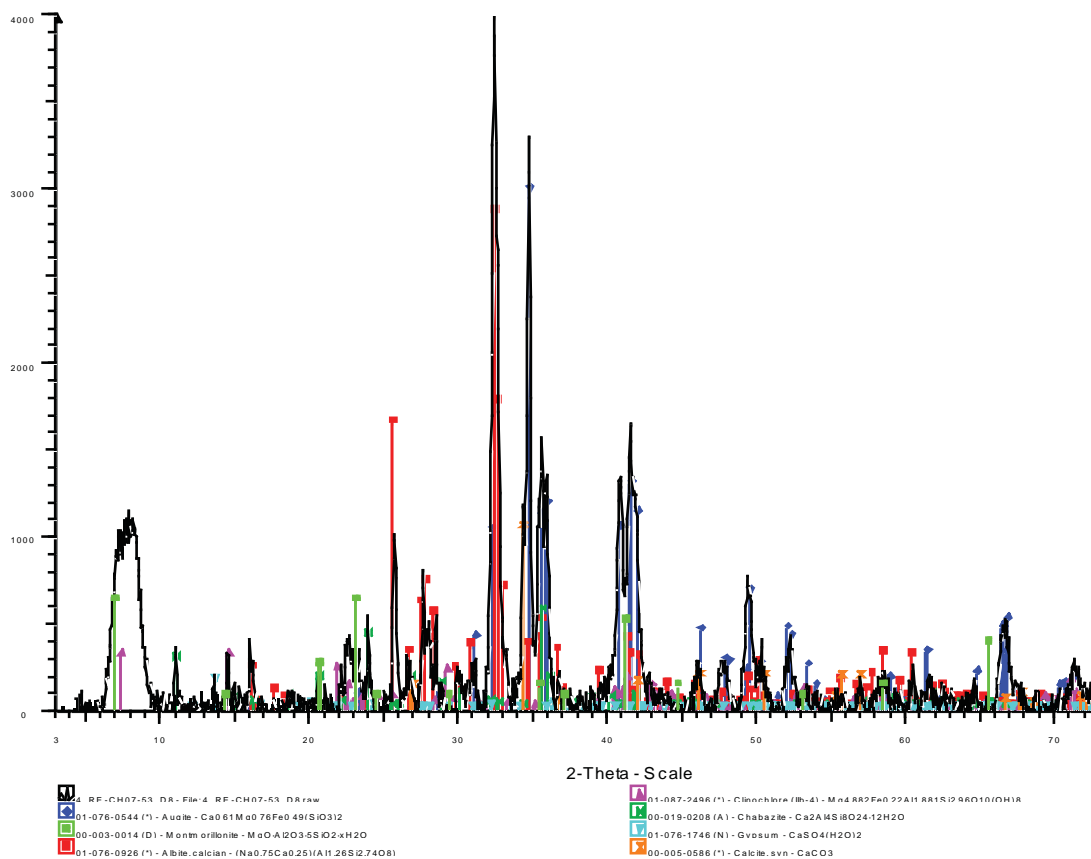


**Figure E4:** X-ray diffractogram of sample RE-CH07-53

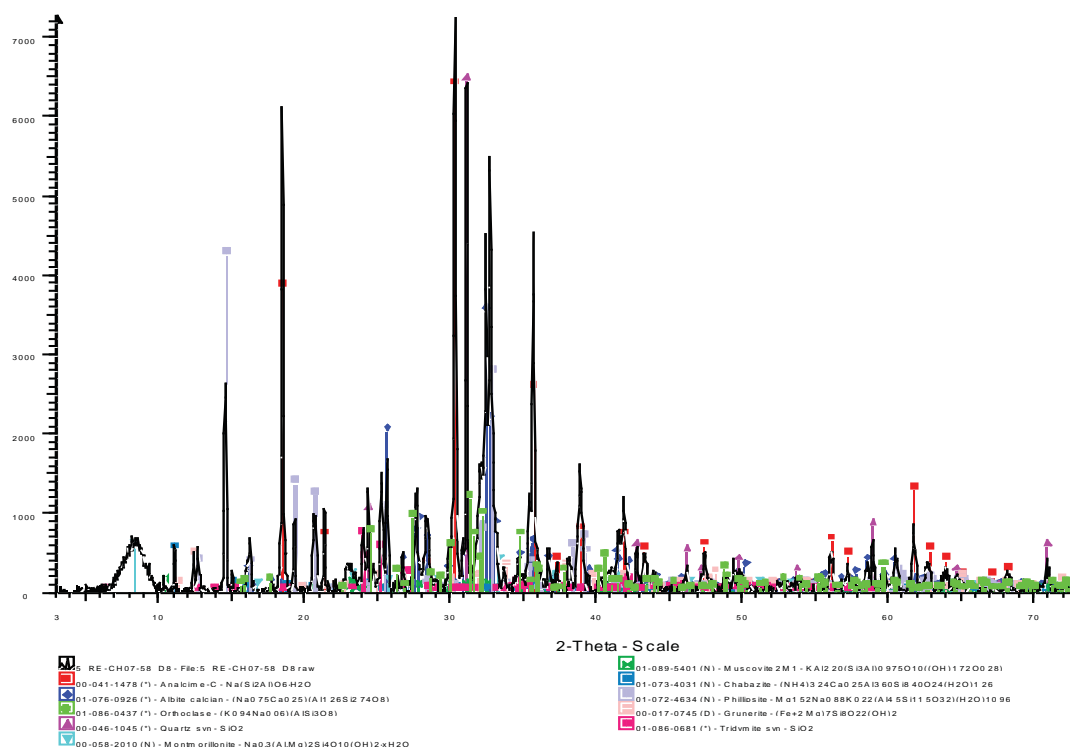


**Figure E5:** X-ray diffractogram of sample RE-CH07-58